The Eocene-Oligocene transition: a review of marine and terrestrial proxy data, models and model-data comparisons

David K. Hutchinson[1], Helen K. Coxall[1], Daniel J. Lunt[2], Margret Steinthorsdottir[1,3], Agatha M. De Boer[1], Michiel Baatsen[4], Anna von der Heydt[4,5], Matthew Huber[6], Alan T. Kennedy-Asser[2], Lutz Kunzmann[7], Jean-Baptiste Ladant[8], Caroline H. Lear[9], Karolin Moraweck[7], Paul N. Pearson[9], Emanuela Piga[9], Matthew J. Pound[10], Ulrich Salzmann[10], Howie D. Scher[11], Willem P. Sijp[12], Kasia K. Śliwińska[13], Paul A. Wilson[14], Zhongshi Zhang[15,16]

1. Department of Geological Sciences and Bolin Centre for Climate Research, Stockholm University, Stockholm, Sweden
2. School of Geographical Sciences, University of Bristol, UK
3. Department of Palaeobiology, Swedish Museum of Natural History, Stockholm, Sweden
4. Institute for Marine and Atmospheric Research, Department of Physics, Utrecht University, Utrecht, the Netherlands
5. Centre for Complex Systems Studies, Utrecht University, Utrecht, the Netherlands
6. Department of Earth, Atmospheric, and Planetary Sciences, Purdue University, West Lafayette, USA
7. Senckenberg Natural History Collections Dresden, Germany
8. Department of Earth and Environmental Sciences, University of Michigan, USA
9. School of Earth and Ocean Sciences, Cardiff University, Cardiff, UK
10. Department of Geography and Environmental Sciences, Northumbria University, UK
11. School of the Earth, Ocean and Environment, University of South Carolina, USA
12. Climate Change Research Centre, University of New South Wales, Sydney, Australia
13. Department of Stratigraphy, Geological Survey of Denmark and Greenland (GEUS), Copenhagen, Denmark
14. University of Southampton, National Oceanography Centre Southampton, UK
15. Department of Atmospheric Science, China University of Geoscience, Wuhan, China
16. NORCE Research and Bjerknes Centre for Climate Research, Bergen, Norway

Correspondence to: David K. Hutchinson (david.hutchinson@geo.su.se)

Abstract. The Eocene-Oligocene transition (EOT) from a largely ice-free greenhouse world to an icehouse climate with the first major glaciation of Antarctica was a phase of major climate and environmental change occurring ~34 million years ago (Ma) and lasting ~500 kyr. The change is marked by a global shift in deep sea $\delta^{18}O$ representing a combination of deep-ocean cooling and global ice sheet growth. At the same time, multiple independent proxies for sea surface temperature indicate a surface ocean cooling, and major changes in global fauna and flora record a shift toward more cold-climate adapted species. The major explanations of this transition that have been suggested are a decline in atmospheric CO_2, and changes to ocean gateways, while orbital forcing likely influenced the precise timing of the glaciation. This work reviews and synthesises proxy evidence of paleogeography, temperature, ice sheets, ocean circulation, and CO_2 change from the marine and terrestrial realms. Furthermore, we quantitatively compare proxy records of change to an ensemble of model simulations of temperature change across the EOT. The model simulations compare three forcing mechanisms across the EOT: CO_2 decrease, paleogeographic

changes, and ice sheet growth. We find that CO_2 forcing provides by far the best explanation of the combined proxy evidence, and based on our model ensemble, we estimate that a CO_2 decrease of about 1.6x across the EOT (e.g. from 910 to 560 ppmv)

40   achieves the best fit to the temperature change recorded in the proxies. This model-derived CO_2 decrease is consistent with proxy estimates of CO_2 decline at the EOT.

1 Introduction

1.1 Scope of Review

Since the last major review of the EOT (Coxall and Pearson, 2007) the fields of palaeoceanography and palaeoclimatology

45   have grown considerably. New proxy techniques, drilling and field archives of Cenozoic (66 Ma to present) climates, have expanded global coverage and added increasingly detailed views of past climate patterns, forcings and feedbacks. A plethora of new proxy records capture near and far-field signals of the onset of Antarctic glaciation. Meanwhile, efforts to simulate the onset of the Cenozoic 'icehouse', using the latest and most sophisticated climate models, have also progressed. It is now possible to compare model outputs with one another, as well as against a growing body of climate proxy data. Here we review

50   both observations and modelling literature of the EOT. From the marine realm, we review records of sea surface temperature, as well as deep sea time series of the temperature and land ice proxy $\delta^{18}O$ and carbon cycle proxy $\delta^{13}C$. From the terrestrial realm we cover plant records and biogeochemical proxies of temperature, CO_2 and vegetation change. We summarise the main evidence of temperature, glaciation and carbon cycle perturbations and constraints on the terrestrial ice extent during the EOT, and review indicators of ocean circulation change and deep water formation, including how these changes reconcile with

55   paleogeography, in particular, ocean gateway effects.

Finally, we synthesise existing model experiments that test three major proposed mechanisms driving the EOT: (i) paleogeography changes, (ii) greenhouse forcing and (iii) ice sheet forcing upon climate. We highlight what has been achieved from these modelling studies to illuminate each of these mechanisms, and explain various aspects of the observations. We also

60   discuss the limitations of these approaches, and highlight areas for future work. We then combine and synthesise the observational and modelling aspects of the literature in a model-data intercomparison of the available models of the EOT. This approach allows us to assess the relative effectiveness of the three modelled mechanisms in explaining the EOT observations.

The paper is structured as follows: Section 1.2 defines the chronology of events around the EOT, and clarifies the terminology

65   of associated events, transitions, and intervals, thereby setting the framework for the rest of the review. Section 2 reviews our understanding of palaeogeographic change across the EOT, and discusses proxy evidence for changes in ocean circulation and ice sheets. Section 3 synthesises marine proxy evidence for sea surface temperatures (SST) and deep-ocean temperature change. Section 4 synthesises terrestrial proxy evidence for continental temperature change, with a focus on pollen-based reconstructions. Section 5 presents estimates of CO_2 forcing across the EOT, from geochemical and stomatal-based proxies.

70   Section 6 qualitatively reviews previous modelling work, and Section 7 provides a new quantitative intercomparison of previous modelling studies, with a focus on model-data comparisons to elucidate the relative importance of different forcings across the EOT. Section 8 provides a brief conclusion.

1.2 Terminology of the Eocene-Oligocene transition

Palaeontological evidence has long established Eocene (56 to 34 Ma) warmth in comparison to a long term Cenozoic cooling
75   trend (Lyell and Deshayes 1830, p99-100). As modern stratigraphic records improved, a prominent step in that cooling emerged towards the end of the Eocene. This became evident in early oxygen isotope records ($\delta^{18}O$) from deep-sea benthic foraminifera, which show an isotope shift towards higher $\delta^{18}O$ values (Kennett and Shackleton, 1976; Shackleton and Kennett, 1975), subsequently attributed to a combination of continental ice growth and cooling (Lear et al., 2008). In the 1980s the search was on for a suitable Global Stratotype Section and Point (GSSP) to define the Eocene-Oligocene boundary (EOB).
80   Much of the evidence was brought together in an important synthesis edited by Pomerol and Premoli Silva (1986). The GSSP was eventually fixed at the Massignano outcrop section in the Marche region of Italy in 1992 (Premoli Silva and Jenkins, 1993) at the 19.0 m mark which corresponds to the extinction of the planktonic foraminifer family Hantkeninidae (Coccione, 1988; Nocchi et al., 1986). Massignano is the only place where the EOB is defined unambiguously; everywhere else the EOB must be correlated to the Massignano section, whether by biostratigraphy, magnetostratigraphy, isotope stratigraphy or other
85   methods.

Coxall and Pearson, (2007, p 352) described the EOT as "a phase of accelerated climatic and biotic change lasting 500 kyr that began before and ended after the E/O boundary". Recognizing and applying this in practice turns out to be problematic due to variability in the pattern of $\delta^{18}O$ between records and different timescales in use. Widespread records now show the positive
90    $\delta^{18}O$ shift with increasing detail. A high-resolution record from ODP Site 1218 in the Pacific Ocean revealed two $\delta^{18}O$ and $\delta^{13}C$ 'steps' separated by a more stable 'plateau interval' (Coxall et al., 2005; Coxall and Wilson, 2011). The EOT brackets these isotopic steps with the EOB falling in the plateau between them (Coxall and Pearson, 2007; Coxall and Wilson, 2011; Dunkley Jones et al., 2008; Pearson et al., 2008). However, while two-step $\delta^{18}O$ patterns have now been interpreted in other deep sea records, thus far largely from the Southern Hemisphere (Figure 1) (Bohaty et al., 2012; Borrelli et al., 2014; Coxall
95   and Wilson, 2011; Langton et al., 2016; Pearson et al., 2008; Wade et al., 2012; Zachos et al., 1996), there is often ambiguity in their identification. In particular, while the second $\delta^{18}O$ step, 'Step 2' of Coxall and Pearson (2007), is an abrupt and readily correlated feature, the first step (Step 1 of Pearson et al., 2008; EOT-1 of Coxall and Wilson, 2011) is less often prominent than at Site 1218, particularly in benthic records (Fig. 1). Furthermore, some records have been interpreted to show more than two $\delta^{18}O$ steps (e.g. Katz et al. 2008). Benthic $\delta^{13}C$ records provide a powerful stratigraphic tool in deep ocean sediments. At
100   Site 1218 the prominent EOT steps in benthic $\delta^{13}C$, while closely coupled to those in $\delta^{18}O$ are not synchronous (Coxall et al., 2005) and further complications arise in correlation to other sites (Coxall and Wilson, 2011). In attempting to synthesize the

pattern across multiple sites we suggest that attempts to define and correlate an initial 'Step 1' are probably premature at this point and should await better resolved records. Nonetheless, we maintain a tentative Step-1 in our terminology because it is important for differentiating phases of cooling vs ice growth during the EOT.

105

Settling on a consistent terminology for the other features of the EOT is also problematic because usage of certain terms has changed through time. The important climatic event that corresponds to the larger second δ^{18}O step (in some records) has frequently been termed 'Oi-1' after Miller et al. (1991). However, that term was originally defined as an isotope stratigraphic 'zone' between one oxygen isotope peak and another, corresponding to a duration of several millions of years. In that original

110 meaning, Oi-1 encompasses and extends well above the interval of maximum early Oligocene δ^{18}O that corresponds to most of Chron C13n and is interpreted as the Early Oligocene Glacial Maximum (EOGM; Liu et al. 2004) (Fig. 1). Moreover, being a peak-to-peak interval, by definition it excludes the interval of δ^{18}O increase that led up to the δ^{18}O peak. Because Oi-1 has variously been used as a term to describe 1) an extended isotope zone, 2) the peak δ^{18}O value at the base of that zone, 3) an extended phase of high δ^{18}O values in the lower Oligocene approximately synonymous with the EOGM, and 4) the 'step' that

115 led up to the peak value (see discussion and references in Coxall and Pearson, 2007, p. 352), we avoid the term here. Instead we suggest that if it is to be used, it should be employed in its original sense (Miller et al., 1991). Similarly the term 'Oi-1a' and 'Oi-1b' have been applied inconsistently in the literature and are now arguably an impediment to clear communication. Katz et al. (2008) referred to prominent oxygen isotope steps within the EOT as 'EOT-1' and 'EOT-2', which might seem a convenient nomenclature for the steps referred to here, but whereas 'EOT-1' arguably corresponds to the 'Step 1' of Coxall and

120 Pearson (2007), 'EOT-2' was a separate feature identified in the St. Stephen's Quarry record some way below the level identified as 'Oi-1' (Katz et al. 2008, p330; in that paper used to denote the δ^{18}O maximum). Hence it is not appropriate to use 'EOT-2' to denote the second step. Insofar as it is useful to have a term for the important isotope step that occurs well after the EOB and within the lower part of Chron C13n, we here suggest "**E**arliest **O**ligocene oxygen **I**sotope **S**tep" (EOIS) to distinguish it from Oi-1, EOGM, and the extended (~500 kyr) EOT isotope 'shift'. Note, for absolute clarity, that the EOIS is not

125 instantaneous and several records show some 'intermediate' values (Figure 1); its inferred duration in the records presented here is in the tens of kyr (40 krys at Site 1218, Coxall et al., 2005).

Based on the stratigraphic record from Tanzania, Dunkley Jones et al. (2008) and Pearson et al. (2008) placed the base of the EOT at the extinction of the tropical warm-water nannofossil *Discoaster saipanensis,* which they regarded as the first sign of

130 biotic extinction associated with the late Eocene cooling. This extinction event has long been used to mark the base of nannofossil Zone NP21 (Martini, 1971) or more recently Zone CNE21 (Agnini et al., 2014). On the timescale used by Dunkley Jones et al. (2008) it was estimated to be 500 kyr before the top of the EOIS. However, a subsequent calibration from ODP Site 1218 (Blaj et al., 2009) placed this event significantly earlier than previously suggested. In the record from Site 1218 the *D. saipanensis* extinction is coincident (within 80 kyr analytical error; Coxall et al., 2005) with the base of a significant δ^{18}O

135   increase that seems to be visible in many of the records (including Tanzania) and has been termed the 'Late Eocene Event' by
       Katz et al., (2008). It seems desirable to include these biotic and climatic events within the definition of the EOT rather than
       insist on an arbitrary 500 kyr duration. On the most commonly used current timescale, 'Geological Timescale 2012' (GTS2012;
       Gradstein et al., 2012), the critical levels are calibrated as follows: top of the EOIS at 33.65 Ma, base of Chron C13n at 33.705
       Ma, EOB at 33.9 Ma, and extinction of *D. saipanensis* at 34.44 Ma. Hence the stratigraphic interval of the EOT according to
140   our preferred definition is now given an estimated duration of 790 kyr (Figure 1).
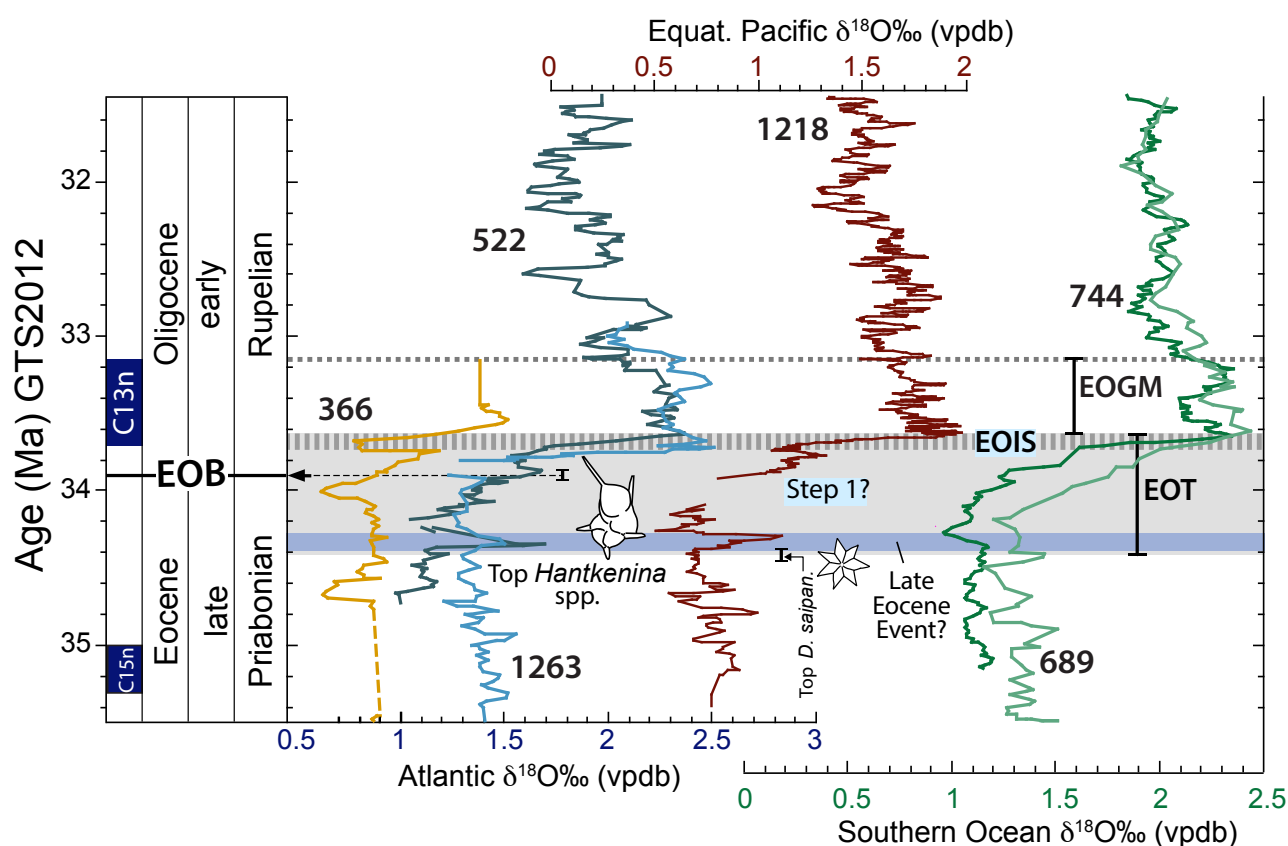
Figure 1: Oxygen stable isotope and chrono-stratigraphic characteristics of the Eocene-Oligocene transition (EOT) from deep marine records and EOT terminology on the GTS 2012 time scale. Benthic foraminiferal δ18O from six deep sea drill holes are shown: Atlantic Sites 366,
145   522 and 1263 (Zachos et al. 1996; Langton et al., 2016); Southern Ocean Sites 744 and 689 (Zachos et al. 1996; Diester-Haass and Zahn 1996) and the Equatorial Pacific Site 1218 (Coxall and Wilson 2011). Due to different sample resolutions, running means are applied using a 3-point filter for Sites 522, 689 and 1263, 5-point filter for Sites 366 and 744 and a 7-point filter for Site 1218. Time scale conversions were made by aligning common magneto-stratigraphic tie points. The EOT is defined as a 500 kyr long phase of accelerated climatic and biotic change that began before and ended after the Eocene-Oligocene boundary (EOB) (after Coxall and Pearson (2007)). Benthic data are
150   all *Cibicidoides* spp. or 'Cibs. Equivalent' and have not been adjusted to sea water equilibrium values. 'Step-1' comprises a modest δ18O increase linked to ocean cooling (Lear et al., 2008. Bohaty et al., 2012) 'Step-2' corresponds to the Early Oligocene oxygen Isotope Step (EOIS), defined herein. The 'Top (T) *Hantkenina* spp.' marker corresponds to the position of this extinction event at DSDP Site 522 (including sampling bracket) with respect to the corresponding Site 522 δ18O curve. That it coincides with the published calibrated age of this event (33.9 Ma) is entirely independent. The 'Late Eocene Event' δ18O maximum (after Katz et al., 2008) may represent a failed
155   glaciation.

Combined $\delta^{18}O$ and trace element investigations (see Section 3.2) have led to the suggestion that the initial $\delta^{18}O$ increase commonly referred to as Step-1 Figure 1) is mostly attributable to ocean cooling, with subordinate ice sheet growth, whereas the more prominent $\delta^{18}O$ increase at the end of the EOT largely represents ice growth with a modest further cooling (Bohaty

160   et al., 2012; Katz et al., 2008; Lear et al., 2008). Estimates of the combined total sea-level fall across the EOT are on the order of 70 m (Miller et al., 2008; Wilson et al., 2013) and microfacies and paleontological records from shelf environments (Houben et al., 2012) are consistent with this generalization. The prominent isotope step that marks the end of the EOT (i.e., the EOIS in our terminology) is the sharpest feature in most records, culminating with the highest $\delta^{18}O$ values of the Eocene and Oligocene. It is widely suggested that it signifies the initiation of major sustained Antarctic glaciation, most likely an early

165   East Antarctic Ice Sheet (EAIS) (Bohaty et al., 2012; Coxall et al., 2005; Galeotti et al., 2016; Miller et al., 1987; Shackleton and Kennett, 1975; Zachos et al., 1992). The approximately 500 kyr interval of maximum early Oligocene $\delta^{18}O$ that corresponds to most of Chron C13n is interpreted as an the Early Oligocene Glacial Maximum (EOGM; Liu et al. 2004) (Fig. 1). Oxygen isotope maxima in the late Eocene imply substantial ephemeral precursor glaciations on the approach to the EOT (Galeotti et al., 2016; Houben et al., 2012; Katz et al., 2008; Scher et al., 2011, 2014). The oldest and most prominent of these

170   hypothesized transient glacial events occurs at 37.3 Ma (Scher et al., 2014). Although precise correlation of the records is uncertain due to the limited stratigraphic resolution, two younger hypothesized events are shown in Figure 1: one at about 34.15 Ma ('Late Eocene Event', of Katz et al., 2008) and another at ~33.9 Ma, which corresponds to $\delta^{18}O$ 'Step- 1', and is apparently coincided with the E/O boundary. This 33.9 Ma step has been previously referred to as the 'Precursor glaciation' (Scher et al., 2011) and EOT-1 (Katz et al., 2008).

175

A detailed discussion of the *Hantkenina* extinction and associated bioevents at the EOB was recently provided by Berggren et al., (2018, p 30-32). The highest stratigraphic occurrence of the planktonic foraminifera family Hantkeninidae denotes the EOB in its type section (Nocchi et al., 1986). This is thought to have involved simultaneous extinction of all five morphospecies and two genera of late Eocene hantkeninids (Coxall and Pearson, 2007) (Fig. 1). Insofar as the principles of biostratigraphy

180   require a particular species to denote a biozone boundary, the commonest species *Hantkenina alabamensis* is used to define the base of Zone O1 (Berggren et al., 2018; Berggren and Pearson, 2005; Wade et al., 2011). The extinction of *H. alabamensis* can be considered the 'primary marker' for worldwide correlation of the EOB. It occurs at a slightly higher (later) level than another set of prominent planktonic foraminifer extinctions, namely *Turborotalia cerroazulensis* and the related species *T. cocoaensis* and *T. cunialensis*. DSDP Site 522 (South Atlantic), thus far, is one of the few deep sea records to have both a

185   detailed $\delta^{18}O$ stratigraphy and planktonic foraminifera assemblages that capture these evolutionary events. Here, the *Hantkenina* extinction horizon occurs approximately two thirds of the way through the EOT (Figure 1). It occurs at a similar relative position in the hemipelagic EOT sequence in Tanzania (Pearson et al., 2008), also in unpublished data from Indian Ocean ODP Site 757 (Coxall et al, unpublished). This finding implies that the extinction of the hantkeninids was globally

synchronous and may have been a response to the EOT cooling phase of the late Eocene. Existing constraints on the
190   hantkeninid extinction horizon remain rather coarse in terms of sampling resolution compared to many isotopic records and
the matter will benefit greatly from incoming high-resolution records from Site U1411, which boasts both excellent (glassy)
preservation and orbital level sampling.

Dating and correlation of non-marine records, which usually lack $\delta^{18}O$ stratigraphy, is more challenging and there are far fewer
195   well-dated records on land. Here a strict concept of the EOT is difficult to apply and relies on correlations using other
stratigraphic approaches, including magnetostratigraphy and palynomorph or mammal tooth biostratigraphy that have been
cross calibrated in a few marine and marginal-marine sections (Abels et al., 2011; Dupont-Nivet et al., 2007, 2008; Hooker et
al., 2004). Central Asian sections are the exception where even the step features of the EOT can be identified using magneto,
bio- and cyclostratigraphy (Xiao et al., 2010). Moreover, combined $\delta^{18}O$ and clumped isotopes analyses on fresh water
200   gastropod shells from a terrestrial EOT section in the south of England has permitted the first direct correlation of marine and
non-marine realms and identified coupling between cooling and hydrological changes in the terrestrial realm (Sheldon et al.,
2016). This finding strengthens the case that the large evolutionary turnover in mammals that occurred during the EOT (the
'Grande Coupure') coincides with the onset of earliest Oligocene glaciation, and therefore was linked with the associated
climate change (Hooker et al., 2004; Sheldon et al., 2016).

205

In shallow water carbonate successions, the EOB has traditionally been approximated by the prominent extinctions of a series
of long-ranging larger benthic foraminifers (LBFs) often called orthophragminids (corresponding to the Families
Discocylinidae and Asterocyclinidae; Adams et al. 1986). The general expectation was that these extinctions likely occurred
at the time of maximum ice growth and sea level regression – in our terminology the EOIS. However this view is not supported
210   by evidence from Tanzania (Cotton and Pearson, 2011) and Indonesia (Cotton et al., 2014), which suggest that the extinctions
occurred within the EOT. In Tanzania the extinctions occur quite precisely at the level of the EOB, hinting that the EOB itself
may have had a global cause affecting different environments, possibly independent of the events that caused the isotope
increases (Cotton and Pearson, 2011).

215   The definition of the EOT used here excludes the long-term Eocene cooling trend. That trend began in the Ypresian (early
Eocene) and continued through much of the Lutetian and Bartonian (middle Eocene; albeit interrupted by the Middle Eocene
Climatic Optimum; MECO; Bohaty and Zachos 2003) and Priabonian (late Eocene) (Cramwinckel et al., 2018; Inglis et al.,
2015; Liu et al., 2018; Zachos et al., 2001). In particular, prominent extinctions in various marine groups occurred around the
beginning of the Priabonian (late Eocene), possibly connected with global cooling (e.g. Wade and Pearson 2008; although we
220   note that the base of the Priabonian has yet to be defined by GSSP). These data are excluded by our definition from the EOT
but may be part of the same general long-term pattern. In some stratigraphic records, especially terrestrial ones, it may not be
easy to distinguish these longer-term events from the EOT.

2 Proxy evidence for paleogeography, ocean circulation, and terrestrial ice evolution

Here we discuss proxy evidence for the global paleogeography of the EOT (Section 2.1) including the state and evolution of
225   ocean gateways (Section 2.2), and proxy evidence for ocean circulation (Section 2.3) and Antarctic glaciation (Section 2.4).
We then briefly discuss the timing of the Northern Hemisphere glaciation (Section 2.5).

2.1 Tectonic Reconstruction

The tectonic evolution of the southern continents, opening a pathway for the Antarctic Circumpolar Current, has long been
linked with long-term Eocene cooling and the EOT (Kennett et al., 1975). However, there remain major challenges in
230   reconstructing the paleogeography at or around the EOT, requiring a series of methodological steps (Baatsen et al., 2016;
Kennett et al., 1975; Markwick, 2007, 2019; Markwick and Valdes, 2004; Müller et al., 2008). The first step is to use modern
day geography and relocate the continental and ocean plates according to a plate tectonic evolution model, used in software
such as GPlates (Boyden et al., 2011). This software uses the interpretation of seafloor spreading and paleomagnetic data to
reconstruct relative plate motion (e.g. Scotese et al. 1988), and an absolute reference frame to position the plates relative to the
235   Earth's mantle (e.g. Dupont-Nivet et al. 2008). Currently, there are two such absolute reference frames: one based on a global
network of volcanic hot-spots (Seton et al., 2012) and one based on a paleomagnetic reference frame (van Hinsbergen et al.,
2015; Torsvik et al., 2012). Importantly, these two reference frames give virtually the same continental outlines, but the
orientation of the continents is shifted. This results in differences in continental positions between the reference frames of up
to 5-6° (Baatsen et al., 2016) around the EOT, creating an uncertainty in reconstructing paleogeography, especially in southern
240   latitudes between 40 to 70 °S where important land and ocean geological archives exist. This latitudinal uncertainty also
impacts the reconstruction of Antarctic glaciation, since glacial dynamics are highly sensitive to latitude.

After the plate tectonic reconstruction has been applied, adjustments are needed to capture the age-depth evolution of the
seafloor (Crosby et al., 2006) and seafloor sedimentation rate (Müller et al., 2008). Adjusting land topography is more difficult,
245   and requires knowledge of paleoaltimetry, including processes such as plate collision processes, uplift, subsidence and erosion.
Several publicly available reconstructions exist for the Eocene; Markwick (2007) reconstructed paleotopography for the late
Eocene (38 Ma), while Sewall et al. (2000) and more recently (Zhang et al., 2011) and Herold et al. (2014) have generated
paleotopographies for the early Eocene (~55 to 50 Ma). These are based on the Hot Spot reference frame. Baatsen et al. (2016)
have recently created a paleogeographic reconstruction of the late Eocene using the Paleomagnetic reference frame. Such
250   efforts to develop realistic paleogeography for each time slice represents a major undertaking in blending geomorphic evidence
with tectonic evolution, and thus includes many specific details that are beyond the scope of this review.

Recently, a stage-by-stage paleogeographic reconstruction of the entire Phanerozoic has been made publicly available in digital
format (Scotese and Wright, 2018). This includes snapshots of the Priabonian (35.9 Ma) and Rupelian (31 Ma). Another stage-

255 by-stage reconstruction of Cenozoic paleogeography evolution originates from Markwick (2007); this reconstruction has been incorporated into a modelling study of climate dependence on paleogeography (Farnsworth et al., 2019; Lunt et al., 2016), and paleogeography changes across the EOT (Kennedy et al., 2015). However, the most recent versions of the (Markwick, 2007) paleogeography reconstructions are proprietary and are thus not included in this paper. Therefore, we present a summary of late Eocene (38 Ma) paleogeography in

260 Figure 2 from the publicly available datasets of Baatsen et al. (2016) and Scotese and Wright (2018). Our aim here is not to evaluate these reconstructions, but to present them such that their differences can be taken as broadly indicative of the uncertainties in paleogeography at this time.
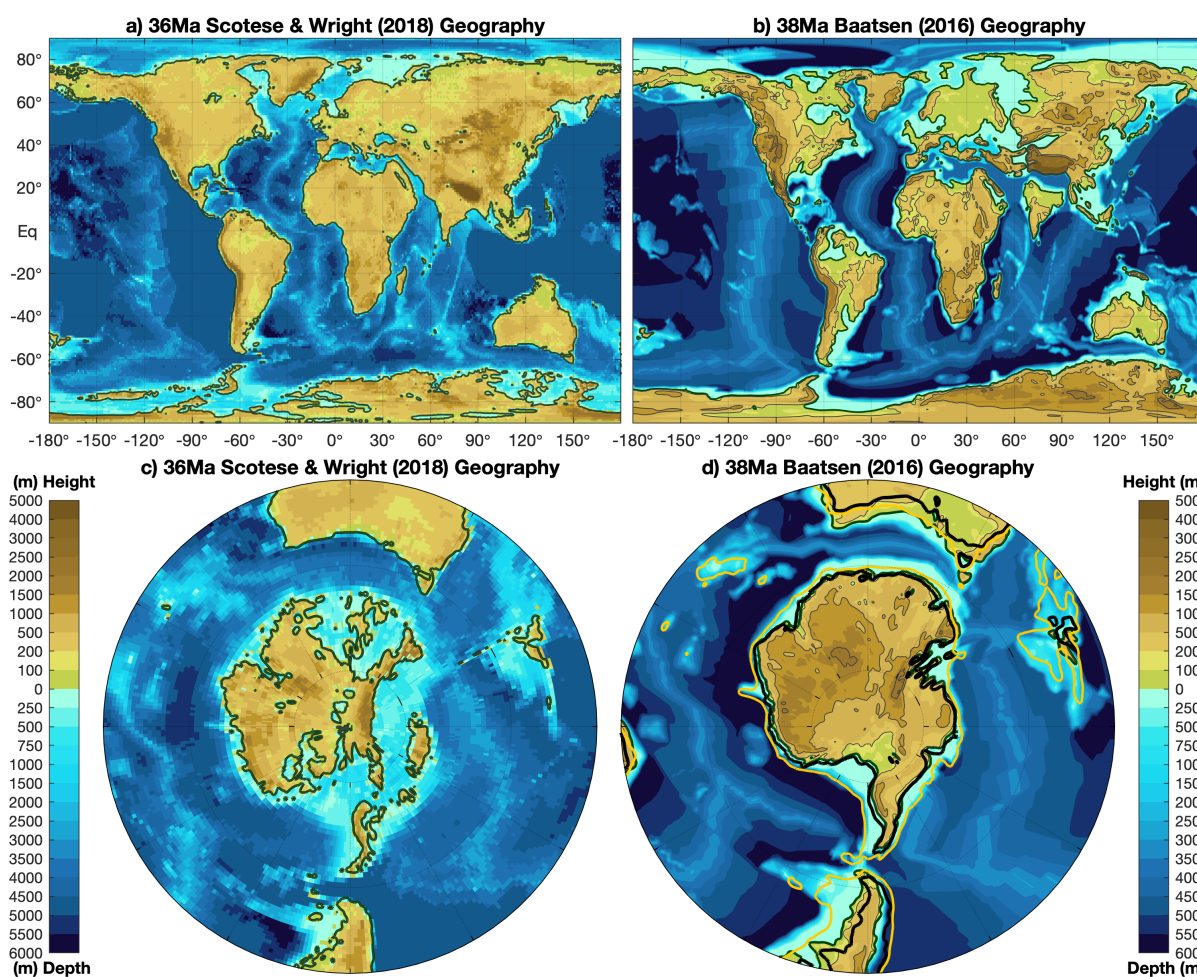
265

Figure 2: Paleogeography at the late Eocene showing two alternative reconstructions. (a) and (c) use the Hot Spot reference frame, using the Scotese and Wright (2018) paleogeography at 36 Ma, while (b) and (d) use the Paleomagnetic reference frame showing the reconstruction of Baatsen et al. (2016) at 38 Ma. These two reconstructions use different methodologies, and are presented as broadly indicative of the

uncertainties in paleogeography at this time. Also shown in (d) are post-EOT coastlines at 30 Ma (black contours) and 1000 m depth (orange contours), which illustrate the widening of the Southern Ocean gateways during the 8 Myr interval around the EOT.

2.2 Southern Ocean Gateways

A long-held hypothesis on the cause of the EOT glaciation is that Antarctica cooled because of tectonic opening of Southern Ocean gateways (Barker and Burrell, 1977; Kennett, 1977). This mechanism suggests that the onset of the Antarctic Circumpolar Current (ACC) reorganised ocean currents from a configuration of subpolar gyres with strong meridional heat transport to predominantly zonal flow, thereby causing thermal isolation of Antarctica (Barker and Thomas, 2004). The hypothesis is supported by foraminiferal isotopic evidence from deep sea drill cores in the Southern Ocean, which indicate a shift from warm to cold currents (Exon et al., 2004). As such, there has been considerable effort to reconstruct the tectonic history of the Southern Ocean gateways.

The Drake Passage opening has been dated to around 50 Ma (Livermore et al., 2007) or even earlier (Markwick, 2007); however it was likely shallow and narrow at this time. The timing of the transition to a wide and deep gateway, potentially capable of sustaining a vigorous ACC, occurred on a timescale of tens of millions of years. Even with substantial widening of Drake Passage, several intervening ridges in the region are likely to have blocked the deep circumpolar flow (Eagles et al., 2005). These barriers may have not have cleared until the Miocene at around 22 Ma (Barker and Thomas, 2004; Dalziel et al., 2013). The evolution of the Tasman Gateway is better constrained. Geophysical reconstructions of continent-ocean boundaries (Williams et al., 2011) place the opening of a deep (greater than ~500 m) Tasmanian Gateway at 33.5 ± 1.5 Ma (Scher et al., 2015; Stickley et al., 2004). Marine microfossil records suggest the circumpolar flow was initially westward (Bijl et al., 2013). Multiproxy based evidence from ODP Leg 189 suggests that the opening of the Tasmanian Gateway significantly preceded Antarctic glaciation and might therefore not been its primary cause (Huber et al., 2004; Stickley et al., 2004; Wei, 2004). The results also indicate that the gateway deepening at the EOT initially produced an eastward flow of warm surface waters into the southwestern Pacific, and not of cold surface waters as previously assumed. Subsequently, the Tasmanian Gateway steadily opened during the Oligocene, hypothesised to cross a threshold when the northern margin of the ACC aligned with the westerly winds (Scher et al., 2015), triggering the onset of an eastward flowing ACC at around 30 Ma. However, the westerly winds can also shift position due to changes in orographic barriers or an increase in the meridional temperature gradient after glaciation. Thus, the opening of Southern Ocean gateways approximately coincides with the EOT, but with large uncertainty on the timing and implications. We discuss modelling of this mechanism in Section 6.1.

2.3 Meridional overturning circulation

Throughout much of the Eocene, deep water formation is suggested to have occurred dominantly in the Southern Ocean and the North Pacific (Ferreira et al., 2018), based on numerical modelling and supported by stable and radiogenic isotope work

(Cramer et al., 2009; McKinley et al., 2019; Thomas et al., 2014). A shift in the north-south gradient of δ^{13}C and decrease in South Atlantic ε_{Nd} around the EOT suggests that North Atlantic convection may have begun or strengthened at this time (Katz et al., 2011; Via and Thomas, 2006), although other studies suggest that some kind of North Atlantic overturning operated from the middle Eocene (Boyle et al., 2017; Hohbein et al., 2012; Vahlenkamp et al., 2018a, 2018b). Significant seafloor
305 spreading was occurring in the Southern Hemisphere, such that these changes in ocean circulation have previously been explained by the opening of Southern Ocean gateways (Borrelli et al., 2014). Moreover, interactions between the Arctic and Atlantic oceans are gaining interest as potential triggers of a late Eocene proto Atlantic meridional overturning circulation (AMOC; Hutchinson et al., 2019). Data from the Labrador Sea and western North Atlantic margin indicate that North Atlantic waters became saltier and denser from 37 to 33 Ma (Coxall et al., 2018). This densification may then have strengthened or
310 even triggered an AMOC, suggesting a possible forcing mechanism for Antarctic cooling that predates the EOT and Southern Ocean gateway openings.

Proxy records suggest that the Arctic Ocean was much fresher during the Eocene than the present day, with typical surface salinities around 20-25 psu and periodic excursions to very low salinity conditions (<10 psu) (Brinkhuis et al., 2006; Kim et
315 al., 2014; Waddell and Moore, 2008). Outflow of this fresh surface water into the North Atlantic can potentially prohibit deep water formation (Baatsen et al., 2020; Hutchinson et al., 2018). A new line of evidence suggests that deepening of the Greenland-Scotland Ridge (GSR) around the EOT may have enabled North Atlantic surface waters to become saltier (Abelson and Erez, 2017; Stärz et al., 2017), by allowing a deeper exchange between the basins. A related hypothesis derived from sea level and paleo-shoreline estimates in the Nordic Seas is that the Arctic likely became isolated during the Oligocene (Hegewald
320 and Jokat, 2013; O'Regan et al., 2011). Thus a gradual constriction of the connection between the Arctic and Atlantic presents a newly hypothesised priming mechanism for establishment of a well-developed AMOC (Coxall et al., 2018; Hutchinson et al., 2019).

2.4 Antarctic glaciation

Although transient glacial events on Antarctica are proposed for the late Eocene, the most significant long term glaciations
325 likely began on eastern Antarctica on the Gamburtsev Mountains and other highlands (Young et al., 2011) as a result of rapid global cooling in the early Oligocene around 33.7 Ma (EOGM, Fig. 1). Evidence for glacial discharge into open ocean basins in the earliest Oligocene is long established, with ice-rafted debris (IRD) appearing in deep-sea Southern Ocean sediment cores (Zachos et al., 1992). Since these initial results, efforts have continued to document and understand early Cenozoic Antarctic ice dynamics (Barker et al., 2007; Francis et al., 2008; McKay et al., 2016). Combining perspectives from marine geology,
330 geophysics, geochemical proxies and modelling, these efforts have largely focused on the evolution and stability of the early Oligocene Antarctic ice sheets, and estimates of ice volume contributions to sea-level change. Other important developments in the study of Antarctic ice include modelled thresholds for Antarctic glaciation (DeConto et al., 2008; Gasson et al., 2014), and improved reconstructions of Eocene-Oligocene subglacial bedrock topography (from airborne radar surveys). These

bedrock reconstructions are important for reconstructing the nucleation centres of precursor ice sheets (Scher et al. 2011, 2014)
335   and subsequent development of continental-sized ice sheets (Bo et al., 2009; Thomson et al., 2013; Wilson et al., 2013; Wilson
and Luyendyk, 2009; Young et al., 2011).

Evidence for glaciation in the Weddell Sea and Ross Sea suggest that there was an increase in physical weathering over West
Antarctica around the EOT (Anderson et al., 2011; Ehrmann and Mackensen, 1992; Huang et al., 2014; Olivetti et al., 2015;
340   Scher et al., 2011; Sorlien et al., 2007). However, in the Ross Sea, evidence suggests that an expansion over West Antarctica
in Marie Byrd Land occurred after the EOT (Olivetti et al., 2013), while in the Weddell Sea sedimentation rates were still
lower than recent times, suggesting the West Antarctic ice sheet was not expanded to modern proportions (Huang et al., 2014).
This is consistent with approximations of ice volume based upon oxygen isotopes (Bohaty et al., 2012; Lear et al., 2008) and
is supported by the record of relatively diverse vegetation around at least coastal regions of Antarctica through the Oligocene
345   (Francis et al., 2008).

Recent evidence has emerged of transient 'precursor' Antarctic glaciations occurred in the late Eocene (Carter et al., 2017;
Escutia et al., 2011; Passchier et al., 2017; Scher et al., 2014), suggesting a 'flickering' transition out of the greenhouse.
Importantly, several Southern Ocean sites revealed evidence that Antarctic glaciation induced crustal deformation and
350   gravitational perturbations resulting in local sea level rise close to the young Antarctic ice sheet (Stocchi et al., 2013). Finally,
detailed core sedimentary records drilled close to Antarctica in the western Ross Sea invoke a transition from a modestly sized
highly dynamic late Eocene-early Oligocene ice sheet, existing from ~34 - 32.8 Ma, to a more stable, continental-scale ice
sheet thereafter, which calved at the coastline (Galeotti et al., 2016).

2.5 Northern hemisphere glaciation

355   While there is clear evidence for Antarctic glaciations at the EOT, the question of contemporaneous northern hemisphere
glaciation remains equivocal. The prevailing view is that the Oligocene represented a non-modern-like state with only
Antarctica glaciated (Zachos et al., 2001). Glaciation in mountain areas around the globe is suggested to have followed through
the Miocene and Pliocene, with evidence for the first significant build-up of ice on Greenland (in the southern highlands)
traced to the late Miocene, sometime between 7.5 - 6 Ma (Bierman et al., 2016; Larsen et al., 1994; Maslin et al., 1998; Pérez
360   et al., 2018) or as early as 11 Ma (Helland and Holmes, 1997). Northern Hemisphere glaciation intensified during the late
Pliocene (~2.7 Ma) when large terrestrial glaciers began rhythmically advancing and retreating across North America,
Greenland, and Eurasia (Bailey et al., 2013; DeConto et al., 2008; Ehlers and Gibbard, 2007; Lunt et al., 2008; Maslin et al.,
1998; Raymo, 1994; De Schepper et al., 2014; Shackleton et al., 1984). It is important to note that delayed northern hemisphere
glaciation is predicted from models—the stabilizing effect of the hysteresis in the height-mass balance feedback becomes
365   weaker with greater distance from the poles (Pollard and DeConto, 2005).

However, a series of studies argue that bipolar glaciation happened earlier than the late Miocene. Evidence for this theory is based on global seawater $\delta^{18}O$ budgets (Tripati et al., 2005) and identification of ice-transported sediment grains inferred to have originated from Greenland in both interior Arctic Ocean and subarctic Atlantic sediment cores associated with the EOT
370 (Eldrett et al., 2007), or earlier (middle Eocene) (St. John, 2008; Tripati and Darby, 2018; Tripati et al., 2008). Certainly, several lines of evidence provide support for winter sea ice in the Arctic from the middle Eocene (Darby, 2014; St. John, 2008; Stickley et al., 2009) and perennial sea ice from 13 Ma (Krylov et al., 2008). It is possible that small mountain glaciers on East Greenland, perhaps comparable to the modern Franz Josef and Fox Glaciers of New Zealand (which extend from the Southern Alps through lush rain forest), reached sea level during cooler orbital phases of the Eocene, intensifying in the late Eocene and
375 early Oligocene (Eldrett et al., 2007). Yet, a recent detailed analysis of expanded EOT sections from the North Atlantic's modern day iceberg alley on the Newfoundland margin found no evidence to support the suggestion of extensive early northern hemisphere glaciation (Spray et al., 2019). Furthermore, it is unlikely that ice growth on land in the Northern Hemisphere was sufficiently extensive to impact global seawater $\delta^{18}O$ budgets sea level at the EOT (Coxall et al., 2005; Lear et al., 2008; Mudelsee et al., 2014). Marine SSTs and floral records from the subarctic and Arctic imply sustained warm temperatures and
380 extensive lowland temperate vegetation well into the middle Miocene (O'Regan et al. 2011), which is hard to reconcile with large continental ice sheets fringing Greenland and other Arctic landmasses then or before this time.

From a theoretical perspective, climate and ice sheet modelling suggest that the CO_2 threshold for Northern Hemisphere ice-sheet inception is fundamentally lower than for Antarctica (DeConto et al., 2008; Gasson et al., 2014), implying that the climate
385 must be cooler to glaciate Greenland than Antarctica. This is also consistent with evidence that the modern Greenland ice sheet is highly sensitive to climatic warming and that Greenland may have been almost ice-free for extended periods even in the Pleistocene (Schaefer et al., 2016). This asymmetry between the northern and southern hemispheres in susceptibility to glaciation has been attributed to (i) the lower latitudes of the continents encircling the Arctic Ocean relative to the Antarctic, together with different ocean and atmospheric circulation patterns (Gasson et al., 2012) and (ii) the ice sheet carrying capacity
390 of the continents; it has been argued that Greenland topography was low during the Paleogene compared to Antarctica and extensive mountain building, providing high-altitude terrain needed for glaciation, did not occur until the late Miocene-Pliocene (Gasson et al., 2012; Solgaard et al., 2013).

But even in the question of Greenland topography there is uncertainty. Reconstructions of plate kinematics in suspected ice
395 sheet nucleation sites (e.g., northern Greenland, Ellesmere Island) are equivocal. It has been argued that Greenland topography was low during the Paleogene compared to Antarctica and extensive mountain building, providing high-altitude terrain needed for glaciation, did not occur until the late Miocene-Pliocene (Gasson et al., 2012; Japsen et al., 2006; Solgaard et al., 2013). However, sophisticated new approaches to the plate kinematic history of the Eurekan orogeny, taking into account crustal shortening (Gurnis et al., 2018), now indicate a period of significant compression in northern Greenland and Ellesmere from
400 55-35 Ma (Gion et al., 2017) that was probably associated with uplift (Piepjohn et al., 2016). The new kinematic insights are

compatible with the onset of a rapid phase of exhumation—based on apatite fission track and helium data—of the East Greenland margin around 30 +/- 5 Ma (Bernard et al., 2016; Japsen et al., 2015). Together, these approaches support a view of high mountains on Greenland/Ellesmere that began eroding in the late Eocene to early Oligocene with a greater possibility of supporting glaciers.

405 **3 Marine observations**

3.1 Sea surface temperature observations

A key requirement for understanding the cause and consequences of the Eocene-Oligocene climatic transition is good spatial and temporal constraints on global temperatures and our most numerous and well-resolved records of this undoubtedly come from the oceans. Quantitative reconstruction of sea surface and deep ocean temperatures has been ongoing for decades. This
410 requires use of various geochemical proxies, both to provide independent support for absolute temperature estimates and because different proxy options are available for different ocean/sedimentary settings, and deep sea versus surface ocean water masses. Each method has its own limitations and uncertainties resulting in a currently patchy but steadily improving view of global change. Quantitative assemblage-based SST proxies akin to transfer functions are not available because there are no living plankton relatives during the EOT. For a thorough review of pre-Quaternary marine SST proxies, and their strengths
415 and weaknesses, see Hollis et al., (2019).

While more heterogeneous than the deep sea, reconstruction of SST in the EOT is in some ways currently more achievable than bottom water temperatures because more proxies are available, although there are still multiple confounding factors to consider. Classical marine $\delta^{18}O$ paleothermometry extracted from the calcium carbonate shells of fossil planktonic (surface
420 floating) foraminifera is especially complicated because of the combining influences of (i) compromised fossil preservation under the shallow late Eocene ocean calcite compensation depth, limiting the availability of planktonic records, (ii) increasing $\delta^{18}O$ of sea water as a consequence of ice sheet expansion, which enriches ocean water and thus increases calcite $\delta^{18}O$; a signal which can otherwise indicate cooling. However, a growing number of clay-rich hemipelagic marine sequences containing exceptionally well-preserved (glassy) fossil material are yielding $\delta^{18}O$ paleotemperatures that provide useful SST perspectives.
425 $\delta^{18}O$ SSTs derived from glassy foraminifera contrast greatly from those measured on recrystalized 'frosty' material (Pearson et al., 2001; Sexton et al., 2006). A detailed compilation of glassy versus recrystalized foraminiferal $\delta^{18}O$ proxies around the EOT is given in Piga (2020).

Planktonic foraminifera Mg/Ca paleothermometry provides another means of quantifying SSTs (Evans et al., 2016; Lear et
430 al., 2008), however such records are even more sparse than $\delta^{18}O$ equivalents due to the scarcity of appropriate EOT fossils. This method is especially useful since, in theory, unlike $\delta^{18}O$ it should be independent of Antarctic glaciation and, when

coupled with $\delta^{18}O$ paleothermometry, past variations in the $\delta^{18}O$ composition of seawater, and thus ice volume changes may also be estimated (Lear et al., 2004, 2008; Mudelsee et al., 2014). The two key existing records are from Tanzania (Lear et al., 2008) and the Gulf of Mexico (Evans et al., 2016; Wade et al., 2012). The Tanzanian planktonic Mg/Ca record provides

435 cornerstone evidence for a permanent 2.5 °C tropical surface and bottom water, ocean cooling, and therefore likely global cooling, associated with the Step 1 of the EOT (Figure 1). The Gulf of Mexico Mg/Ca temperature record resembles the biomarker-derived (i.e. TEX_{86}, see below) SST record from this site (Wade et al., 2012). Both imply a distinct and slightly larger surface cooling of 3-4°C limited to Step 1. To what extent secular change in seawater Mg/Ca reconstruction might have influenced these actual numbers is an ongoing question (Evans et al., 2018). Clumped isotope paleothermometry (Ghosh et

440 al., 2006; Zaarur et al., 2013), also independent of seawater $\delta^{18}O$, is still in its infancy, but this is a third method applicable to calcitic microfossils that will help address some of these problems. Thus far only one clumped isotope (Δ_{47}) record from Maud Rise spans the EOT (Petersen and Schrag, 2015). This record shows cooling preceding the EOT, and then relatively minor changes across the EOT. Early to middle Eocene clumped isotope SST records are consistent with other proxies, specifically cooler values at high southern latitudes compared to the early and middle Eocene (Evans et al., 2018). Many new SST records

445 base on Mg/Ca and Δ_{47} are expected in coming years.

In some regions, Eocene-Oligocene age sediments lack biogenic calcium carbonates (e.g. Bijl et al., 2009). Therefore low- and non-calcareous areas, like the Arctic and high-latitudes of the North Atlantic and North Pacific, have suffered for lack of data. However, the development of independent organic proxies based on biomarkers such as alkenones ($U^{K'}_{37}$ index; Brassell et al.

450 1986) and glycerol dialkyl glycerol tetraethers (GDGTs) from the membrane lipids of Thaumarchaeota (TEX_{86} index; Schouten et al. 2002), which can be preserved in high sedimentation settings close to continental margins or restricted basins where carbonate is often scarce, have helped fill this gap. Importantly, these organic biomarkers are often the only marine archive for paleothermometry at high latitudes, where SST constraints are particularly useful for model-data comparisons.

455 While the $U^{K'}_{37}$ index is well established, the TEX_{86} index is relatively new and its accuracy as a paleotemperature proxy is under critical review. There have been several different TEX_{86} indices developed, with different SST calibrations (e.g. TEX'_{86} by Sluijs et al. 2009; TEX_{86}^{H} and TEX_{86}^{L} by Kim et al. 2010; Bayspar by Tierney and Tingley 2015). As suggested by some of the recent studies conducted on cultures of Thaumarchaeota, GDGT composition may be sensitive not only to SST but also other factors such as oxygen (O_2) concentration (Qin et al., 2015) or ammonia oxidation rate (Hurley et al., 2016). Furthermore,

460 there is uncertainty in the source of the GDGTs used for SST estimations, i.e. the production level in the water column and possible summer biases, and therefore their value as an SST proxy. Recent reviews are available for both the paleotemperatures $U^{K'}_{37}$ (Brassell, 2014) and for TEX_{86} (Hurley et al., 2016; Pearson and Ingalls, 2013; Qin et al., 2015; Tierney and Tingley, 2015). Despite these issues, in some studies where both $U^{K'}_{37}$ and TEX_{86} indices were applied, temperature estimations show remarkably similar results (Liu et al., 2009) suggesting that TEX_{86}, after an evaluation of the source and the distribution of

465   GDGTs (Inglis et al., 2015), can successfully be applied as a paleotemperature proxy. TEX_{86} is especially useful at lower latitudes, since the $U^{K'}_{37}$ index saturates at about 28°C (Müller et al., 1998).

Cross-latitude biomarker proxy records ($U^{K'}_{37}$ and TEX_{86}) suggest that SSTs were higher than today in both the late Eocene and early Oligocene SSTs with annual means of up to 20 °C at both 60 °N and 60 °S respectively and low meridional

470   temperature gradients (Hollis et al., 2009; Liu et al., 2009; Wade et al., 2012). One record from the Gulf of Mexico (Wade et al., 2012) consistently suggests higher sea surface temperatures derived from TEX_{86} than from inorganic proxies (Hollis et al., 2009, 2012; Liu et al., 2009). Where records span the EOT (i.e. ~33-34 Ma), between 1 to 5 °C of surface cooling in both hemispheres is found. To date, temperature records from the high northern latitudes are sparse but coverage from the high southern latitudes is richer where several records suggest a cooling of subantarctic waters across the EOT of 4 to 8°C, although

475   some records are indistinguishable from 0°C change (Figure 3). In the low latitude Pacific, Atlantic and Indian Ocean tropical SSTs were significantly warmer than today in the late Eocene, with SSTs up to 31°C (Liu et al., 2009) or even ~33°C (Lear et al., 2008; Wade et al., 2012). One TEX_{86} record from the Gulf of Mexico implies gradual surface cooling of 3-4 °C between ~34 and 33 Ma (Wade et al., 2012). TEX_{86} data from elsewhere in the tropical Atlantic shows a large transient cooling of up to 6°C across the EOT (Liu et al., 2009), although some equatorial records show minimal change (Figure 3). Newly available

480   records from the North Atlantic region are starting to challenge earlier evidence of homogeneous bipolar cooling (Liu et al., 2018; Śliwińska et al., 2019). Furthermore, comparison of a uniquely well-resolved record from the Newfoundland margin, western North Atlantic (Liu et al., 2018), with data from the subantarctic South Atlantic, confirms this in new detail, leading the authors to the conclusion that surface ocean cooling during the EOT was strongly asymmetric between hemispheres. Liu et al. (2018) interpret this finding as evidence for 'transient thermal decoupling of the North Atlantic Ocean from the southern

485   high latitudes', as a result of changes in ocean circulation-driven heat transport associated with Antarctic glaciation. A summary of SST records across the EOT is shown in Figure 3.
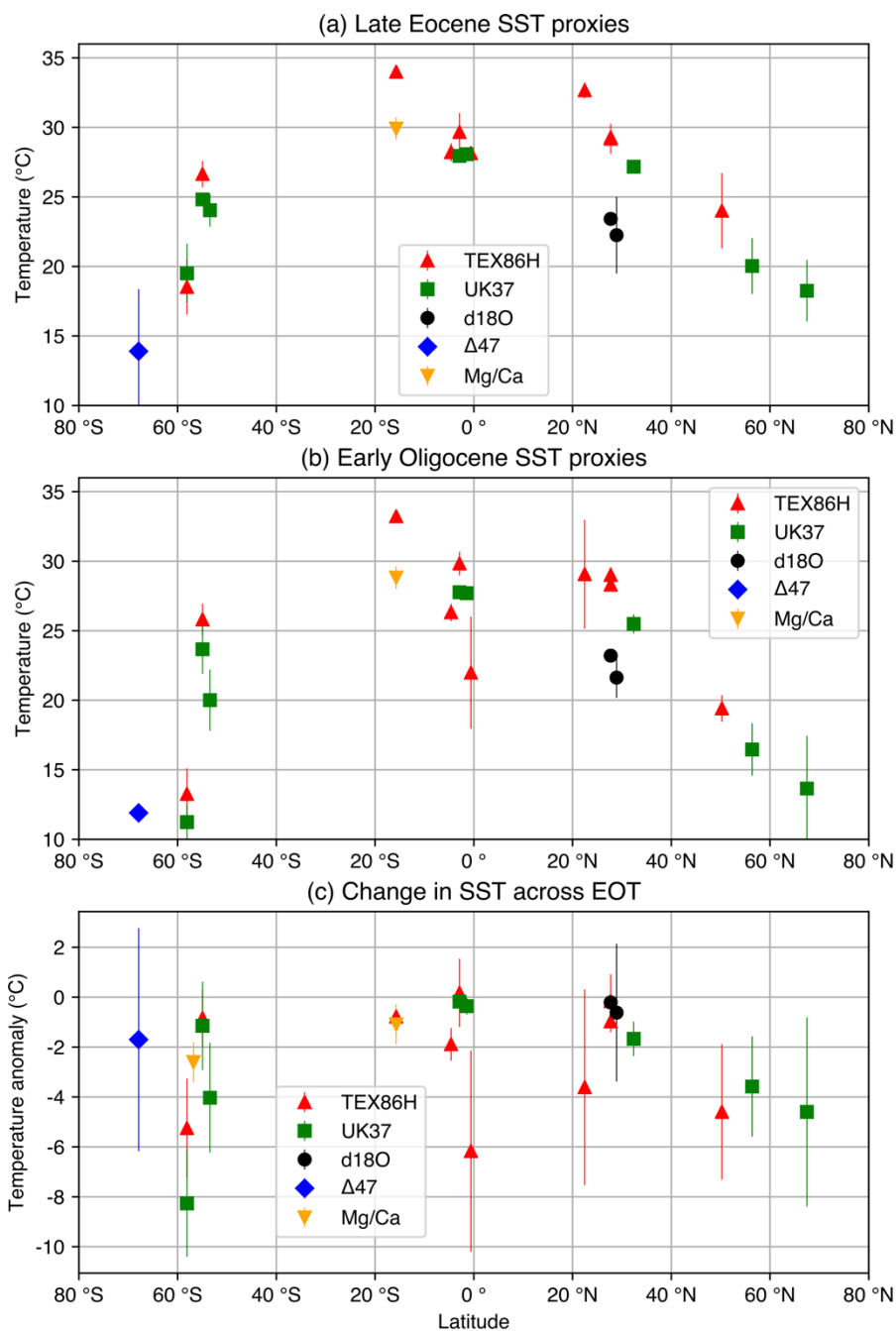
Figure 3: Summary of sea surface temperature (SST) change across the EOT from proxies, TEX$_{86}$^{H}, UK^{37}, δ^{18}O, Δ_{47}, and Mg/Ca. (a) Late Eocene, (b) early Oligocene and (c) change in SST across the EOT. Data shown in (a) and (b) are only from locations that record a temperature signal on both sides of the EOT. Data compiled from (Bohaty et al., 2012; Cramwinckel et al., 2018; Inglis et al., 2015; Kobashi et al., 2004; Lear et al., 2008; Liu et al., 2009, 2018; Pearson et al., 2007; Petersen and Schrag, 2015; Piga, 2020; Śliwińska et al., 2019; Wade et al., 2012; Zhang et al., 2013). The late Eocene value was calculated as an average between 38 and 34.2 Ma (pre-EOT), while the early Oligocene value was calculated as the average between 33.7 and 30 Ma (post-EOT), and the change across the EOT is the difference between these values. The data compilation is provided in digital form in Supplementary Table S1.

495

3.2 Deep sea temperature changes

As described in Section 1.2, the Eocene-Oligocene climate transition is defined by high-resolution benthic foraminiferal oxygen isotope (δ^{18}O) records from deep sea sites (Coxall et al., 2005; Zachos et al., 1996). These records describe a benthic

500 δ^{18}O increase of about 1.5‰, a combination of deep sea cooling and terrestrial ice growth. While surface ocean temperature changes have been constrained using organic and inorganic proxies (Section 3.1), there are fewer proxies for the deep sea temperature and, thus, the picture of deep ocean cooling remains uncertain. This is because, on its own, it is impossible to deconvolve the temperature and ice volume components of δ^{18}O records, and hence quantify the timing, magnitude and spatial distribution of deep ocean temperature change through the climate transition. Indeed, an early interpretation of the Cenozoic

505 benthic oxygen isotope record suggested that the δ^{18}O increase at the EOT represented a pure cooling signal (Shackleton and Kennett, 1975), whereas numerous lines of evidence have since shown that a substantial component of the δ^{18}O shift reflects the glaciation of Antarctica (e.g. Zachos et al. 1996). Independent paleotemperature proxies provide a potential means to deconvolve the two contributors to δ^{18}O records, and benthic foraminiferal Mg/Ca paleothermometry has been applied to several marine EOT sections (Billups and Schrag, 2003; Bohaty et al., 2012; Katz et al., 2008; Lear et al., 2000, 2004, 2008,

510 2010; Peck et al., 2010; Pusz et al., 2011; Wade et al., 2012). Yet, calculating absolute bottom water temperatures from benthic foraminiferal Mg/Ca ratios requires an estimate of the Mg/Ca ratio of seawater, while the Mg-partitioning into foraminiferal calcite shows modest sensitivity to temperature at low temperatures and is subject to the competing influence of seawater carbonate chemistry (Evans et al., 2018; Lear et al., 2015). Relative temperature trends over short time intervals are generally considered more robust than absolute temperatures, although the residence time of calcium in seawater (~ 1 Myr; Broecker

515 and Peng 1982) compared with the duration of the entire climate transition (~500 kyr) does add some uncertainty to calculated relative temperature changes across the EOT. High resolution reconstructions of seawater Mg/Ca are therefore required to improve both absolute and relative temperature changes using Mg/Ca paleothermometry.

Furthermore, although the benthic foraminiferal Mg/Ca paleothermometer appears to capture the long-term cooling trend since

520 the early Eocene Climatic Optimum, the concomitant ~1km deepening of the CCD hinders its use across the EOT (Coxall et al., 2005; Lear et al., 2004). Specifically, the increase in bottom water calcite saturation state across the EOT acts to increase benthic foraminiferal Mg/Ca, and mask the deep sea cooling signal (Coxall et al., 2005; Lear et al., 2004). Attempts have been made to use Li/Ca to correct this ΔCO_3^{2-} effect from Mg/Ca records (Lear et al., 2010; Peck et al., 2010; Pusz et al., 2011), but this approach brings with it additional uncertainties including the species-specific sensitivities to both temperature and ΔCO_3^{2-}

525 . An alternative, and perhaps more robust approach at present, is to combine planktonic δ^{18}O records with salinity-independent sea surface paleotemperature records to calculate the change in the surface water δ^{18}O (δ^{18}O$_{sw}$). If it can be assumed, in some

regions, that the surface $\delta^{18}O_{sw}$ signal is dominated by ice volume signal (as opposed to a local change in the salinity) then these records can be used in conjunction with the benthic $\delta^{18}O$ records to estimate changes in bottom water temperature across the climate transition (Kennedy et al., 2015). The overall change in surface $\delta^{18}O_{sw}$ across the EOT has been estimated using
530 planktonic $\delta^{18}O$ and Mg/Ca at many sites, including a section in Tanzania containing exceptionally well-preserved (glassy) foraminifera (Lear et al., 2008). The similarity between this $\Delta\delta^{18}O_{sw}$ estimate from the Indian Ocean (~0.6‰; Lear et al. 2008) and those from other sites, e.g., the Southern Ocean (Bohaty et al., 2012) and the southeast Atlantic (Peck et al., 2010) suggests that the surface $\delta^{18}O_{sw}$ change is dominated by a global (ice volume) signal. The associated estimated volume of Antarctic ice depends upon the assumed isotopic composition of the ice sheet, but was likely between 70 and 110% of the size of the
535 modern day Antarctic ice sheet (Bohaty et al., 2012; Lear et al., 2008), representing a sea level difference to modern of approximately minus 18 metres to plus 6 metres. Spatial heterogeneities in the deep ocean temperature history may therefore be inferred by calculating inter-site offsets in benthic foraminiferal $\delta^{18}O$ records (Abelson and Erez, 2017; Bohaty et al., 2012; Cramer et al., 2009).

540 There is a growing consensus based on southern hemisphere and low latitude records that the step 1 of the EOT was associated with a cooling of both surface and deep waters on the order of 2 °C, associated with a relatively minor increase in global ice volume (Bohaty et al., 2012; Lear et al., 2004, 2008, 2010; Peck et al., 2010; Pusz et al., 2011). We note that the combination of this magnitude of cooling and an overall increase in $\delta^{18}O_{sw}$ of ~0.6‰ is enough to account for the average ~1.0‰ shift in benthic foraminiferal $\delta^{18}O$ observed in deep sea records (Mudelsee et al., 2014). However, this overall shift across the entire
545 climate transition ignores the apparent $\delta^{18}O$ "overshoot" (Zachos et al., 1996) observed in some high resolution records, at the base of the EOGM (Coxall and Pearson, 2007). Determining whether the "overshoot" reflects deep sea cooling, a transient further increase in global ice volume, or a combination of the two has implications for our understanding of Antarctic ice sheet dynamics and indeed the cause of the EOT itself. Unfortunately, it is Step 2 (EOIS) of the transition, into the EOGM where the CCD reaches its maximum depth and benthic foraminiferal Mg/Ca records appear most compromised by the ΔCO_3^{2-} effect
550 (Lear et al., 2004, 2010), even at depths above the implied depth of CCD deepening (Peck et al., 2010), so we currently have no robust and direct evidence of deep ocean cooling across this step. Future work may go some way to address these problems using clumped isotopes or by generating high resolution B/Ca records across the transition, and by using deep infaunal benthic species (e.g. Elderfield et al. 2012). However, by combining benthic and planktonic records, it appears that the EOGM in the deep Pacific Ocean reflects, at least in part, a transient cooling of deep waters associated with the major expansion of the
555 Antarctic ice sheet (Kennedy et al., 2015).

An additional complication is that the Mg/Ca composition of seawater may itself have shifted during the EOT, as suggested by incoming constraints from other proxies, including paired Mg/Ca and clumped isotope temperature constraints in shallow living larger benthic foraminifera (Evans et al., 2018). Further investigation into this possibility is required, which could

560 ultimately help identify Mg/Ca adjustment factors needed to improve the ability to extract paleotemperature estimates for this
geological time interval.

4 The terrestrial realm at the EOT

There are several proxy indicators of past terrestrial climate change. These include geochemical indices, leaf margin analysis,
Climate Leaf Analysis Multivariate Program (CLAMP) (Yang et al., 2011), and pollen assemblages (see review in Hollis et
565 al. 2019). Here we focus on pollen assemblages as a broad indicator of terrestrial change across the EOT, because an EOT
synthesis of these data already exists (Pound and Salzmann, 2017). This dataset, a global paleo-biome reconstruction of pollen
and spore assemblages, indicates that the terrestrial realm of the late Eocene and early Oligocene has a vegetation distribution
that in general indicates a warmer and wetter world than today. The response of the terrestrial realm to the EOT is more
heterogeneous than the marine realm, with no evidence for a global scale uniform response (Pound and Salzmann, 2017).
570 Terrestrial biomes record not only global climate change but also regional changes due to local factors. These include
orographic uplift, which reduces local temperature and changes regional precipitation patterns. Further changes in precipitation
are induced by the retreat of a number of inland seaways due to sea-level changes and tectonics (Chamberlain et al., 2012;
Dupont-Nivet et al., 2008; Kocsis et al., 2014; Sheldon et al., 2016). These complicating factors mean that changes in
vegetation must be interpreted within the context of local paleoenvironmental changes. Thus, we present the terrestrial records
575 on a continent-by-continent basis below. For a summary of strengths and limitations of deriving quantitative climate estimates
from the pre-Quaternary plant record, see Hollis et al. (2019).

4.1 North America

In North America, the paleobiome distribution of the EOT ranges from tropical mangroves, swamps and forests in the south
of the continent to cool-temperate forests at the high latitudes (Breedlovestrout et al., 2013; Pound and Salzmann, 2017;
580 Wolfe, 1985, 1994). Gradual cooling and drying from the middle Eocene until the late Oligocene allowed the mixed coniferous
and deciduous broadleaf forests to become more dominant (Wing, 1987). Fossil leaves found in Washington State
(Breedlovestrout et al., 2013) indicate no clear temperature trend from the middle Eocene to the EOT. Instead variations are
attributed to differing paleoaltitude, combined with a gradual long-term cooling. Pollen records from Texas indicate a long
term cooling and aridification from the middle Eocene to the early Oligocene (Yancey et al., 2003), whereas pollen records
585 from 5° longitude further east show no turnover at the EOT boundary (Oboh-Ikuenobe and Jaramillo, 2003). Pollen from the
far north Yukon Territory show a transition from warmer adapted angiosperm forests in the Late Eocene to cooler adapted
gymnosperm forests during the Early Oligocene (Ridgway and Sweet, 1995).

In Oregon, well dated floras and marine invertebrates show no evidence for a rapid change at the EOT (Retallack et al., 2004),
590 but rather a gradual cooling during the early to middle Oligocene. By contrast, paleosols indicate a 2.8±2.1°C drop across the

EOT in the same region (Gallagher and Sheldon, 2013). Isotopic data from horse teeth indicate a 8±3.1°C drop in MAT across the EOT, but with a 400 kyr lag behind the marine realm (Zanazzi et al., 2007), though part of this shift is due to changes in the hydrological cycle (Chamberlain et al., 2012; Hren et al., 2013). Conversely a study on White River mammals interprets no significant change in MAT, but an aridification of the local environment (Boardman and Secord, 2013). This conclusion is

595 in line with paleosol studies, which suggest a change in vegetation structure from a forest to a more open environment (Retallack, 1983).

Oxygen isotope analyses in the western North American Cordillera suggest the changing hydrological regime of North America (Chamberlain et al., 2012) was influenced by factors other than large-scale climate. Rising orography, starting in

600 British Colombia at ~50 Ma and moving south to Nevada by ~23 Ma shifted the North American Monsoon further south during this time. This not only impacts terrestrial oxygen isotopes, but also the regional vegetation – creating an aridification not linked to global climatic events (Chamberlain et al., 2012). No response to the EOT is evident from North American mammals (Figueirido et al., 2012; Prothero, 2012, 2004), while fossil Equidae analyses from North America indicate that horses had a browsing diet before, at and after the EOT (Mihlbachler et al., 2011).

605

4.2 South America

Late Eocene and early Oligocene paleo-biome distributions of South America indicate tropical evergreen rainforest in the north and cool-temperate biomes in the south (Pound and Salzmann, 2017). In South America there was a greater change in vegetation from the middle Eocene into the late Eocene, rather than at the EOT (Barreda and Palazzesi, 2007). Patagonian

610 pollen floras from the middle Eocene to the end of the early Oligocene are termed the "Mixed Paleoflora". These show a long-term cooling trend rather than a step change at the EOT (Quattrocchio et al., 2013). Phytolith and oxygen isotope records from Patagonia show no change in vegetation across the EOT (Kohn et al., 2004, 2015; Strömberg et al., 2013). Faunal turnovers in South America began at approximately 42 – 39 Ma (Woodburne et al., 2014). This relates to the end of the MECO, but also correlates with the appearance of rodents from Africa. The mammal turnover associated with the EOT is no more dramatic

615 than those during the late Eocene or late Oligocene (Woodburne et al., 2014). The Amazonian region had a diverse, primarily frugivorous fauna during the EOT, suggesting productive stable forest (Negri et al., 2009).

4.3 Africa

Vegetation in Africa shows little change in structure from the Late Eocene into the Early Oligocene, but there is a documented drop in palm diversity (Jacobs et al., 2010; Pan et al., 2006; Pound and Salzmann, 2017). There are significant gaps in the

620 paleobotanical record for Africa over this time interval, with most information coming from the region between 10° north and south of the Equator (Jacobs et al., 2010; Pound and Salzmann, 2017). One exception is the Fayum Depression in Egypt which

contains macrofossil and microfossil evidence for tropical vegetation in the late Eocene (Tiffney and Wing, 1991; Wing et al., 1995).

4.4 Eurasia

625   In Eurasia there was a progressive change from para-tropical evergreen forests in the middle Eocene to warm-temperate evergreen and deciduous mixed forests by the early Oligocene (Collinson and Hooker, 2003; Teodoridis and Kvaček, 2015). The paleo-biome reconstructions show a dominance of subtropical and warm-temperate mixed forests throughout Eurasia with seasonal biomes in the Iberian Peninsula and arid biomes in central Asia (Pound and Salzmann, 2017). A change from a diverse mixed broad-leaved to a cooler conifer- dominated pollen flora in North Atlantic cores through the Eocene indicates increasing

630   seasonality in Europe (Eldrett et al., 2009). However, leaf floras from Bulgaria show no significant change in vegetation at the EOT (Bozukov et al., 2009). There is a greater change in Iberian pollen floras from the early to late Oligocene than at the EOT (Postigo Mijarra et al., 2009). Between the late Eocene and early Oligocene no change in mean annual temperature or precipitation is reconstructed in the Ebro Basin in Spain, but there is a decrease in chemical weathering across the EOT (Sheldon et al., 2012).

635

In Germany and Czechia, macrofloras show a stepwise disappearance of subtropical species and immigration of evergreen and deciduous warm-temperate species during the late Eocene (Kunzmann et al., 2016). The first mixed evergreen/deciduous forest in azonal biomes is recorded prior to the EOT from Roudniky (Kvaček et al., 2014) referring to a latest Eocene cooling event (Teodoridis and Kvaček, 2015). However, evergreen broadleaved forests were still present in the early Oligocene (Kovar-

640   Eder, 2016; Teodoridis and Kvaček, 2015) indicating the low impact of global EOT changes in terrestrial central Europe. Most of the subtropical to warm-temperate genera survived in that region until the Miocene Climatic Optimum (Mai, 1995). Based on proxies from macrofloras, MAT was almost stable at the EOT (Teodoridis and Kvaček, 2015) with ongoing prevailing seasonality in precipitation but which is not monsoonal (Moraweck et al., 2019).

645   Recent investigations on late Eocene and earliest Oligocene macrofloras in SE Tibet and Yunnan revealed multiple evidence for the modernization of the vegetation by establishment of present-day genera and families (Linnemann et al., 2017; Su et al., 2018). However, regional vegetation change across EOT from subtropical to temperate and partly cool temperate in SW China is masked by the uplift of the Tibetan Plateau (Su et al., 2018). Paleoaltimetric studies show that the already elevated proto-Tibetan highland (Lhasa Terrain) achieved its modern elevation during EOT by uplift of (only) about 1km (Spicer, 2017; Su

650   et al., 2018). An Eocene appearance of a modern subtropical / tropical aspect of vegetation is also recorded from Chinese low latitude floras (Hainan; Guangdong) indicating an Eocene establishment of monsoonal climate (Jin et al., 2017) which seems to have had a much higher impact on the evolution of regional vegetation than the EOT or any later climatic event (Dupont-Nivet et al., 2008).

Freshwater gastropods from southern Britain show that growing season temperatures (Spring – Summer) may have dropped from around 34°C to about 20°C across the Eocene – Oligocene boundary (Hren et al., 2013). This has been translated into a MAT drop of 4 - 6°C (Hren et al., 2013), which is comparable to the UK'37 estimated SST change from the high latitude North Atlantic ODP Site 913, but not the smaller SST change at the more comparable latitude ODP Site 336 (Liu et al., 2009). Summer temperatures for the Hampshire Basin fell by around 4°C during the EOT (Grimes et al., 2005), but did not drop again during the EOIS (see section 1.2). Paleosols of the Hampshire Basin show minimal changes in temperature but an increase in precipitation (Sheldon and Tabor, 2009).

4.5 Australia and New Zealand

In Australia, the EOT is associated with the loss of rarer taxa in pollen records rather than significant turnovers (Macphail, 2007). There is a diversity drop from the middle to late Eocene into the latest Eocene – early Oligocene (Martin, 2006). The distribution of paleo-biomes in Australia shows no change between the late Eocene and the early Oligocene (Pound and Salzmann, 2017), though data coverage is sparse apart from in the south of the continent. Terrestrial paleoclimate reconstructions of temperature do show a cooling at around 36 Ma (Pound and Salzmann, 2017). The New Zealand records show a warm humid forest with a gradual turnover of palynomorphs through the late Eocene and the early Oligocene (Homes et al., 2015; Pocknall, 1991).

4.6 Antarctica

On Antarctica it is known that from the equable climates of the middle Eocene there was a progressive drop in plant diversity and stature, from evergreen forests to low-lying vegetation (Francis et al., 2008; Pound and Salzmann, 2017). Changing $\delta^{13}C$ measurements from late Eocene leaves and pollen have been interpreted as decreasing moisture availability on the Antarctic Peninsula (Griener et al., 2013). Vegetation at Wilkes Land, East Antarctic, changed from an early Eocene subtropical to a cool temperate forest, indicating a 5°C decline in mean annual temperature (Pross et al., 2012). A further change towards a less diverse, cool-temperate shrubland and forest indicates further cooling at Wilkes Land at the onset of the Oligocene (Strother et al., 2017). Other evidence supporting decreasing moisture availability is demonstrated by a shift from chemical weathering in a humid environment, to physical weathering associated with a colder more arid regime (Basak and Martin, 2013; Dingle et al., 1998; Ehrmann and Mackensen, 1992; Robert and Kennett, 1997; Wellner et al., 2011). This aridification of the Antarctic continent is attributable to a partly glaciated continent in the late Eocene. A new bedrock topography for Antarctica allows for an early Oligocene ice sheet of greater areal extent than today (Wilson et al., 2012), raising the possibility that the temperature component of the EOT $\delta^{18}O$ increase was more modest than previously suggested (Wilson et al., 2013).
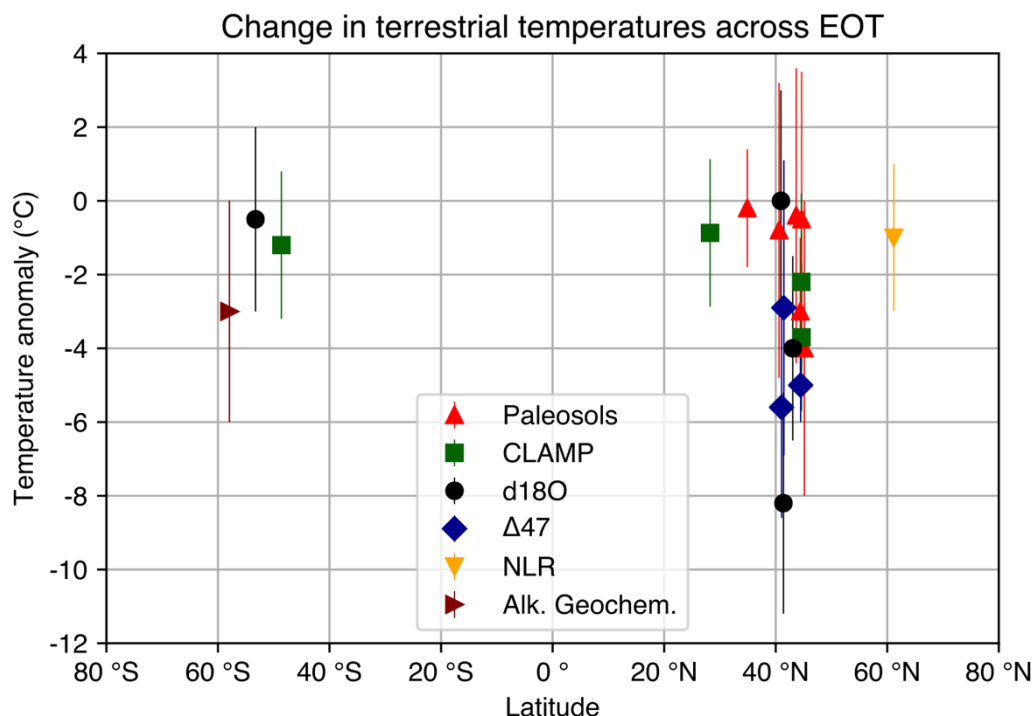
Figure 4: Summary of terrestrial air temperature change across the EOT from proxies Paleosols, CLAMP, $\delta^{18}O$, Δ_{47}, Nearest Living Relative (NLR) and alkaline geochemistry. Data is compiled from (Boardman and Secord, 2013; Eldrett et al., 2009; Fan et al., 2017; Gallagher and Sheldon, 2013; Héran et al., 2010; Herman et al., 2017; Hinojosa and Villagrán, 2005; Hren et al., 2013; Kohn et al., 2004; Kvaček et al., 2014; Lielke et al., 2012; Meyers, 2003; Page et al., 2019; Passchier et al., 2013; Roth-Nebelsick et al., 2017; Sheldon and Tabor, 2009; Zanazzi et al., 2007). Where possible, we apply the same method as in Figure 3, i.e. the 'late Eocene' is taken the average temperature from 38 to 34.2 Ma and the 'early Oligocene' is taken as the average from 33.7 to 30 Ma, and the temperature change shown here is the difference. However, in a number of cases, only a relative temperature change across the EOT was given in the original literature. We therefore limit our compilation to temperature anomaly only. The compilation shown above is provided in digital form in Supplementary Table S2.

5 CO₂ and carbon cycle dynamics

The concentration of carbon dioxide in the atmosphere (pCO₂) is a primary driver of global climate change on geological timescales (Berner and Kothavala, 2001; Foster et al., 2017; Royer et al., 2004), and changes in pCO₂ have been linked to the phase of acute climate change at the EOT (DeConto and Pollard, 2003; Heureux and Rickaby, 2015; Pearson et al., 2009; Steinthorsdottir et al., 2016). However atmospheric pCO₂ reconstructions for the EOT are sparse, variable and, in some cases, contradictory and not readily reconciled with paleo-temperature proxy records or numerical model hindcasts (Beerling and Royer, 2011; Heureux and Rickaby, 2015; Pagani et al., 2005; Pearson et al., 2009; Royer et al., 2004; Zhang et al., 2013). New well-resolved pCO₂ records with strong age control are pressingly needed. Four proxies have been identified as particularly useful for Cenozoic pCO₂ reconstructions by the Intergovernmental Panel on Climate Change (IPCC, 2013). These are the marine carbon and boron isotope proxies, and the terrestrial paleosol carbon and stomatal density proxies (Beerling and Royer, 2011). Below, we discuss the development and state of the art of existing EOT pCO₂ records constructed using marine and terrestrial proxies.

5.1 Marine pCO$_2$ proxies

705

To date, the most detailed pre-Pleistocene climate records are derived from marine geochemical proxies, including boron isotopes (δ^{11}B) in planktonic foraminiferal calcite (Anagnostou et al., 2016; Foster et al., 2012; Greenop et al., 2017; Pearson et al., 2009; Pearson and Palmer, 1999, 2000) and carbon isotopes (δ^{13}C) in marine organic biomarkers (Heureux and Rickaby, 2015; Liu et al., 2009; Pagani et al., 2005, 2011; Zhang et al., 2013). Each proxy has its own limitations and uncertainties, which initially led to divergent estimates of pCO$_2$ using these different proxies. However, recent efforts to address such uncertainties and limitations have led to a more coherent picture of the evolution of pCO$_2$ through the Cenozoic from marine proxies.

710

While the theoretical basis of the boron isotope proxy is well understood, a major uncertainty in reconstructing surface ocean pH is estimating the boron isotopic composition of seawater (Greenop et al., 2017). A further major uncertainty comes into play when a second carbonate system parameter (e.g. total alkalinity) is required to calculate pCO$_2$ from seawater pH, as well as the major ion composition of seawater, which impacts key dissociation constants. Nevertheless, significant progress has been made to reduce these uncertainties (Anagnostou et al., 2016; Greenop et al., 2017; Sosdian et al., 2018). For the Eocene pCO$_2$ estimates, seawater δ^{11}B has been estimated using the δ^{11}B-pH relationship, while self-consistent estimates of the second carbonate parameter have been determined using Earth System modelling (Anagnostou et al., 2016). For the alkenone δ^{13}C proxy, there are many factors that can impact algal growth conditions and inaccurate temperature reconstructions have also been known to bias pCO$_2$ reconstructions (Pagani et al., 2011; Zhang et al., 2013). Algal carbon-concentrating mechanisms may also lead to biased pCO$_2$ reconstructions when using the alkenone δ^{13}C proxy in low-CO$_2$ intervals of the Neogene, but is unlikely to be a significant issue at the EOT (Zhang et al., 2013).

715

720

725

The boron isotope proxy suggests atmospheric pCO$_2$ was 1400±470 ppm in the early Eocene, and decreased by several hundred ppm through the Eocene over several million years (Anagnostou et al., 2016). In the late Eocene (Bartonian-Priabonian), pCO$_2$ reconstructions are variable, but the boron isotope and alkenone proxy both indicate pCO$_2$ concentrations around 1000 ppm (Anagnostou et al., 2016; Zhang et al., 2013). The EOT itself appears to be associated with a further, and perhaps steeper, decline in pCO$_2$, with both proxies supporting the passing of a modelled glaciation threshold of ~750 ppm (DeConto and Pollard, 2003; Pagani et al., 2011; Pearson et al., 2009; Zhang et al., 2013), although this modelled threshold itself is highly uncertain (Gasson et al., 2014). A δ^{11}B-based record from Tanzania sediments also suggests an intriguing transient pCO$_2$ increase associated with the second δ^{18}O step (Pearson et al., 2009).

730

5.2 Terrestrial proxies

735

The stomatal CO$_2$ proxy is based on the empirically and experimentally demonstrated inverse relationship between the density of stomata on the leaf surfaces of most land plants and pCO$_2$ (Beerling, 1998; Franks et al., 2014; Hincke et al., 2016; Konrad

et al., 2008; Kürschner et al., 2008; McElwain and Chaloner, 1995; Royer et al., 2001; Steinthorsdottir et al., 2016, 2019, 2011, 2013; Steinthorsdottir and Vajda, 2015; Wagner et al., 1996; Woodward, 1987). Previous studies using the stomatal proxy method of pCO_2 reconstructions for the time intervals either side of the EOT (here Bartonian-Rupelian) are still relatively few,

740 derived from mostly low-resolution datasets consisting of a variety of fossil plant taxa, and marred by limitations in chronological accuracy and correlation to marine records. Consequently, the pCO_2 records have so far been highly heterogeneous.

Early results based on datasets of the gymnosperms *Ginkgo biloba* and *Metasequoia glyptostroboides* from the USA suggested

745 that pCO_2 was more or less stable between 300 and 450 ppm during the Eocene and Oligocene (Royer et al., 2001) - however, the fossil leaf record was of too low resolution to draw strong conclusions. Another early study, based on data gathered mainly from published images of fossil *Ginkgo* specimens from Russia and USA, suggested a decrease in pCO_2 across the EOT (Retallack, 2001), from ~1300 ppm in the Bartonian, to ~420 ppm at the EOT, and ~330 ppm in the Rupelian. A further stomatal dataset from Germany, based on fossil leaves from the angiosperm Fagacaeae species *Eotrigonobalanus furcinervis*

750 and *Laurophyllum acutimontanum,* again of low temporal resolution, suggested that pCO_2 was higher before than after the EOT (Roth-Nebelsick et al., 2004). A more recent study from a temporally restricted sedimentary succession in Canada suggested high but decreasing pCO_2 at the Bartonian/Priabonian boundary (from ~1000–700 ppm to ~450 ppm), based on a dataset of *Metasequoia* fossil needles (Doria et al., 2011), but does not include the EOT or the Rupelian. In contrast, a study based on various angiosperm species using a leaf gas exchange model suggested more modest as well as stable pCO_2 of ~470

755 ppm during the Bartonian and Priabonian, decreasing to ~400 ppm after the EOT in the Rupelian (Grein et al., 2013). A subsequent study from the same region compiled all data in broad temporal bins and reconstructed early Oligocene to early Miocene pCO_2 to ~400 ppm throughout, despite significant changes in stomatal densities (Roth-Nebelsick et al., 2012, 2014). Two studies with restricted temporal ranges reconstructed pCO_2 in the Bartonian, indicating 400-500 ppm using *Metasequoia* from Canada (Maxbauer et al., 2014) and ~390 ppm using the podocarp conifer *Nageia maomigensis* from China (Liu et al.,

760 2016).

Recently, a new relatively high-resolution dataset consisting of *Eotrigonobalanus furcinervis* from Germany was published, including data points thought to be temporally located immediately before and after the EOT (Steinthorsdottir et al., 2016). The results show pCO_2 of ~650 ppm in the Bartonian, decreasing to ~550–400 ppm in the Priabonian, and ~410 ppm at the

765 EOT and the earliest Rupelian (Steinthorsdottir et al., 2016). This higher-resolution record shows a distinct ~40% Bartonian-Priabonian decrease in pCO_2, highly comparable to the marine isotope temperature records, but reaching stable levels by the EOT, and not recording a significant pCO_2 decrease at the EOT proper, unlike in the marine temperature records (Steinthorsdottir et al., 2016; Zachos et al., 2001, 2008). This discrepancy between pCO_2 and temperatures suggests that there are factors other than greenhouse forcing that contribute to the threshold climate response of glaciation. New results based on

770 Lauraceae leaf fragments from the Southern Hemisphere (Australia and New Zealand) further confirm Late Eocene pCO_2

mostly in the order of 550–450 ppm, but are not sufficiently chronologically well-constrained to confirm falling pCO_2 prior to the EOT (Steinthorsdottir et al., 2019).

Other results show a significant decrease in stomatal density values (indicating increasing pCO_2) of extinct *Platanus neptuni*
775 before the EOT (Moraweck et al., 2019). This unexpected trend, contradictory to the stomata density-pCO_2 relation previously recorded, is not yet understood but is consistent with the suggestion that pCO_2 change prior to the EOT caused plant responses. Further, pCO_2 reconstructed using a mechanistic gas exchange model of Konrad et al. (2008) applied to two fossil species from northern central Europe, *Rhodomyrtophyllum reticulosum* and *Platanus neptuni*, records no significant decrease across the EOT (Moraweck et al., 2019), in agreement with Steinthorsdottir et al. (2016), but not recording decreasing pCO_2 before
780 the EOT. It should be noted that the gas-exchange model of Konrad et al. (2008) has recently been tested with modern material and was shown to produce the most accurate pCO_2 estimates when used with multiple species, to derive a consensus pCO_2 (Grein et al., 2013).

When focusing on datasets from central Europe, terrestrial plant based pCO_2 records support the plant-derived temperature
785 records by indicating no abrupt decrease or environmental change across the EOT (Kunzmann et al., 2016; Teodoridis and Kvaček, 2015). A detectable but not fundamental change in vegetation, temperatures and pCO_2 is however evident from the interval prior to the EOT (Kunzmann et al., 2016; Kvaček et al., 2014; Steinthorsdottir et al., 2016; Teodoridis and Kvaček, 2015). Preliminary results of MAT estimations based on sedimentary GDGT values from some central German sites are in accordance with temperature estimates from plant fossils, i.e. based on CLAMP and the Nearest Living Relative (NLR)
790 approach. In combination these data refer to a successive decrease in MAT across the Priabonian and the EOT but not to a significant drop during the EOT.

5.3 Synthesis of EOT pCO_2 change

The most recent marine records indicate pCO_2 of ~1000 ppm in the Bartonian-Priabonian, decreasing to ~700–800 ppm into the Rupelian. Stomatal proxy-based pCO_2 records generally indicate elevated Bartonian-Priabonian pCO_2 of ~500–1000 ppm,
795 decreasing ~40% before the EOT to pCO_2 of ~400 ppm, and continuing in the Rupelian with pCO_2 of ~400 ppm or lower. The direction and approximate magnitude of pCO_2 change leading up to the EOT is therefore consistent between proxies, even though the stomatal records consistently yield lower pCO_2 levels than the marine proxies. We consider the higher pCO_2 estimates based on marine proxies to be most robust indicator of pCO_2 at this time, since they have been shown to reproduce ice-core CO_2 well (Foster and Rae, 2016), and to agree better with the available modelling evidence from warm climate
800 simulations of the Eocene, and estimated thresholds for glaciation of Antarctica (section 6.2). Some terrestrial records also indicate a decrease in CO_2 but the decrease is more gradual and long term than in the marine records.
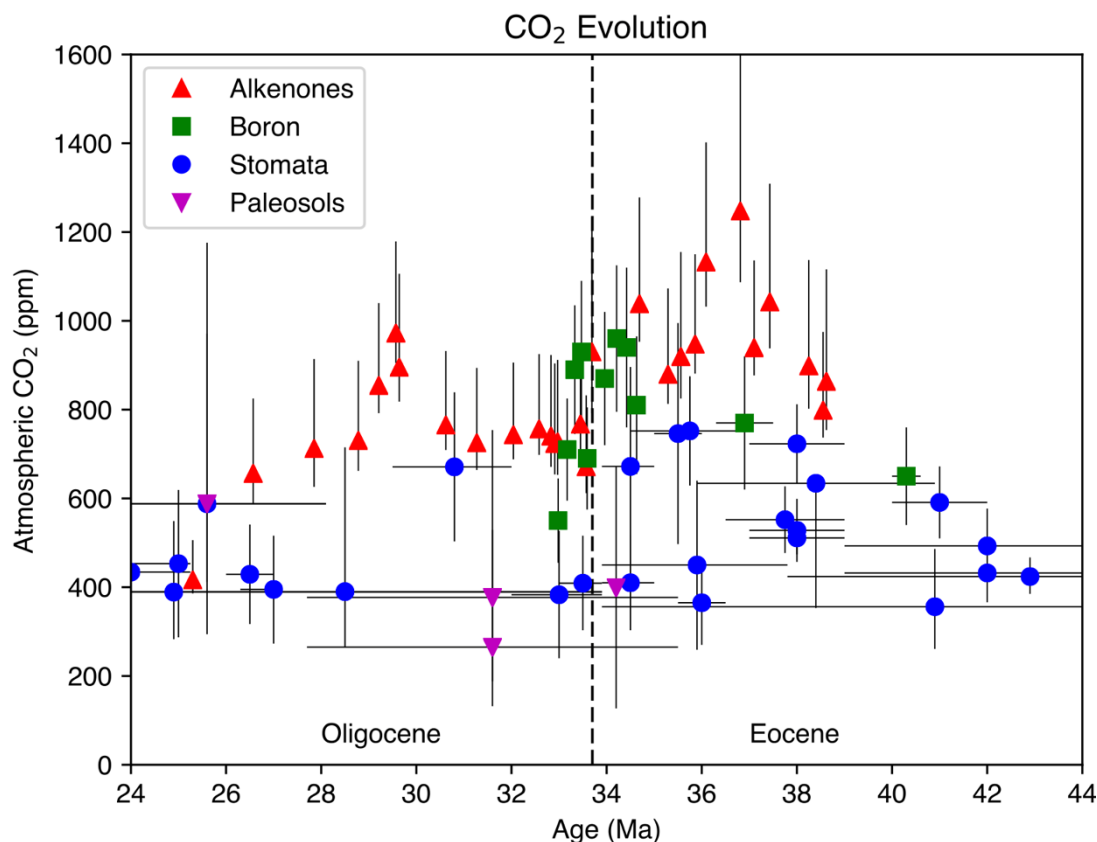
Figure 5: Atmospheric CO_2 evolution from 44 to 24 Ma from the compilation of Foster et al., (2017), incorporating data from its original data sources (Anagnostou et al., 2016; Doria et al., 2011; Erdei et al., 2012; Franks et al., 2014; Pearson et al., 2009; Roth-Nebelsick et al., 2012, 2014; Steinthorsdottir et al., 2016; Zhang et al., 2013), and Steinthorsdottir et al., (2019).

6 Insights into the EOT from modelling studies

In this section we qualitatively synthesise previous modelling studies that have focussed on the EOT. In particular, we discuss the modelled response to changing paleogeography (Section 6.1) and to changes in CO_2 (Section 6.2). Finally, we describe carbon-cycle models that have explored mechanisms behind CO_2 changes at the EOT (Section 6.3).

6.1 Modelling the response to changing paleogeography at the EOT

The widening of the Southern Ocean Drake Passage and Tasman gateways has long been considered as a primary driver for the initiation of the AMOC and Antarctic glaciation at the EOT (Section 2.2). Many climate modelling studies have tested the effect of opening these Southern Ocean gateways and found cooling effects on the southern high latitudes (Cristini et al., 2012; Elsworth et al., 2017; England et al., 2017; Mikolajewicz et al., 1993; Sijp et al., 2009, 2014; Sijp and England, 2004; Toggweiler and Bjornsson, 2000; Viebahn et al., 2016; Yang et al., 2014). These studies have variously found that opening Southern Ocean gateways can decrease southward heat transport (e.g. Sijp et al., 2009), trigger the onset of an AMOC (e.g.

Yang et al. 2014), and enable some degree of cooling over Antarctica. However, these approaches do not reconcile the timing and evolution of the gateway evolution of the EOT, since they employed either modern-day or idealised geography with specific gateway perturbations. In contrast, climate model simulations that do employ Eocene boundary conditions indicate
820 that Southern Ocean gateway opening caused only a modest change in ocean poleward heat transport and could therefore not be directly responsible for the initiation of the AIS (Goldner et al., 2014; Huber et al., 2004; Huber and Nof, 2006; Huber and Sloan, 2001; Sijp et al., 2011; Zhang et al., 2011). Furthermore, opening the Southern gateways under Eocene-like CO_2 forcing may result in a weaker ACC than under pre-industrial conditions (Lefebvre et al., 2012). The long-term evolution of Southern Ocean gateway opening has been found to cause ~3°C of bottom water cooling (Sijp et al., 2014), which may explain some of
825 the observed benthic cooling (Section 3.2). However, Drake Passage opening probably affected deep ocean temperatures and the strength of the ACC. Hill et al. (2013) showed that despite deep water connections through both Drake Passage and the Tasman Gateway, a coherent ACC could not develop until the Australian continent was sufficiently equatorward such that it no longer inhibited strong zonal flow in the Southern Ocean.

830 Imposing an ice sheet in a climate model has been shown to have a significant impact on the ocean circulation and deep water formation regions (Goldner et al., 2014; Kennedy et al., 2015). In particular, the presence of an ice sheet may enhance westerly winds over the Southern Ocean, leading to enhanced Southern Ocean deep ocean formation and benthic cooling (Goldner et al., 2014). This theory suggests that Southern Ocean gateway changes play a secondary role to radiative forcing, since the ocean circulation change are a consequence of the glaciation, rather than a cause. Other ocean gateways may also play an
835 important role. In the late Eocene continental configuration, the Central American Seaway and the Tethys gateway, connecting the Indian and Atlantic oceans, were wider than today. The importance of the open Tethys gateway for the EOT circulation has not received much attention but Zhang et al. (2011) found that the tropical seaways need to be sufficiently constricted before the southern high latitudes can cool substantially. This cooling is related to a transition from an ocean circulation with southern hemisphere deep water formation to the modern-like circulation with deep water formation in the North Atlantic.

840

Recently, focus has shifted to the role of Arctic-Atlantic gateways around the EOT. The evolution of the Arctic-Atlantic gateways has been shown to have a strong influence on the salinity of the North Atlantic and therefore on the AMOC (Hutchinson et al., 2019; Roberts et al., 2009; Stärz et al., 2017; Vahlenkamp et al., 2018b). The deepening of the Greenland-Scotland ridge at the EOT has been proposed as a trigger for the AMOC (Abelson and Erez, 2017; Stärz et al., 2017). According
845 to this hypothesis, the deepening changes the flow across the ridge from a shallow unidirectional flow to a deeper bi-directional flow which allows salty subtropical water to penetrate further north and enable North Atlantic sinking. Hutchinson et al. (2019) recently proposed that it is the tectonic closing of the shallow Barents Sea gateway, just prior to the EOT, that initiated the AMOC, by closing off the pathway of extremely fresh Arctic water to the North Atlantic. Neither Southern Ocean gateways changes, Greenland-Scotland Ridge changes, or CO_2 forcing changes could similarly overcome the freshening effect of the
850 Arctic to allow an AMOC. However, their study did not test the feedback of these circulation changes on the carbon cycle,

making it unclear what the climatic impact of the Arctic closure would have been. Using an Earth System Model, (Vahlenkamp et al., 2018a, 2018b) experimented with similar changes in the North Atlantic gateways to investigate an alternative idea of significant AMOC behaviour since the early–middle Eocene. They were able to initiate an AMOC when the Greenland Scotland Ridge reached a threshold depth of deeper than 200 m but, only when the Arctic Ocean brackish water outlets were

855   shut off from the North Atlantic. Timing of changes in Arctic-Atlantic 'plumbing', thus, appear to be a critical factor in allowing an AMOC to start up in the Warm Paleogene, and a key area for future research.

In all these studies, it is assumed that the final state of the simulation is the only steady solution for that climate and boundary conditions. While there is no consensus yet (Nof et al., 2007), the present day climate is thought to have two global circulation

860   modes; the observed AMOC with sinking in the north, and a southern-sinking only mode with no AMOC (Liu et al., 2017; Srokosz and Bryden, 2015). In continental geometries other than the present day different circulation patterns and co-existing equilibria may be possible but have not been systematically searched for so far (Baatsen et al., 2018). In coupled Eocene simulations, centers of deepwater formation include the North and South Pacific (Hutchinson et al., 2018; Thomas et al., 2014) and the North and South Atlantic (Huber et al., 2003; Huber and Sloan, 2001). Conceptual climate models have suggested a

865   potential role for meridional overturning circulation transitions in the EOT (Tigchelaar et al., 2011).

6.2 Modelling the response to CO_2 decrease at the EOT

A reduction in atmospheric CO_2 is hypothesised to be a primary cause of the EOT, because it can plausibly explain both long term cooling during the Eocene, and provide a trigger for the glaciation of Antarctica (DeConto and Pollard, 2003). Although proxy reconstructions of atmospheric CO_2 during the Eocene have large uncertainties (Section 5), there is general agreement

870   that climate cooled and CO_2 declined through the Eocene (Anagnostou et al., 2016; Foster et al., 2017), making long-term CO_2 drawdown from the atmosphere a prime underlying forcing mechanism for the EOT. Furthermore, CO_2-forced climate-ice sheet model experiments yield $\delta^{18}O$ series (DeConto and Pollard, 2003) that closely match the overall form of our best-resolved EOT data sets (Coxall et al., 2005; Coxall and Wilson, 2011).

875   A long-standing problem in modelling the Eocene climate is to reproduce the low meridional temperature gradient recorded in observations. Proxies suggest that high latitude SSTs were more than 20°C warmer than present day during the early Eocene (Bijl et al., 2009), terrestrial anomalies were 20-40°C (Huber and Caballero, 2011), while tropical temperatures were some 5-10°C warmer than modern (Huber, 2008; Huber and Sloan, 2000). Evidence of frost intolerant flora and fauna in high latitudes (Greenwood and Wing, 1995) provides a challenge to explain how the climate maintained such a low meridional temperature

880   gradient.

When climate models are forced using proxy data-based estimates of Eocene CO_2, they generally fail to capture these flatter meridional temperature gradients (Huber et al., 2003; Roberts et al., 2009; Shellito et al., 2003). One method that has been

used to address this high-latitude cold bias is to increase the CO_2 to extremely high values (2240 or 4480 ppm) (Cramwinckel
885 et al., 2018; Eldrett et al., 2009; Huber and Caballero, 2011; Winguth et al., 2010). These extremely high CO_2 experiments
yield an improved match to high-latitude temperature proxies and temperature gradients (Huber and Caballero, 2011; Lunt et
al., 2012). Because these extremely high CO_2 concentrations are greater than those implied by proxies, this finding also
suggests that modelled climate sensitivity to CO_2 forcing may be too low, probably because of positive feedbacks that are
either missing or too weak in the models. Several missing feedbacks suggested recently are those associated with cloud physics
890 and/or greenhouse gases in addition to CO_2 (Beerling et al., 2011; Kiehl and Shields, 2013; Sagoo et al., 2013; Zhu et al.,
2019). We also note that recent proxy data from the warmest regions of the tropics (Tanzania, Java) indicate tropical
temperatures of up to 35°C in the middle-late Eocene (Evans et al., 2018; Pearson et al., 2007). These temperatures imply a
somewhat larger meridional gradient than previously suggested, helping to reduce the magnitude (but not eliminate) the model-
data mismatch. In addition, several models have now achieved lower meridional temperature gradients through a combination
895 of higher resolution, which tends to increase poleward heat transport, and improved Eocene boundary conditions (Baatsen et
al., 2020; Hutchinson et al., 2019; Zhu et al., 2019).

Despite the challenges faced in modelling the early Eocene, the observed cooling during the Eocene of bottom waters (Zachos
et al., 2001) and high latitude SSTs (Bijl et al., 2009) and terrestrial temperatures can plausibly be explained by a reduction in
900 CO_2 in climate model simulations (Eldrett et al., 2009; Liu et al., 2009). Furthermore, crossing a CO_2 threshold of Antarctic
glaciation may also explain several degrees of bottom water cooling, through consequent shifts in Southern Ocean winds and
changes to Southern Ocean circulation (Goldner et al., 2014). A key challenge to adequately testing the CO_2 forcing hypothesis
is to derive a threshold level of CO_2 for glaciation from climate model reconstructions. The first study to do so found a
glaciation threshold of around 780 ppm (DeConto and Pollard, 2003), in approximate agreement with CO_2 proxies. However,
905 a recent inter-comparison of Eocene climate models used to force an ice sheet model found that this threshold varied
significantly between models, from roughly 560 to 920 ppm (Gasson et al., 2014). Differences in the lapse-rate feedback were
identified as the leading cause of this spread, although there were also differences in the paleogeographic boundary conditions.

All ice-sheet modelling studies of the EOT to date have used prescribed climate states to force the glaciation. Likewise, coupled
910 ocean-atmosphere-sea ice models currently prescribe ice sheets as either present or absent. Running a full-complexity climate
model synchronously with an ice sheet model remains a major technical challenge, and has yet to be implemented for the
Eocene or Oligocene. However, innovative asynchronous coupling, such as the "matrix-method" (Pollard, 2010), has shown
some promise by allowing a better representation of the ice albedo feedback, leading to a similar yet slightly revised upward
glaciation threshold of ~900 ppm (Ladant et al., 2014b).
915

6.3 Carbon Cycle Modelling

Slow decline in atmospheric CO_2 remains a likely priming mechanism for the inception of large ice sheets on Antarctica and this pivotal transition in Cenozoic climate was associated during the EOT with pronounced rapid perturbation to the global carbon cycle as indicated by a transient increase in ocean $\delta^{13}C$ and a permanent deepening of the calcite compensation depth

920 (CCD) (Coxall et al., 2005). Thus, numerical carbon cycle model experiments provide useful insight to forcing mechanisms and feedback processes involved.

Many hypotheses have been posited to explain the carbon cycle perturbations at the EOT (Armstrong McKay et al., 2016; Coxall and Wilson, 2011; Merico et al., 2008). Some of the leading hypotheses include a shift from shelf to basin carbonate

925 fractionation (Opdyke and Wilkinson, 1988), increases in organic carbon burial (Olivarez Lyle and Lyle, 2006), feedbacks between ice sheet coverage and silicate weathering (Zachos and Kump, 2005), and an ecological shift from calcareous to siliceous plankton (Falkowski et al., 2004). Carbon cycle box model experiment results suggest that the best fit to observations is achieved by glacio-eustatic sea level-led shelf-to-basin fractionation in global carbonate burial and a spike in riverine carbonate weathering together with carbon sequestration in C12-enriched carbon capacitors such as terrestrial peatlands or

930 marine methane clathrate (Armstrong McKay et al., 2016; Merico et al., 2008).

Palike et al. (2012) investigated causes of carbon cycle changes over the Eocene using the intermediate complexity climate model cGENIE. They suggest several mechanisms are needed to explain the CCD change in addition to the shelf-basin fractionation hypothesis; (i) perturbations to continental weathering and solute input to the deep ocean, or (ii) changes in the

935 partition of organic carbon flux between labile and refractory components.

The longer-term decline in CO_2 over the Eocene needs to be reconciled with the negative feedback between silicate weathering and surface temperature (Walker et al., 1981). Higher CO_2 causes warming and enhances the hydrological cycle, which leads to an increase in silicate weathering. The increase in weathering eventually lowers CO_2 and subsequent cooling, creating a

940 dynamic equilibrium. This silicate weathering feedback is regulated by tectonic processes (Raymo and Ruddiman, 1992), since mountain ranges give rise to greater weathering than low-lying regions (Maher and Chamberlain, 2014).

A climate model study suggests that opening and deepening of the Drake Passage could lower atmospheric CO_2 via the silicate weathering feedback (Elsworth et al., 2017). They suggested that the gateway transition enhanced the AMOC, leading to

945 greater precipitation over land regions and a warmer northern hemisphere, both of which enhance silicate weathering and thus drawdown of CO_2 (Maher and Chamberlain, 2014). However, this study used modern geography with selected gateway perturbations, whereas climate models using paleogeography from the late Eocene have yielded different patterns of overturning (Baatsen et al., 2020; Hutchinson et al., 2019). Furthermore, a hypothesised change in silicate weathering must be

weighed against the CCD record, because silicate weathering changes have implications for carbonate weathering and
950 bicarbonate ion supply to the ocean (Armstrong McKay et al., 2016; Merico et al., 2008). Fyke et al. (2015) found opening
Drake Passage led to a decrease in Atlantic carbon storage and an increase in Pacific and Southern Ocean storage, due to the
enhancement of a modern-like AMOC. This led to an overall increase in global carbon storage in the ocean, though their
implied drop in atmospheric CO_2 is relatively small (10-30 ppm). Incorporating carbon cycle processes into full complexity
climate models with Eocene or Oligocene paleogeography thus remains an outstanding challenge (e.g. Goddéris et al., 2014).
955

Experiments using a model of intermediate complexity, cGENIE, report an increase in carbon re-mineralisation near the ocean
surface when temperatures are very warm, such as in the early Eocene (John et al., 2013, 2014). The more temperature
dependent re-mineralisation results in a shallower CCD, and a decrease in organic carbon burial, an effect which then decreased
over the Eocene as temperatures decreased. This modelled mechanism is consistent with tropical records of $\delta^{13}C$ during the
960 Eocene (John et al., 2013, 2014), providing a positive feedback on carbon dioxide changes, in opposition to the silicate
weathering feedback.

7 Model-data intercomparison of temperature change across the EOT

Until this point, this review paper has synthesised the existing literature but has not presented any new quantitative analysis.
Furthermore, we have in general presented the proxy and model-derived insights separately. Here, we combine the information
965 from proxies and models and present a new model-data comparison and quantitative analysis of the mechanisms behind
temperature change at the EOT. This section is in two parts: (7.1) a quantitative intercomparison of temperature change across
the EOT from a subset of these previous studies, in which we identify those changes that are robust across models; and (7.2)
a comparison of the modelled temperature changes with proxy SST and SAT data, in which we assess which models best fit
the proxy reconstructions, and which mechanisms most likely explain the observed proxy temperature changes.

7.1 Intercomparison of modelled SAT change across the EOT
970

Here we present an intercomparison of some previous model results of surface air temperature (SAT) change across the EOT.
We use SAT data because it provides a consistent surface temperature over both ocean and land regions that reflects changes
across the globe. It also enables comparison with proxies of both marine and terrestrial data to be readily included. We include
those models and studies for which the authors have provided their model results in digital form. The models and simulations
975 included in this intercomparison are shown in Table 7.1. This itself is a subset of the simulations that were available – here we
show only those simulations that allow us to compare the response of the models to a consistent forcing, for as many models
as possible.

We first consider pairs of simulations that represent the response of the climate system to a perturbation in forcing that may
980 have occurred across the EOT. These pairs can broadly be divided into three categories corresponding to three forcings: a CO_2 decrease, an increase in the volume and extent of the Antarctic ice sheet, and a paleogeographic change. Although these forcing factors are in reality interdependent (for example the ice sheet change may itself be caused by a CO_2 change), for the purposes of modelling they are treated as independent mechanisms.

985 For the CO_2 forcing, we consider a halving of atmospheric CO_2, which for most models is from 1120 to 560 ppmv. However, for GFDL this is from 800 to 400 ppmv, and for NORESM there are CO_2 simulations at 980 and 560 ppmv. For the NORESM case, we scale the anomaly by a factor of $\log(2)/\log(980/560)$ in order to approximate the radiative forcing of halving CO_2. For the ice sheet forcing, we consider a change from an ice-free Antarctic, to an ice sheet similar in volume and area to that of today. However, the configuration of these ice sheets, and the ice-free state, does vary from model to model (see
990 Supplementary Figure S1). The paleogeographic forcing is less consistent across the models, and includes modelled changes to gateways only (CESM and UVic), to west Antarctic geography (FOAM), or to global paleogeography (HadCM3BL) (see Supplementary Figure S3).

Before examining the SAT response of the system to these three forcings, it is useful to explore the absolute temperatures in
995 the model simulations. The annual global mean SAT in each simulation is shown in Figure 6, while the spatial patterns for each individual model are shown in Supplementary Figures S1-S3. In terms of global mean surface temperature, the models fall approximately into two groups: (i) a cooler group, consisting of CESM_H, FOAM, HadCM3BL, NorESM-L, have global mean surface temperatures of around 17-19 °C at 560 ppm, and 21 to 23 °C at 1120 ppm; and (ii) a warmer group consisting of CESM_B, CESM_H (x2) and GFDL CM2.1, where temperatures are roughly 4 °C warmer for the equivalent level of CO_2
1000 (Figure 6). A common factor in this split is that the warmer models have higher horizontal resolution (~1° ocean for CESM_B and GFDL CM2.1; ~2° atmosphere for CESM_H (x2) and CESM_B), although this is likely to be depend strongly on the individual model and boundary conditions used. It is also clear from Figure 6 and Supplementary Figures S1-S3 that the CO_2 forcing has a much greater effect on global mean SST than the ice or paleogeographic forcing.

Model	Atmos resolution	Ocean resolution	Publication	Paleogeography	CO2 [ppm]	Antarc. ice	Tasman	Drake	CO2 expts	ICE expts	GEO expts	Model years
CESM_B (CESM 1.0.5)	144 x 96 x 26	384 x 320 x 60	Baatsen et al (2020)	38 Ma	560	N	open	open	L			3600
				Baatsen et al (2016)	1120	N	open	open	H			4600
CESM_H (CESM1.1)	96 x 48 x 26	122 x 100 x 25	Goldner et al (2014)	45 Ma	560	N	closed	open	L	NI		3400
				Sewall et al (2000)	560	Y	closed	open		I		3000
					1120	N	closed	open	H			3300
					1120	N	closed	closed			B	1300
					1120	N	open	open			A	1000
CESM_H (x2)	144 x 96 x 26	122 x 100 x 25	* 2° atmosphere		560	N	closed	open				1500
FOAM	48 x 40 x 18	128 x 128 x 24	Ladant et al (2014a)	34Ma	560	N	open	open	L	NI	B	2000
			Ladant et al (2014b)		560	Y	open	open		I		2000
					1120	N	open	open	H			2000
				30Ma	560	N	open	open			A	2000
GFDL CM2.1	96 x 60 x 24	240 x 175 x 50	Hutchinson et al (2018)	38 Ma	400	N	open	open	L			6500
				Baatsen et al (2016)	800	N	open	open	H		B	6500
			Hutchinson et al (2019)	* Arctic closed	800	N	open	open			A	6500
HadCM3BL	96 x 73 x 19	96 x 73 x 20	Kennedy et al (2015)	Rupelian (28-34Ma)	560	N	open	open	L	NI		1422
					1120	N	open	open	H			1422
					560	Y	open	open		I		1422
				Chattian (23-28Ma)	560	N	open	open			A	1422
				Priabonian (34-38Ma)	560	N	open	open			B	1422
NorESM-L	96 x 48 x 26	100 x 116 x 32	Zhang et al (2012, 2014)	40 Ma	560	N	open	open	L			2200
				Scotese (2001)	980	N	open	open	H			2200
UVic	150 x 100 x 1	150 x 140 x 40	Sijp et al (2016)	45 Ma	1600	N	open	open			A	9000
				Sewall et al (2000)**	1600	N	open	closed			B	9000

l005 **Table 1:** Details of model simulations that are included in this intercomparison. For each model, the response to CO2, ΔTCO2, is given by H-L; ΔTICE is given by I-NI; and ΔTGEO is given by A-B.
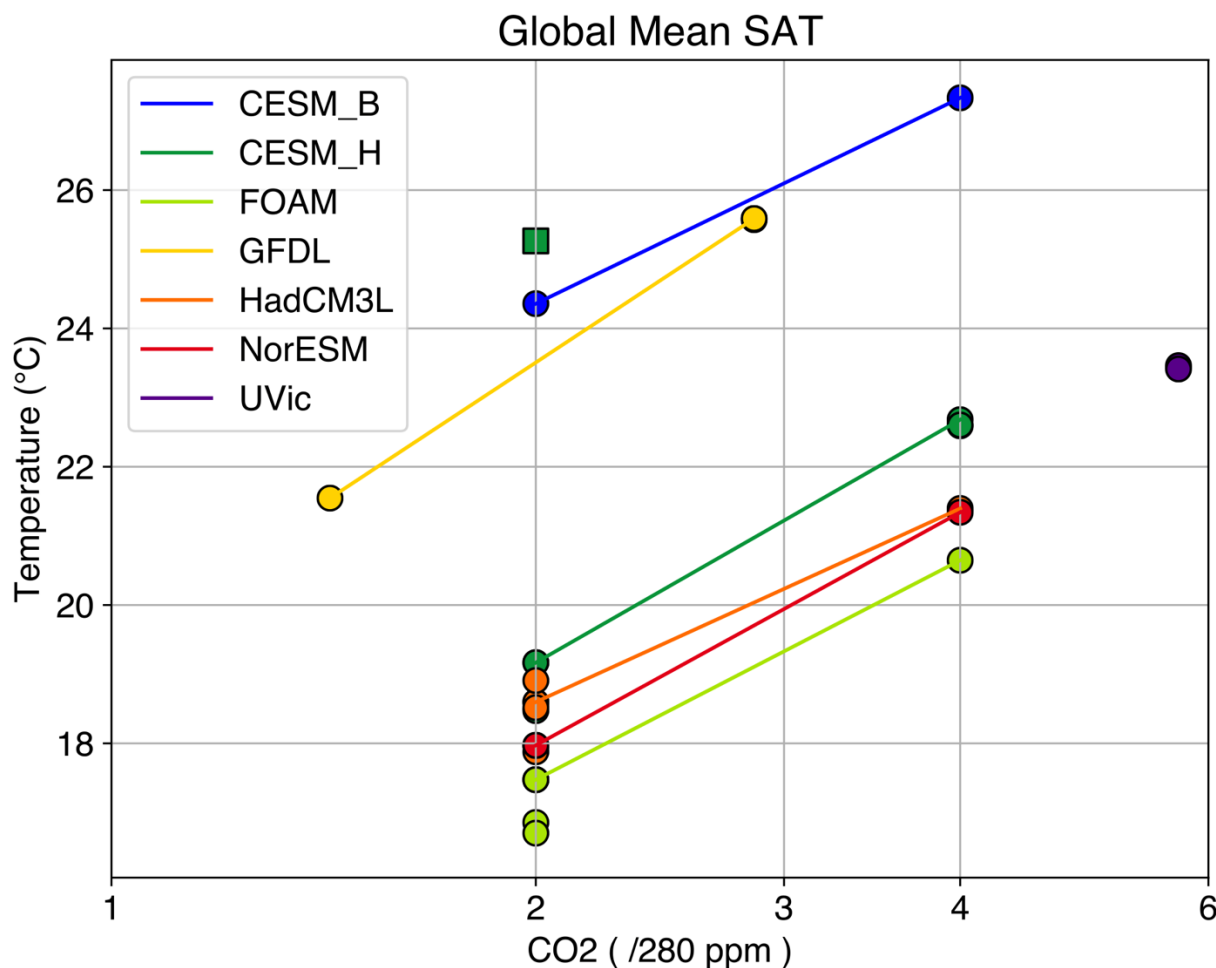
Figure 6: Global mean surface air temperature (SAT) for all models included in this intercomparison as a function of CO_2 concentration. The lines join simulations from a single model at different CO_2 concentrations. References for each model are CESM_H: (Goldner et al., 2014), UVic: (Sijp et al., 2016), FOAM : (Ladant et al., 2014a, 2014b), GFDL: (Hutchinson et al., 2018, 2019), HadCM3BL: (Kennedy et al., 2015), NorESM: (Zhang et al., 2014), CESM_B: (Baatsen et al., 2020). The dark green square is an additional simulation of CESM_H with 2° atmosphere resolution (Table 1).

The responses of each of the individual models to the three forcings, ΔT_{CO2}, ΔT_{ICE}, ΔT_{GEO}, are also shown in Supplementary Figures S1, S2, S3 respectively. It is important to highlight that the changes shown have not necessarily been chosen to best represent the EOT transition. In particular, the CO_2 forcing shown is a halving of CO_2 in all models, and although proxy CO_2 estimates are not inconsistent with this change (Pagani et al., 2011; Pearson et al., 2009), the data come with large uncertainties, albeit more so for absolute concentrations than for relative changes. In Section 7.3 we will explore this further, but here we recognise that the model responses are highly idealised and we treat them as sensitivity studies.

7.1.1 SAT response to CO_2 decrease, ΔT_{CO_2}

1020

Here we consider the response to halving CO_2 in the absence of an ice sheet. There appear to be two different modes of SAT response to a halving of CO_2 (Supplementary Figure S1). In the first mode, CESM_H, CESM_B, FOAM, and GFDL respond with a cooling over all the globe, with greatest cooling in the higher latitudes. In the second mode, HadCM3BL and NorESM-L respond with cooling in most regions (with greatest cooling in the north Pacific), but with warming in the Pacific sector of

1025 the Southern Ocean. In HadCM3BL, this is associated with a switch in regions of deep water formation from dominant sinking in the southern Atlantic and north Atlantic at high CO_2, to dominant sinking in the southern Pacific and north Atlantic at low CO_2. The onset of sinking in the southern Pacific at low CO_2 leads to increased heat transport from the equatorial Pacific southwards, to such an extent that it leads to net warming in the Pacific sector of the Southern Ocean, despite the decrease in CO_2. Similar but weaker changes in ocean circulations happen in the NorESM-L. However, this warming response is highly

1030 sensitive to the boundary conditions, with other qualitatively similar simulations behaving very differently in the region, with some showing only cooling (Kennedy-Asser et al., 2019). In CESM, a switch in the mode of ocean circulation does not occur, with deep water formation in the Pacific sector of the Southern Ocean at both high and low CO_2 (albeit increased in intensity at low CO_2). Similarly, for GFDL there is no switch, with deep water formation in the South and North Pacific at high and low CO_2, and for FOAM there is no switch, with deep water formation predominantly in the North Pacific at high and low CO_2.

1035 The patterns of change in HadCM3BL and NorESM-L are remarkably similar except in the Arctic, where NorESM-L shows much more cooling than HadCM3BL. In this region FOAM also has very little cooling. This is because both HadCM3BL and FOAM have Arctic sea ice in both high and low CO_2 simulations, which maintains the SST close to 0°C.

The ensemble mean SAT change due to a halving of CO_2 is shown in Figure 7a. This shows that the greatest cooling is in the

1040 North Pacific and in the Atlantic and Indian sectors of the Southern Ocean. Most of the regional cooling is "robust" in that all models show a change of the same sign and are all within ±2 °C of the ensemble mean change. Exceptions are in the south Pacific (because some models show warming rather than cooling) and in the North Pacific and Arctic (because there is large variability in the amount of cooling predicted). Overall, the zonal mean cooling is approximately symmetric about the equator, with equatorial cooling of -2.6 °C and mid-high latitude cooling of -5.0 °C. While this symmetry is at odds with an inferred

1045 northward migration of the intertropical convergence zone from dust geochemistry (Hyeong et al., 2016), we stress that this result reflects the fact that the far-field cooling induced by imposing an Antarctic ice sheet (see Figure 7b) is much smaller than the global cooling induced by CO_2 forcing in these models.

Climate of the Past
Discussions
(a) ensemble mean 2x-4x
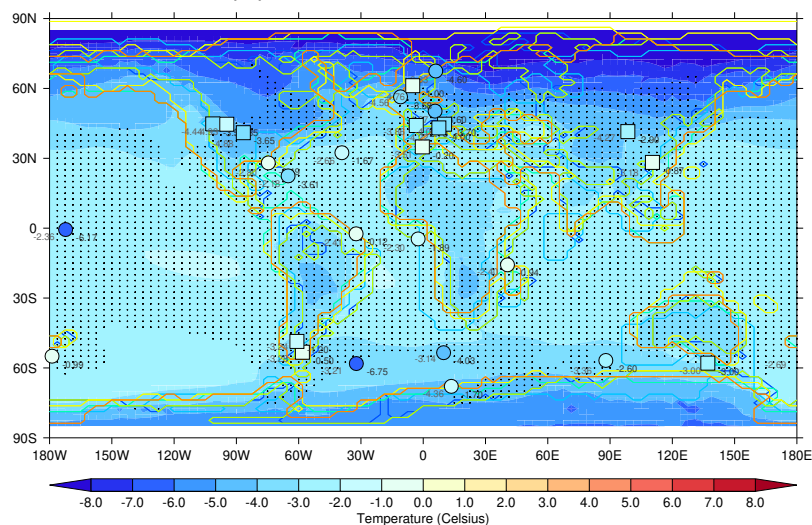
(b) ensemble mean 2xice-2x
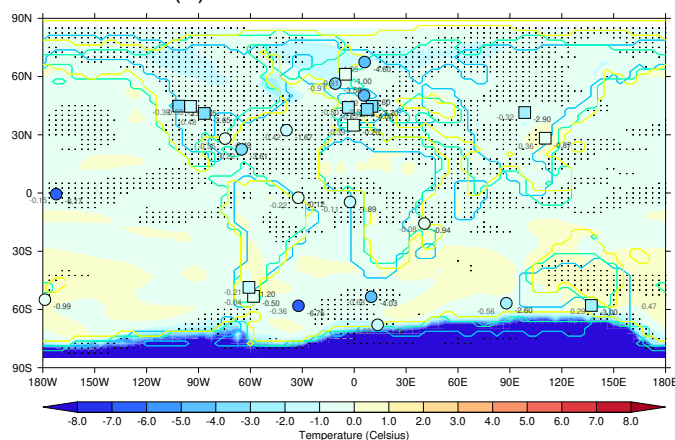
(c) ensemble mean postEOT-preEOT
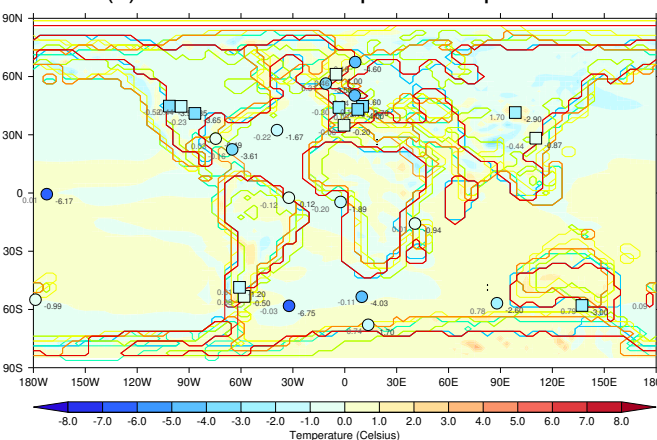
Figure 7: Ensemble mean modelled SAT response to (a) CO2 halving (ΔTCO2), (b) onset of ice on Antarctica (ΔTICE), and (c) paleogeographic change (ΔTGEO) across the EOT. Stippled regions are those where the change is defined as 'robust', in that all models have a response of the same sign and within ±2 °C of the ensemble mean. The continental outlines for all models in each ensemble are shown. The marine proxy data are shown as filled circles, while the terrestrial proxy data are shown as filled squares. The values of SAT change at each proxy site are shown for the data and model on the left and right of each site respectively.

7.1.2 SAT response to Antarctic ice, ΔT$_{ICE}$

The three models that have carried out simulations with and without an Antarctic ice sheet show differing responses to the forcing (Supplementary Figure S2). CESM shows a cooling around the margins of Antarctica, and in the Pacific and Atlantic sectors of the Southern Ocean; FOAM shows cooling around the margins of Antarctica but warming throughout much of the Southern Ocean, and HadCM3BL shows cooling in the Southern Ocean except in the southern Pacific. The mechanisms behind

1060   the changes are described in the respective papers. In brief, Kennedy et al. (2015) attribute the warming in the Pacific sector of the Southern Ocean in HadCM3BL to an increased N-S pressure gradient close to the polar front leading to stronger westerlies, intensification of the Ross Sea gyre, and a resulting increase in oceanic poleward heat transport. Goldner et al. (2014) focus on changes to deep ocean temperatures, highlighting the importance of increased easterly winds around the margins of Antarctica and resulting Ekman transport for bringing cold water to depths. They do not discuss mechanisms for

1065   the warming around Australia. Ladant et al. (2014a) do not discuss the mechanism of SST change following glaciation, but Ladant et al. (2014b) do, for a similar pair of simulations. In their model, the presence of the Antarctic ice sheet enhances the strength of the Antarctic Circumpolar Current, and as a result, the Ross Gyre and Weddell Gyre initiate. They also highlight the importance of sea ice changes in amplifying the changes in SSTs. More recent work (Kennedy-Asser et al., 2019) has highlighted that the particularly strong Southern Ocean warming response in the HadCM3BL simulations could be an artefact

1070   of insufficient spin-up, with very long simulations showing a more muted temperature response. As a result, these HadCM3BL results should be treated with caution.

In terms of the ensemble mean (Figure 7b), there are only a few regions where there is a robust SST signal. Robust cooling in response to the addition of the Antarctic ice sheet are around the margins of the East Antarctic ice sheet, in the Drake Passage,

1075   south of southern Africa, and the tropical and North Atlantic. There is a seemingly robust warming east of Australia, but this is a small region and as such it is unclear if it occurs by chance.

7.1.3 SAT response to paleogeographic change, ΔT_{GEO}

For examining the response to paleogeographic change (Supplementary Figure S3), for each model we first identify the pair of simulations for each model that represents the largest change in paleogeography across the EOT. For CESM this is an

1080   idealised gateway change from a closed Tasman and Drake Passages to open Tasman and Drake Passages. This forcing results in a cooling in the Pacific sector of the Southern Ocean, and a slight warming in the rest of the Southern Ocean, but these changes are all small compared with those caused by CO_2 or ice sheet changes. For UVic the forcing is an idealised gateway change from a closed to an open Drake Passage. This has a large impact on SSTs in the Southern Ocean, with cooling south of southern Africa, and a N-S dipole of warming and cooling in the Pacific sector of the Southern Ocean, associated with the

1085   transition from a gyre circulation to an Antarctic Circumpolar Current. For FOAM the forcing consists of a localised change in West Antarctica in which continent becomes ocean. However, despite the relatively small forcing the response is quite substantial, leading to global cooling of about 1 °C (Figure 6), especially in the south west Pacific. For HadCM3BL, the forcing is global in nature, but consists of relatively small changes to continental position and topography and bathymetry associated with plate tectonic movements from the Priabonian (34-38 Ma) to the Chattian (23-28 Ma). As a global mean the response is

1090   very small, but regionally it is quite large, for example in the North Pacific where there is a N-S dipole response, cooling in the North Atlantic, and warming in the Southern Ocean. These changes are associated with the strengthening of deep water

formation in the Atlantic sector of the Southern Ocean. NorESM-L shows a relatively muted response, but a substantial cooling of about 2 °C in the southwest Pacific.

1095 Given that all models have carried out different simulations to differing forcings, interpreting the differences in response is challenging. However, the ensemble mean response, shown in Figure 7c, can be interpreted as the best estimate of the SAT-response to paleogeographic change across the EOT, given the uncertainty in the paleogeographic forcing itself, as well as in the different models. The only substantial region of robust change is in the tropical Atlantic, where all models indicate a cooling response of about 1 °C.

1100 **7.2 Model-data comparison across the EOT**

It is important to assess the realism (or otherwise) of the model simulations by comparison with evidence from the geological record. Such model-data comparison can also improve our understanding of the likely mechanisms that drove change. Given the 'snapshot' nature of the model simulations, and uncertainties in dating and limitations due to sparse data coverage, it is necessary to use data that extend throughout the EOT, and that are clearly either 'pre-EOT' or 'post-EOT'. Here we use an

1105 updated compilation of SST (Figure 3) and terrestrial surface temperature proxies (Figure 4), which we present in Supplementary Tables S1 and S2 respectively. In total there are 23 data points from marine sources and 19 data points from terrestrial sources. Before performing the intercomparison, we first combine and average data points that either come from different proxies from the same location, or from neighbouring data points when they are less than one grid cell apart. This process yields a final proxy dataset of 28 data points, shown in Supplementary Table S3. Each data point is then given an equal

1110 weight in determining a root mean square error skill score.

7.2.1 Comparison of model simulations with proxy data

The observed proxy temperature changes compared with the individual model responses to CO_2, Antarctic ice and paleogeography are shown in Supplementary Figures S1-S3. As discussed in Section 7.1.1, when CO_2 is halved, all models predict a cooling at all sites, in agreement with the data, except NorESM-L that warms at one of the Arctic sites. There are no

1115 data to evaluate the warming signal in the southern Pacific in HadCM3BL and NorESM-L. When an Antarctic ice sheet is imposed, the agreement is not so good, with all models showing warming for at least 2 of the sites. When paleogeographic changes are imposed, the model-data agreement is worse again for most models, with all models showing warming for at least 3 of the sites. The exception is FOAM, for which all sites cool, in agreement with the data. The ensemble means capture the broad changes reasonably well, with all sites cooling for the CO_2 case, and all but one site cooling for the ice and

1120 paleogeographic changes.

This model-data comparison is limited by the fact that the models have carried out idealised simulations, especially for CO_2 forcing for which the halving of CO_2 is somewhat arbitrary. Although some proxy CO_2 records do indicate a drop of this order

of magnitude (Pagani et al., 2011; Pearson et al., 2009), the associated uncertainties are large. Similarly, the changes to the

1125 Antarctic ice sheet imposed in the model may be greater or less than in reality, or the imposed changes in paleogeography may

be too extreme. As such, we carry out the model-data comparison such that each model SAT response to each forcing is scaled

by a constant in such a way that it best fits the data. To assess the goodness-of-fit, we calculate a skill score, *s*, for each pair

of model simulations, simply as the RMS difference between the proxy temperature and modelled temperature, calculated

from model gridpoint that is in closest proximity to the data. For the purposes of the skill score we treat neighbouring sites

1130 (e.g. tropical sites 925 and 929) as a single data point by averaging the proxy and the scaled modelled temperatures at the two

sites. The values of *s* for each modelled best-fit change to the proxy SSTs are shown in Table 7.2. When comparing models

and proxies, it is informative to consider what may be called a "good agreement", and to provide a point of reference for

assessing the skill scores. As such, in Table 7.2 we also show the skill score that would be obtained in the case of an idealised

model simulating (i) no SAT change across the EOT, (ii) a global mean change that best fits the data, and (iii) a zonal-mean

1135 change of the form $\Delta SST = A + B\cos(\phi)$, (where ϕ is latitude), that best fits the data.

Model	s for best-fit ΔT_{CO2}	s for best-fit ΔT_{ice}	s for best-fit ΔT_{geog}
CESM_B	0.328		
CESM_H	0.343	0.564	0.588
FOAM	0.330	0.533	0.455
GFDL	0.329		0.588
HadCM3BL	0.361	0.509	0.588
Nor-ESM	0.360		0.588
UVic			0.577
Ensemble mean	0.326	0.523	0.588
	s for idealised ΔT		
No change	0.588		
Constant change	0.329		
cos(ø) change	0.322		

Table 2: Skill scores, s, for the best-fit modelled changes in response to CO₂, ice, and paleogeographic forcing, for each model and for the ensemble mean (a lower value of s represents a better fit to data). Also shown are the values of s for three idealised SAT changes. The
1140 models all achieve their best skill performance with CO₂ forcing (UVic does not include CO₂ forcing). Only one model (FOAM) achieves a better skill than an idealised constant temperature change, however, the spread in skill across the different models is narrow.

It is clear from Table 2 that the best modelled fit to the SAT proxy data arises from changes to CO₂. In particular, the ensemble

mean response to a decrease in atmospheric CO₂ has the best (lowest) skill score, and better than a constant change fit, but

1145   slightly poorer than a cos(ø). We note however, that a cos(ø) fit to the data produces only a 2% improved skill score over the constant change fit. The CESM_B and GFDL models perform marginally better than the constant change fit to the data, while CESM_H, FOAM, HadCM3BL and Nor-ESM all perform slightly worse than this, but all skills scores are within a margin of 10% of the constant change fit. The CO_2 change provides by far the best temperature fit over the ICE and GEOG changes. The UVic model does not apply a CO_2 change, and consequently achieves a poorer skill score. We note however, that in several

1150   cases (CESM_H, FOAM and HadCM3BL), the ICE changes also improve the skill score, while the GEOG changes improve the skill score in the FOAM model. Since those forcing factors are independent to CO_2, they also improve the overall skill score in combination, as we show below. These results broadly agree with a recent Southern Ocean-only model-data comparison, which showed that CO_2 forcing provided the best explanation of temperature changes across the EOT, with secondary improvements made from ice and paleogeography changes (Kennedy-Asser et al., 2020).

1155   **7.2.2 Mechanisms of change**

The above analysis implies that the change in SST at the EOT can be best explained by a decrease in CO_2, as opposed to changes in ice or paleogeography. However, it is possible that changes in ice or paleogeography, combined with CO_2 change, may fit even better with the data. To test this possibility, we assume that the various responses add together linearly, and find the best scaled combination of each mechanism, i.e. we find α, β, γ such that the skill score, s, of ($\alpha\Delta T_{CO2} + \beta\Delta T_{ice} + \gamma\Delta T_{geo}$)

1160   is minimised. The result of this exercise for each model and for the ensemble mean is shown in Table 3. This shows that CESM_H and HadCM3BL achieve a better fit to the data when including the full response to ice sheet change and no paleogeographic change, while FOAM achieves a better fit when including both a paleogeographic change and a small fraction of ice sheet change. The ensemble mean agrees best with the proxies when incorporating a CO_2 shift of 910 to 560 ppm (α=0.7), which is achieved from CO_2 forcing alone in the ensemble mean case. This best-fit ensemble mean change is shown in Figure

1165   8. Given the close agreement between the models in fitting a CO_2 change to the data, we can estimate from the full model spread that the CO_2 drop was by a factor of 1.60 ± 0.13. If for example we assume an Oligocene CO_2 value of 2x pre-industrial levels, the CO_2 drop would be from 910 ± 90 ppmv to 560 ppmv. However, we would caution that this estimate reflects the model spread in matching this particular set of data, and that the true uncertainty is larger. Additionally, the models that included changes due to ice sheet forcing or paleogeographic forcing achieved some improvement in fitting the data, but this

1170   played a lesser role than CO_2 forcing, as measured by these skill metrics.

Model	s for best-fit $\alpha\Delta T_{CO2}$ + $\beta\Delta T_{ice}$ + $\gamma\Delta T_{geo}$	α [CO2 change ppmv]	β	γ
CESM_B	0.328	0.74 [935 to 560]		
CESM_H	0.325	0.6 [848 to 560]	1.0	0
FOAM	0.329	0.66 [885 to 560]	0	0.25

GFDL	0.329	0.56 [826 to 560]		
HadCM3BL	0.359	0.62 [860 to 560]	0.49	0
Nor-ESM	0.356	0.72 [922 to 560]		0.5
UVic	0.577			0.78
Ensemble mean	0.326	0.7 [910 to 560]	0.06	0.26
	s for idealised ΔT			
No change	0.588			
Constant change	0.329			
cos(ø) change	0.322			

Table 3: Skill scores, s, for the best-fit modelled changes in response to a combination of CO2, ice, and paleogeographic forcing, for each model and for the ensemble mean (a lower value of s represents a better fit to data). Also shown are the values of α, β, and γ that give the best fit, and the CO2 change corresponding to α, assuming a post-EOT value of 560 ppmv. Also shown are the values of s for three idealised SAT changes. Changes highlighted in green are better than or equal to the idealised constant change case, while no models achieve better than the idealised cos(ø) case.

1175
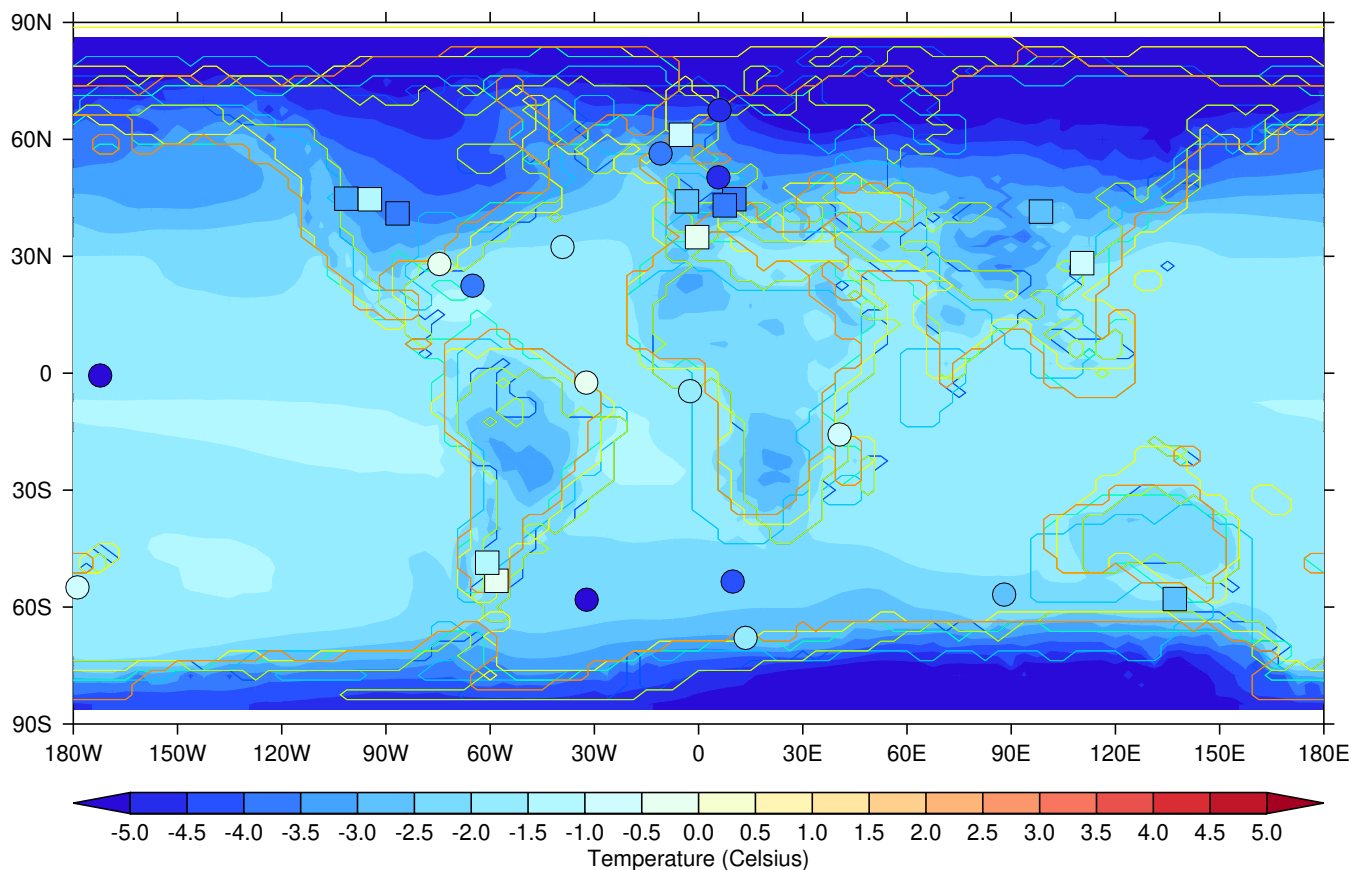
180   **Figure 8:** Ensemble mean modelled SAT response to a CO2 decrease from 900 to 560 ppmv, representing the best fit to the proxy data. The marine proxy data are shown as filled circles, while the terrestrial proxy data are shown as filled squares. Coastlines from each model are plotted to illustrate the uncertainties associated with the paleogeographic reconstructions.

7.2.3 Uncertainties associated with the modelling

There are several uncertainties that should be considered when interpreting the results above. Some of these are discussed

185   here. There is uncertainty in the models themselves. These models could be characterised as AR4-class or even TAR-class in

that they were state-of-the-art at the time of the 4th or 3rd IPCC assessment report, as opposed to the most recent AR5, or the

upcoming AR6. The use of less complex models can be an advantage for deep-time paleoclimate work, as these models allow

greater length of simulation, which is especially important for the deep ocean where the initial condition may be far from the

equilibrium state, which is unknown at the start of the simulation. However, there is a trade- off between simulation length

190   and model complexity, and some of the model simulations presented here are relatively short (e.g. HadCM3BL; Table 1). A

potential manifestation of this lack of complexity relates to the modelled change in land-sea contrast. The EOT temperature

change from marine records is larger (-2.9 °C) than that recorded from land temperature proxies (-2.2 °C). This in part reflects the heterogeneous pattern of changes in plant species, from which the land temperature proxies are derived, but is in general a globally robust signal. On the other hand, the temperature changes recorded in the model simulations show the opposite; land temperature changes are more sensitive to greenhouse cooling than ocean temperature changes. This makes it challenging to achieve a close fit to all of the temperature records available. However, by including both marine and terrestrial temperature changes, we derive an estimate of CO_2 decline that of a factor of 1.6, which is broadly in line with proxy estimates (Figure 5).

The boundary conditions applied to the models is a large source of uncertainty. The spread in paleogeographic forcing between models is testament to the fact that the paleogeography both pre-EOT and post-EOT is relatively uncertain (See Section 2.1 and 2.2). The proxy dataset we have used is somewhat limited in areal coverage. As such, the models remain untested in several key regions, such as the North and tropical Pacific, or the Indian Ocean. New data in the regions predicted to warm in response to a CO_2 drop in HadCM3BL and NorESM-L would be particularly useful for discriminating between models. The model-data comparison does not consider any uncertainty in the proxy estimates themselves. In reality, each site is associated with a different and substantial uncertainty in its estimate of SST change across the EOT.

Here we have considered only the change in temperature across the EOT, rather than absolute temperatures. However, this can mask biases in the simulated base state of the pre-EOT and post-EOT simulations. Not all models do a good job of simulating the base state (see e.g. discussion of meridional temperature gradients in Section 6.2). Although the ensemble results achieve the best fit from CO_2 forcing (with a small contribution form ice sheet forcing), it is worth noting that the ultimate cause of the CO_2 drop itself remains unclear; it could itself be driven by changes to geological sources and sinks, changes in weathering rates, or feedbacks associated with ocean and land sinks due to circulation changes (see Section 6.3).

8 Conclusions

Earth's modern 'icehouse' climate is defined by the presence of significant terrestrial ice at both poles but that ice is now disappearing. Understanding the drivers and scale of polar ice growth during the initial inception of this icehouse at the EOT, which involved cooling and glaciation under a yet still warm Eocene-Oligocene climate, can provide crucial insights into ice sheet stability and behaviour under a warm climate, something that is more critical than ever. Here we have reviewed current literature regarding the EOT, in terms of stratigraphic definitions, geological records of paleogeographic and Earth system change, and modelling insights into mechanisms of change. Marine records currently provide the most extensive global record of temperature change across the EOT, with a SST cooling found across most regions. These records suggest a global average temperature change of approximately -2.9 °C across the EOT, although individual records range from approximately 0 to -8 °C change. Terrestrial records of temperature change are more geographically limited, with a concentration of records in the midlatitude Northern Hemisphere, and very little coverage of the Southern Hemisphere. Overall, terrestrial records average a

Climate
of the Past
Discussions

-2.2 °C, but like the marine records, the change recorded at individual locations ranges from approximately 0 to -8 °C across the EOT. Records of CO_2 across the EOT also indicate some differences between marine and terrestrial records. Marine records suggest a higher concentration of CO_2 overall and a clearer transition towards lower CO_2 across the EOT. Terrestrial records, by contrast, indicate a lower CO_2 concentration overall and a more gradual CO_2 decline with no obvious shift coinciding with the EOT. There is therefore a

A new model-data comparison presented in this paper reveals that a halving of atmospheric CO_2 across the EOT has a substantially greater effect on global mean and regional SAT than either the onset of Antarctic glaciation or changes in paleogeography. The response to CO_2 forcing is robust across models, with cooling increasing towards higher latitudes, helping to explain high latitude cooling in the marine records. While individual models achieved a better fit to the data by including paleogeographic forcing and ice sheet forcing, these changes are more variable across the models. As a result, the best fit in the ensemble mean is achieved by including the CO_2 forcing only, with a decrease in CO_2 of 1.6x. Assuming an Oligocene value of 560 ppmv, the corresponding pre-EOT value is 910 ppmv. However, we do not exclude the importance of contributions from other forcings. Indeed, several models in the ensemble achieve their best fit to the temperature records with a combination of CO_2 and ice-sheet induced changes, while one model shows an improved fit when paleogeographic changes are combined with CO_2 forcing. Paleogeographic changes and ice sheet feedbacks are inherently regional and harder to aggregate across different model experiments. Nevertheless, it remains possible that gateway-induced ocean circulation change is somehow implicated in CO_2 decline. For a more complete understanding of these feedbacks, future climate modelling of the EOT must incorporate dynamic feedbacks between these different forcing factors.

Appendix – List of Acronyms

AMOC: Atlantic meridional overturning circulation

CCD: Calcite compensation depth

CLAMP: Climate Leaf Analysis Multivariate Program

EAIS: East Antarctic ice sheet

EOGM: Early Oligocene glacial maximum

EOB: Eocene-Oligocene boundary

EOT: Eocene-Oligocene transition

EOIS: Early Oligocene oxygen isotope step

GSSP: Global boundary stratotype section and point

MECO: Middle Eocene climatic optimum

NLR: Nearest Living Relative

ODP: Ocean drilling program

PrOM: Priabonian oxygen isotope maximum

SAT: Surface air temperature

SST: Sea surface temperature

Data Availability

1260 The data compilation plotted in the manuscript are included in the supplementary material. The model data are available upon request from the lead authors listed in Table 1.

Author Contributions

The manuscript was conceived and planned by DKH, AMdB, HKC, and MS, in collaboration with all authors. Section 1 was led by HKC, PNP and PAW. Section 2 was led by DKH, MB, HDS and AvdH. Section 3 was led by KKS, HKC and CHL.
1265 Section 4 was led by MS, MJP and LK, with contributions from KM. Section 5 was led by MS, CHL and LK. Section 6 was led by DKH and AMdB. Section 7 was led by DJL and DKH. Compilations of SST records were made by KKS and MH, terrestrial records by MJP, US and MH, coordinated by DKH. δ^{18}O records were compiled by EP. Model simulation data were contributed by DKH, ATK-A, J-BL, MB, MH, WPS, ZZ. All authors contributed to editing and review of the manuscript.

Competing interests

1270 The authors declare that they have no conflict of interest.

Acknowledgments

This work originated from a workshop on the Eocene-Oligocene Transition in Stockholm in February 2017, funded by the Bolin Centre for Climate Research, Research Area 6. This work was also supported by the Swedish Research Council project 2016-03912 and FORMAS project 2018-01621.

1275 **References**

Abels, H. A., Dupont-Nivet, G., Xiao, G., Bosboom, R. and Krijgsman, W.: Step-wise change of Asian interior climate preceding the Eocene–Oligocene Transition (EOT), Palaeogeogr. Palaeoclimatol. Palaeoecol., 299(3), 399–412, doi:10.1016/j.palaeo.2010.11.028, 2011.

Abelson, M. and Erez, J.: The onset of modern-like Atlantic meridional overturning circulation at the Eocene-Oligocene
1280 transition: Evidence, causes, and possible implications for global cooling, Geochemistry, Geophys. Geosystems, 18(6), 2177–2199, doi:10.1002/2017GC006826, 2017.

Adams, C. G., Butterlin, J. and Samanta, B. K.: Larger Foraminifera and Events at the Eocene/Oligocene Boundary in the Indo-West Pacific Region, in termbal eocene events, vol. 9, edited by C. Pomerol and I. B. T.-D. in P. and S. Premoli-Silva, pp. 237–252, Elsevier., 1986.

1285 Agnini, C., Fornaciari, E., Raffi, I., Catanzariti, R., Pälike, H., Backman, J. and Rio, D.: Biozonation and biochronology of Paleogene calcareous nannofossils from low and middle latitudes, Newsletters Stratigr., 47(2), 131–181, doi:10.1127/0078-0421/2014/0042, 2014.

Anagnostou, E., John, E. H., Edgar, K. M., Foster, G. L., Ridgwell, A., Inglis, G. N., Pancost, R. D., Lunt, D. J. and Pearson, P. N.: Changing atmospheric CO2 concentration was the primary driver of early Cenozoic climate, Nature, 533(7603), 380–
1290 384, doi:10.1038/nature17423, 2016.

Anderson, J. B., Warny, S., Askin, R. A., Wellner, J. S., Bohaty, S. M., Kirshner, A. E., Livsey, D. N., Simms, A. R., Smith, T. R., Ehrmann, W., Lawver, L. A., Barbeau, D., Wise, S. W., Kulhanek, D. K., Weaver, F. M. and Majewski, W.: Progressive Cenozoic cooling and the demise of Antarctica's last refugium, Proc. Natl. Acad. Sci., 108(28), 11356 LP – 11360, doi:10.1073/pnas.1014885108, 2011.

1295 Armstrong McKay, D. I., Tyrrell, T. and Wilson, P. A.: Global carbon cycle perturbation across the Eocene-Oligocene climate transition, Paleoceanography, 31(2), 311–329, doi:10.1002/2015PA002818, 2016.

Baatsen, M., van Hinsbergen, D. J. J., von der Heydt, A. S., Dijkstra, H. A., Sluijs, A., Abels, H. A. and Bijl, P. K.: Reconstructing geographical boundary conditions for palaeoclimate modelling during the Cenozoic, Clim. Past, 12(8), 1635–1644, doi:10.5194/cp-12-1635-2016, 2016.

1300 Baatsen, M., von der Heydt, A. S., Huber, M., Kliphuis, M. A., Bijl, P. K., Sluijs, A. and Dijkstra, H. A.: The middle-to-late Eocene greenhouse climate, modelled using the CESM 1.0.5, Clim. Past Discuss., 2020, 1–44, doi:10.5194/cp-2020-29, 2020.

Baatsen, M. L. J., von der Heydt, A. S., Kliphuis, M., Viebahn, J. and Dijkstra, H. A.: Multiple states in the late Eocene ocean circulation, Glob. Planet. Change, 163, 18–28, doi:https://doi.org/10.1016/j.gloplacha.2018.02.009, 2018.

Bailey, I., Hole, G. M., Foster, G. L., Wilson, P. A., Storey, C. D., Trueman, C. N. and Raymo, M. E.: An alternative suggestion
1305 for the Pliocene onset of major northern hemisphere glaciation based on the geochemical provenance of North Atlantic Ocean ice-rafted debris, Quat. Sci. Rev., 75, 181–194, doi:https://doi.org/10.1016/j.quascirev.2013.06.004, 2013.

Barker, P. F. and Burrell, J.: The opening of Drake Passage, Mar. Geol., 25(1–3), 15–34, doi:10.1016/0025-3227(77)90045-7, 1977.

Barker, P. F. and Thomas, E.: Origin, signature and palaeoclimatic influence of the Antarctic Circumpolar Current, Earth-
1310 Science Rev., 66(1–2), 143–162, doi:10.1016/j.earscirev.2003.10.003, 2004.

Barker, P. F., Filippelli, G. M., Florindo, F., Martin, E. E. and Scher, H. D.: Onset and role of the Antarctic Circumpolar Current, Deep Sea Res. Part II Top. Stud. Oceanogr., 54(21–22), 2388–2398, doi:10.1016/j.dsr2.2007.07.028, 2007.

Barreda, V. and Palazzesi, L.: Patagonian Vegetation Turnovers during the Paleogene-Early Neogene: Origin of Arid-Adapted Floras, Bot. Rev., 73(1), 31–50, doi:10.1663/0006-8101(2007)73[31:PVTDTP]2.0.CO;2, 2007.

1315 Basak, C. and Martin, E. E.: Antarctic weathering and carbonate compensation at the Eocene–Oligocene transition, Nat. Geosci., 6, 121, doi:10.1038/ngeo1707, 2013.

Beerling, D. J.: Preface to Vegetation-climate-atmosphere interactions: past, present and future, the proceedings of a Discussion Meeting held at the Royal Society, Philos. Trans. R. Soc. B Biol. Sci., 353(1365), 3–4, doi:10.1098/rstb.1998.0185, 1998.

1320   Beerling, D. J. and Royer, D. L.: Convergent Cenozoic CO2 history, Nat. Geosci., 4, 418, doi:10.1038/ngeo1186, 2011.

Beerling, D. J., Fox, A., Stevenson, D. S. and Valdes, P. J.: Enhanced chemistry-climate feedbacks in past greenhouse worlds, Proc. Natl. Acad. Sci., 108(24), 9770 LP – 9775, doi:10.1073/pnas.1102409108, 2011.

Berggren, W. A. and Pearson, P. N.: A Revised Tropical to Subtropical Paleogene Planktonic Foraminiferal Zonation, J. Foraminifer. Res., 35(4), 279–298, doi:10.2113/35.4.279, 2005.

1325   Berggren, W. A., Wade, B. S. and Pearson, P. N.: Oligocene chronostratigraphy and planktonic foraminiferal biostratigraphy: Historical review and current state-of-the-art, in Atlas of Oligocene Planktonic Foraminifera, edited by B. S. Wade, R. K. Olsson, P. N. Pearson, B. T. Huber, and W. A. Berggren, pp. 29–54, Cushman Foundation for Foraminiferal Research: Lawrence, USA., 2018.

Bernard, T., Steer, P., Gallagher, K., Szulc, A., Whitham, A. and Johnson, C.: Evidence for Eocene–Oligocene glaciation in 1330   the landscape of the East Greenland margin, Geology, 44(11), 895–898, doi:10.1130/G38248.1, 2016.

Berner, R. A. and Kothavala, Z.: GEOCARB III: a revised model of atmospheric CO2 over Phanerozoic time, Am. J. Sci., 301(2), 182–204, doi:10.2475/ajs.301.2.182, 2001.

Bierman, P. R., Shakun, J. D., Corbett, L. B., Zimmerman, S. R. and Rood, D. H.: A persistent and dynamic East Greenland Ice Sheet over the past 7.5 million years, Nature, 540, 256, doi:10.1038/nature20147, 2016.

1335   Bijl, P. K., Schouten, S., Sluijs, A., Reichart, G.-J., Zachos, J. C. and Brinkhuis, H.: Early Palaeogene temperature evolution of the southwest Pacific Ocean, Nature, 461(7265), 776–779, doi:10.1038/nature08399, 2009.

Bijl, P. K., Bendle, J. A. P., Bohaty, S. M., Pross, J., Schouten, S., Tauxe, L., Stickley, C. E., McKay, R. M., Röhl, U., Olney, M., Sluijs, A., Escutia, C., Brinkhuis, H. and Scientists, E. 318: Eocene cooling linked to early flow across the Tasmanian Gateway, Proc. Natl. Acad. Sci., 110(24), 9645–9650, doi:10.1073/pnas.1220872110, 2013.

1340   Billups, K. and Schrag, D. P.: Application of benthic foraminiferal Mg/Ca ratios to questions of Cenozoic climate change, Earth Planet. Sci. Lett., 209(1), 181–195, doi:10.1016/S0012-821X(03)00067-0, 2003.

Blaj, T., Backman, J. and Raffi, I.: Late Eocene to Oligocene preservation history and biochronology of calcareous nannofossils from paleo-equatorial Pacific Ocean sediments, Riv. Ital. di Paleontol. e Stratigr., 115, 67–85, doi:10.13130/2039-4942/5920, 2009.

1345   Bo, S., Siegert, M. J., Mudd, S. M., Sugden, D., Fujita, S., Xiangbin, C., Yunyun, J., Xueyuan, T. and Yuansheng, L.: The Gamburtsev mountains and the origin and early evolution of the Antarctic Ice Sheet, Nature, 459, 690, doi:10.1038/nature08024, 2009.

Boardman, G. S. and Secord, R.: Stable isotope paleoecology of White River ungulates during the Eocene–Oligocene climate transition in northwestern Nebraska, Palaeogeogr. Palaeoclimatol. Palaeoecol., 375, 38–49, 1350   doi:https://doi.org/10.1016/j.palaeo.2013.02.010, 2013.

Bohaty, S. M. and Zachos, J. C.: Significant Southern Ocean warming event in the late middle Eocene, Geology, 31(11), 1017–1020, doi:10.1130/G19800.1, 2003.

Bohaty, S. M., Zachos, J. C. and Delaney, M. L.: Foraminiferal Mg/Ca evidence for Southern Ocean cooling across the Eocene–Oligocene transition, Earth Planet. Sci. Lett., 317–318(Supplement C), 251–261, doi:10.1016/j.epsl.2011.11.037, 1355   2012.

Borrelli, C., Cramer, B. S. and Katz, M. E.: Bipolar Atlantic deepwater circulation in the middle-late Eocene: Effects of

Southern Ocean gateway openings, Paleoceanography, 29(4), 308–327, doi:10.1002/2012PA002444, 2014.

Boyden, J. A., Müller, R. D., Gurnis, M., Torsvik, T. H., Clark, J. A., Turner, M., Ivey-Law, H., Watson, R. J. and Cannon, J. S.: Next-generation plate-tectonic reconstructions using GPlates, in Geoinformatics: Cyberinfrastructure for the Solid Earth Sciences, edited by G. R. Keller and C. Baru, pp. 95–114, Cambridge University Press., 2011.

Boyle, P. R., Romans, B. W., Tucholke, B. E., Norris, R. D., Swift, S. A. and Sexton, P. F.: Cenozoic North Atlantic deep circulation history recorded in contourite drifts, offshore Newfoundland, Canada, Mar. Geol., 385, 185–203, doi:10.1016/j.margeo.2016.12.014, 2017.

Bozukov, V., Utescher, T. and Ivanov, D.: Late Eocene to early Miocene climate and vegetation of Bulgaria, Rev. Palaeobot. Palynol., 153(3), 360–374, doi:10.1016/j.revpalbo.2008.10.005, 2009.

Brassell, S. C.: Climatic influences on the Paleogene evolution of alkenones, Paleoceanography, 29(3), 255–272, doi:10.1002/2013PA002576, 2014.

Brassell, S. C., Eglinton, G., Marlowe, I. T., Pflaumann, U. and Sarnthein, M.: Molecular stratigraphy: a new tool for climatic assessment, Nature, 320, 129, doi:10.1038/320129a0, 1986.

Breedlovestrout, R. L., Evraets, B. J. and Parrish, J. T.: New Paleogene paleoclimate analysis of western Washington using physiognomic characteristics from fossil leaves, Palaeogeogr. Palaeoclimatol. Palaeoecol., 392, 22–40, doi:10.1016/j.palaeo.2013.08.013, 2013.

Brinkhuis, H., Schouten, S., Collinson, M. E., Sluijs, A., Damsté, J. S. S., Dickens, G. R., Huber, M., Cronin, T. M., Onodera, J., Takahashi, K., Bujak, J. P., Stein, R., van der Burgh, J., Eldrett, J. S., Harding, I. C., Lotter, A. F., Sangiorgi, F., Cittert, H. van K., de Leeuw, J. W., Matthiessen, J., Backman, J., Moran, K. and Scientists, the E. 302: Episodic fresh surface waters in the Eocene Arctic Ocean, Nature, 441(7093), 606–609, doi:10.1038/nature04692, 2006.

Broecker, W. S. and Peng, T.-H.: Tracers in the sea, Eldigio Press, Columbia University, Palisades, NY., 1982.

Carter, A., Riley, T. R., Hillenbrand, C.-D. and Rittner, M.: Widespread Antarctic glaciation during the Late Eocene, Earth Planet. Sci. Lett., 458, 49–57, doi:10.1016/j.epsl.2016.10.045, 2017.

Chamberlain, C. P., Mix, H. T., Mulch, A., Hren, M. T., Kent-Corson, M. L., Davis, S. J., Horton, T. W. and Graham, S. A.: The Cenozoic climatic and topographic evolution of the western North American Cordillera, Am. J. Sci., 312, 213–262, doi:10.2475/02.2012.05, 2012.

Coccione, R.: The genera Hantkenina and Cribrohantkenina (foraminifera) in the Massignano Section (Ancona, Italy), in International Subcommission on Paleogeography and Stratigraphy, Eocene/Oligocene Meeting, pp. 81–96., 1988.

Collinson, M. E. and Hooker, J. J.: Paleogene vegetation of Eurasia: framework for mammalian faunas, Deinsea, 10(1), 41–84, 2003.

Cotton, L. J. and Pearson, P. N.: Extinction of larger benthic foraminifera at the Eocene/Oligocene boundary, Palaeogeogr. Palaeoclimatol. Palaeoecol., 311(3), 281–296, doi:10.1016/j.palaeo.2011.09.008, 2011.

Cotton, L. J., Pearson, P. N. and Renema, W.: Stable isotope stratigraphy and larger benthic foraminiferal extinctions in the Melinau Limestone, Sarawak, J. Asian Earth Sci., 79, 65–71, doi:https://doi.org/10.1016/j.jseaes.2013.09.025, 2014.

Coxall, H. K. and Pearson, P. N.: The Eocene-Oligocene transition, Deep Time Perspect. Clim. Chang. Marrying Signal From Comput. Model. Biol. Proxies, 351–387, 2007.

Coxall, H. K. and Wilson, P. A.: Early Oligocene glaciation and productivity in the eastern equatorial Pacific: Insights into global carbon cycling, Paleoceanography, 26(2), PA2221, doi:10.1029/2010PA002021, 2011.

1395 Coxall, H. K., Wilson, P. A., Palike, H., Lear, C. H. and Backman, J.: Rapid stepwise onset of Antarctic glaciation and deeper calcite compensation in the Pacific Ocean, Nature, 433(7021), 53–57, doi:10.1038/nature03135, 2005.

Coxall, H. K., Huck, C. E., Huber, M., Lear, C. H., Legarda-Lisarri, A., O'Regan, M., Sliwinska, K. K., van de Flierdt, T., de Boer, A. M., Zachos, J. C. and Backman, J.: Export of nutrient rich Northern Component Water preceded early Oligocene Antarctic glaciation, Nat. Geosci., 11(3), 190–196, doi:10.1038/s41561-018-0069-9, 2018.

1400 Cramer, B. S., Toggweiler, J. R., Wright, J. D., Katz, M. E. and Miller, K. G.: Ocean overturning since the Late Cretaceous: Inferences from a new benthic foraminiferal isotope compilation, Paleoceanography, 24(4), PA4216, doi:10.1029/2008PA001683, 2009.

Cramwinckel, M. J., Huber, M., Kocken, I. J., Agnini, C., Bijl, P. K., Bohaty, S. M., Frieling, J., Goldner, A., Hilgen, F. J., Kip, E. L., Peterse, F., van der Ploeg, R., Röhl, U., Schouten, S. and Sluijs, A.: Synchronous tropical and polar temperature 1405 evolution in the Eocene, Nature, 559(7714), 382–386, doi:10.1038/s41586-018-0272-2, 2018.

Cristini, L., Grosfeld, K., Butzin, M. and Lohmann, G.: Influence of the opening of the Drake Passage on the Cenozoic Antarctic Ice Sheet: A modeling approach, Palaeogeogr. Palaeoclimatol. Palaeoecol., 339–341, 66–73, doi:10.1016/j.palaeo.2012.04.023, 2012.

Crosby, A. G., McKenzie, D. and Sclater, J. G.: The relationship between depth, age and gravity in the oceans, Geophys. J. 1410 Int., 166(2), 553–573, doi:10.1111/j.1365-246X.2006.03015.x, 2006.

Dalziel, I. W. D., Lawver, L. A., Pearce, J. A., Barker, P. F., Hastie, A. R., Barfod, D. N., Schenke, H.-W. and Davis, M. B.: A potential barrier to deep Antarctic circumpolar flow until the late Miocene?, Geology, 41(9), 947–950, doi:10.1130/G34352.1, 2013.

Darby, D. A.: Ephemeral formation of perennial sea ice in the Arctic Ocean during the middle Eocene, Nat. Geosci., 7, 210, 1415 doi:10.1038/ngeo2068, 2014.

DeConto, R. M. and Pollard, D.: Rapid Cenozoic glaciation of Antarctica induced by declining atmospheric CO2, Nature, 421(6920), 245–249, doi:10.1038/nature01290, 2003.

DeConto, R. M., Pollard, D., Wilson, P. A., Palike, H., Lear, C. H. and Pagani, M.: Thresholds for Cenozoic bipolar glaciation, Nature, 455(7213), 652–656, doi:10.1038/nature07337, 2008.

1420 Dingle, R. V, Marenssi, S. A. and Lavelle, M.: High latitude Eocene climate deterioration: evidence from the northern Antarctic Peninsula, J. South Am. Earth Sci., 11(6), 571–579, doi:10.1016/S0895-9811(98)00035-2, 1998.

Doria, G., Royer, D. L., Wolfe, A. P., Fox, A., Westgate, J. A. and Beerling, D. J.: Declining atmospheric CO2 during the late Middle Eocene climate transition, Am. J. Sci., 311(1), 63–75, doi:10.2475/01.2011.03, 2011.

Dunkley Jones, T., Bown, P. R., Pearson, P. N., Wade, B. S., Coxall, H. K. and Lear, C. H.: Major shifts in calcareous 1425 phytoplankton assemblages through the Eocene-Oligocene transition of Tanzania and their implications for low-latitude primary production, Paleoceanography, 23(4), doi:10.1029/2008PA001640, 2008.

Dupont-Nivet, G., Krijgsman, W., Langereis, C. G., Abels, H. A., Dai, S. and Fang, X.: Tibetan plateau aridification linked to global cooling at the Eocene–Oligocene transition, Nature, 445, 635, doi:10.1038/nature05516, 2007.

Dupont-Nivet, G., Hoorn, C. and Konert, M.: Tibetan uplift prior to the Eocene-Oligocene climate transition: Evidence from

1430   pollen analysis of the Xining Basin, Geology, 36(12), 987–990, doi:10.1130/G25063A.1, 2008.

Eagles, G., Livermore, R. A., Fairhead, J. D. and Morris, P.: Tectonic evolution of the west Scotia Sea, J. Geophys. Res. Solid Earth, 110(B2), B02401, doi:10.1029/2004JB003154, 2005.

Ehlers, J. and Gibbard, P. L.: The extent and chronology of Cenozoic Global Glaciation, Quat. Int., 164–165, 6–20, doi:10.1016/j.quaint.2006.10.008, 2007.

1435   Ehrmann, W. U. and Mackensen, A.: Sedimentological evidence for the formation of an East Antarctic ice sheet in Eocene/Oligocene time, Palaeogeogr. Palaeoclimatol. Palaeoecol., 93(1), 85–112, doi:10.1016/0031-0182(92)90185-8, 1992.

Elderfield, H., Ferretti, P., Greaves, M., Crowhurst, S., McCave, I. N., Hodell, D. and Piotrowski, A. M.: Evolution of Ocean Temperature and Ice Volume Through the Mid-Pleistocene Climate Transition, Science, 337(6095), 704 LP – 709, doi:10.1126/science.1221294, 2012.

1440   Eldrett, J. S., Harding, I. C., Wilson, P. A., Butler, E. and Roberts, A. P.: Continental ice in Greenland during the Eocene and Oligocene, Nature, 446, 176, doi:10.1038/nature05591, 2007.

Eldrett, J. S., Greenwood, D. R., Harding, I. C. and Huber, M.: Increased seasonality through the Eocene to Oligocene transition in northern high latitudes, Nature, 459(7249), 969–973, doi:10.1038/nature08069, 2009.

Elsworth, G., Galbraith, E., Halverson, G. and Yang, S.: Enhanced weathering and CO2 drawdown caused by latest Eocene
1445   strengthening of the Atlantic meridional overturning circulation, Nat. Geosci, 10(3), 213–216, doi:10.1038/ngeo2888, 2017.

England, M. H., Hutchinson, D. K., Santoso, A. and Sijp, W. P.: Ice–Atmosphere Feedbacks Dominate the Response of the Climate System to Drake Passage Closure, J. Clim., 30(15), 5775–5790, doi:10.1175/JCLI-D-15-0554.1, 2017.

Erdei, B., Utescher, T., Hably, L., Tamas, J., Roth-Nebelsick, A. and Grein, M.: Early Oligocene continental climate of the Palaeogene Basin (Hungary and Slovenia) and the surrounding area, Turkish J. Earth Sci., 21, 153–186, doi:10.3906/yer-1005-
1450   29, 2012.

Escutia, C., Brinkhuis, H., Klaus, A. and the IODP Expedition 318 Scientists: IODP Expedition 318: From Greenhouse to Icehouse at the Wilkes Land Antarctic Margin, Sci. Drill., 12, 15–23, doi:10.2204/iodp.sd.12.02.2011, 2011.

Evans, D., Wade, B. S., Henehan, M., Erez, J. and Müller, W.: Revisiting carbonate chemistry controls on planktic foraminifera Mg / Ca: implications for sea surface temperature and hydrology shifts over the Paleocene–Eocene Thermal Maximum and
1455   Eocene–Oligocene transition, Clim. Past, 12(4), 819–835, doi:10.5194/cp-12-819-2016, 2016.

Evans, D., Sagoo, N., Renema, W., Cotton, L. J., Müller, W., Todd, J. A., Saraswati, P. K., Stassen, P., Ziegler, M., Pearson, P. N., Valdes, P. J. and Affek, H. P.: Eocene greenhouse climate revealed by coupled clumped isotope-Mg/Ca thermometry, Proc. Natl. Acad. Sci., 115(6), 1174 LP – 1179, doi:10.1073/pnas.1714744115, 2018.

Exon, N. F., Kennett, J. P. and Malone, M. J.: Leg 189 Synthesis: Cretaceous – Holocene history of the Tasmanian gateway,
1460   in Proceedings of the Ocean Drilling Program: Scientific Results, 189. [online] Available from: http://www.odp.tamu.edu/publications/189_SR/synth/synth.htm, 2004.

Falkowski, P. G., Katz, M. E., Knoll, A. H., Quigg, A., Raven, J. A., Schofield, O. and Taylor, F. J. R.: The Evolution of Modern Eukaryotic Phytoplankton, Science, 305(5682), 354 LP – 360, doi:10.1126/science.1095964, 2004.

Fan, M., Ayyash, S. A., Tripati, A., Passey, B. H. and Griffith, E. M.: Terrestrial cooling and changes in hydroclimate in the
1465   continental interior of the United States across the Eocene-Oligocene boundary, GSA Bull., 130(7–8), 1073–1084, doi:10.1130/B31732.1, 2017.

Farnsworth, A., Lunt, D. J., O'Brien, C., Foster, G. L., Inglis, G. N., Markwick, P., Pancost, R. D. and Robinson, S. A.: Climate sensitivity on geological timescales controlled by non-linear feedbacks and ocean circulation, Geophys. Res. Lett., doi:10.1029/2019GL083574, 2019.

1470   Ferreira, D., Cessi, P., Coxall, H. K., de Boer, A., Dijkstra, H. A., Drijfhout, S. S., Eldevik, T., Harnik, N., McManus, J. F., Marshall, D. P., Nilsson, J., Roquet, F., Schneider, T. and Wills, R. C.: Atlantic-Pacific Asymmetry in Deep Water Formation, Annu. Rev. Earth Planet. Sci., 46(1), 327–352, doi:10.1146/annurev-earth-082517-010045, 2018.

Figueirido, B., Janis, C. M., Pérez-Claros, J. A., De Renzi, M. and Palmqvist, P.: Cenozoic climate change influences mammalian evolutionary dynamics, Proc. Natl. Acad. Sci., 109(3), 722 LP – 727, doi:10.1073/pnas.1110246108, 2012.

1475   Foster, G. L. and Rae, J. W. B.: Reconstructing Ocean pH with Boron Isotopes in Foraminifera, Annu. Rev. Earth Planet. Sci., 44(1), 207–237, doi:10.1146/annurev-earth-060115-012226, 2016.

Foster, G. L., Lear, C. H. and Rae, J. W. B.: The evolution of pCO2, ice volume and climate during the middle Miocene, Earth Planet. Sci. Lett., 341–344, 243–254, doi:10.1016/j.epsl.2012.06.007, 2012.

Foster, G. L., Royer, D. L. and Lunt, D. J.: Future climate forcing potentially without precedent in the last 420 million years, 1480   Nat. Commun., 8, 14845, doi:10.1038/ncomms14845, 2017.

Francis, J. E., Marenssi, S., Levy, R., Hambrey, M., Thorn, V. C., Mohr, B., Brinkhuis, H., Warnaar, J., Zachos, J., Bohaty, S. and DeConto, R.: Chapter 8 From Greenhouse to Icehouse – The Eocene/Oligocene in Antarctica, in Antarctic Climate Evolution, vol. 8, edited by F. Florindo and M. B. T.-D. in E. and E. S. Siegert, pp. 309–368, Elsevier., 2008.

Franks, P. J., Royer, D. L., Beerling, D. J., Van de Water, P. K., Cantrill, D. J., Barbour, M. M. and Berry, J. A.: New constraints 1485   on atmospheric CO2 concentration for the Phanerozoic, Geophys. Res. Lett., 41(13), 4685–4694, doi:10.1002/2014GL060457, 2014.

Fyke, J. G., D'Orgeville, M. and Weaver, A. J.: Drake Passage and Central American Seaway controls on the distribution of the oceanic carbon reservoir, Glob. Planet. Change, 128(0), 72–82, doi:10.1016/j.gloplacha.2015.02.011, 2015.

Galeotti, S., DeConto, R., Naish, T., Stocchi, P., Florindo, F., Pagani, M., Barrett, P., Bohaty, S. M., Lanci, L., Pollard, D., 1490   Sandroni, S., Talarico, F. M. and Zachos, J. C.: Antarctic Ice Sheet variability across the Eocene-Oligocene boundary climate transition, Science, 352(6281), 76 LP – 80, doi:10.1126/science.aab0669, 2016.

Gallagher, T. M. and Sheldon, N. D.: A new paleothermometer for forest paleosols and its implications for Cenozoic climate, Geology, 41(6), 647–650, doi:10.1130/G34074.1, 2013.

Gasson, E., Siddall, M., Lunt, D. J., Rackham, O. J. L., Lear, C. H. and Pollard, D.: Exploring uncertainties in the relationship 1495   between temperature, ice volume, and sea level over the past 50 million years, Rev. Geophys., 50(1), doi:10.1029/2011RG000358, 2012.

Gasson, E., Lunt, D. J., DeConto, R., Goldner, A., Heinemann, M., Huber, M., LeGrande, A. N., Pollard, D., Sagoo, N., Siddall, M., Winguth, A. and Valdes, P. J.: Uncertainties in the modelled CO2 threshold for Antarctic glaciation, Clim. Past, 10(2), 451–466, doi:10.5194/cp-10-451-2014, 2014.

1500   Ghosh, P., Adkins, J., Affek, H., Balta, B., Guo, W., Schauble, E. A., Schrag, D. and Eiler, J. M.: 13C–18O bonds in carbonate minerals: A new kind of paleothermometer, Geochim. Cosmochim. Acta, 70(6), 1439–1456, doi:10.1016/j.gca.2005.11.014, 2006.

Gion, A. M., Williams, S. E. and Müller, R. D.: A reconstruction of the Eurekan Orogeny incorporating deformation constraints, Tectonics, 36(2), 304–320, doi:10.1002/2015TC004094, 2017.

Goddéris, Y., Donnadieu, Y., Le Hir, G., Lefebvre, V. and Nardin, E.: The role of palaeogeography in the Phanerozoic history of atmospheric CO2 and climate, Earth-Science Rev., 128, 122–138, doi:10.1016/j.earscirev.2013.11.004, 2014.

Goldner, A., Herold, N. and Huber, M.: Antarctic glaciation caused ocean circulation changes at the Eocene-Oligocene transition, Nature, 511(7511), 574–577, doi:10.1038/nature13597, 2014.

Gradstein, F. M., Ogg, J. G., Schmitz, M. and Ogg, G.: The geologic time scale 2012, Elsevier., 2012.

Greenop, R., Hain, M. P., Sosdian, S. M., Oliver, K. I. C., Goodwin, P., Chalk, T. B., Lear, C. H., Wilson, P. A. and Foster, G. L.: A record of Neogene seawater δ11B reconstructed from paired δ11B analyses on benthic and planktic foraminifera, Clim. Past, 13(2), 149–170, doi:10.5194/cp-13-149-2017, 2017.

Greenwood, D. R. and Wing, S. L.: Eocene continental climates and latitudinal temperature gradients, Geology, 23(11), 1044–1048, doi:10.1130/0091-7613(1995)023<1044:ECCALT>2.3.CO;2, 1995.

Grein, M., Oehm, C., Konrad, W., Utescher, T., Kunzmann, L. and Roth-Nebelsick, A.: Atmospheric CO2 from the late Oligocene to early Miocene based on photosynthesis data and fossil leaf characteristics, Palaeogeogr. Palaeoclimatol. Palaeoecol., 374, 41–51, doi:10.1016/j.palaeo.2012.12.025, 2013.

Griener, K. W., Nelson, D. M. and Warny, S.: Declining moisture availability on the Antarctic Peninsula during the Late Eocene, Palaeogeogr. Palaeoclimatol. Palaeoecol., 383–384, 72–78, doi:10.1016/j.palaeo.2013.05.004, 2013.

Grimes, S. T., Hooker, J. J., Collinson, M. E. and Mattey, D. P.: Summer temperatures of late Eocene to early Oligocene freshwaters, Geology, 33(3), 189–192, doi:10.1130/G21019.1, 2005.

Gurnis, M., Yang, T., Cannon, J., Turner, M., Williams, S., Flament, N. and Müller, R. D.: Global tectonic reconstructions with continuously deforming and evolving rigid plates, Comput. Geosci., 116, 32–41, doi:10.1016/j.cageo.2018.04.007, 2018.

Hegewald, A. and Jokat, W.: Relative sea level variations in the Chukchi region - Arctic Ocean - since the late Eocene, Geophys. Res. Lett., 40(5), 803–807, doi:10.1002/grl.50182, 2013.

Helland, P. E. and Holmes, M. A.: Surface textural analysis of quartz sand grains from ODP Site 918 off the southeast coast of Greenland suggests glaciation of southern Greenland at 11 Ma, Palaeogeogr. Palaeoclimatol. Palaeoecol., 135(1), 109–121, doi:10.1016/S0031-0182(97)00025-4, 1997.

Héran, M., Lécuyer, C. and Legendre, S.: Cenozoic long-term terrestrial climatic evolution in Germany tracked by δ18O of rodent tooth phosphate, Palaeogeogr. Palaeoclimatol. Palaeoecol., 285(3–4), 331–342, doi:10.1016/j.palaeo.2009.11.030, 2010.

Herman, A. B., Spicer, R. A., Aleksandrova, G. N., Yang, J., Kodrul, T. M., Maslova, N. P., Spicer, T. E. V, Chen, G. and Jin, J.-H.: Eocene–early Oligocene climate and vegetation change in southern China: Evidence from the Maoming Basin, Palaeogeogr. Palaeoclimatol. Palaeoecol., 479, 126–137, doi:10.1016/j.palaeo.2017.04.023, 2017.

Herold, N., Buzan, J., Seton, M., Goldner, A., Green, J. A. M., Müller, R. D., Markwick, P. and Huber, M.: A suite of early Eocene (~ 55 Ma) climate model boundary conditions, Geosci. Model Dev., 7(5), 2077–2090, doi:10.5194/gmd-7-2077-2014, 2014.

Heureux, A. M. C. and Rickaby, R. E. M.: Refining our estimate of atmospheric CO2 across the Eocene–Oligocene climatic transition, Earth Planet. Sci. Lett., 409, 329–338, doi:10.1016/j.epsl.2014.10.036, 2015.

Hill, D. J., Haywood, A. M., Valdes, P. J., Francis, J. E., Lunt, D. J., Wade, B. S. and Bowman, V. C.: Paleogeographic controls on the onset of the Antarctic circumpolar current, Geophys. Res. Lett., 40, 5199–5204, doi:10.1002/grl.50941, 2013.

Hincke, A. J. C., Broere, T., Kürschner, W. M., Donders, T. H. and Wagner-Cremer, F.: Multi-year leaf-level response to sub-ambient and elevated experimental CO2 in Betula nana, PLoS One, 11(6), e0157400, doi:10.1371/journal.pone.0157400, 2016.

1545 Hinojosa, L. F. and Villagrán, C.: Did South American Mixed Paleofloras evolve under thermal equability or in the absence of an effective Andean barrier during the Cenozoic?, Palaeogeogr. Palaeoclimatol. Palaeoecol., 217(1), 1–23, doi:10.1016/j.palaeo.2004.11.013, 2005.

van Hinsbergen, D. J. J., de Groot, L. V, van Schaik, S. J., Spakman, W., Bijl, P. K., Sluijs, A., Langereis, C. G. and Brinkhuis, H.: A Paleolatitude Calculator for Paleoclimate Studies., PLoS One, 10(6), e0126946, doi:10.1371/journal.pone.0126946, 1550 2015.

Hohbein, M. W., Sexton, P. F. and Cartwright, J. A.: Onset of North Atlantic Deep Water production coincident with inception of the Cenozoic global cooling trend, Geology, 40(3), 255–258, doi:10.1130/G32461.1, 2012.

Hollis, C. J., Handley, L., Crouch, E. M., Morgans, H. E. G., Baker, J. A., Creech, J., Collins, K. S., Gibbs, S. J., Huber, M., Schouten, S., Zachos, J. C. and Pancost, R. D.: Tropical sea temperatures in the high-latitude South Pacific during the Eocene, 1555 Geology, 37(2), 99–102, doi:10.1130/G25200A.1, 2009.

Hollis, C. J., Taylor, K. W. R., Handley, L., Pancost, R. D., Huber, M., Creech, J. B., Hines, B. R., Crouch, E. M., Morgans, H. E. G., Crampton, J. S., Gibbs, S., Pearson, P. N. and Zachos, J. C.: Early Paleogene temperature history of the Southwest Pacific Ocean: Reconciling proxies and models, Earth Planet. Sci. Lett., 349–350, 53–66, doi:10.1016/j.epsl.2012.06.024, 2012.

1560 Hollis, C. J., Dunkley Jones, T., Anagnostou, E., Bijl, P. K., Cramwinckel, M. J., Cui, Y., Dickens, G. R., Edgar, K. M., Eley, Y., Evans, D., Foster, G. L., Frieling, J., Inglis, G. N., Kennedy, E. M., Kozdon, R., Lauretano, V., Lear, C. H., Littler, K., Lourens, L., Meckler, A. N., Naafs, B. D. A., Pälike, H., Pancost, R. D., Pearson, P. N., Röhl, U., Royer, D. L., Salzmann, U., Schubert, B. A., Seebeck, H., Sluijs, A., Speijer, R. P., Stassen, P., Tierney, J., Tripati, A., Wade, B., Westerhold, T., Witkowski, C., Zachos, J. C., Zhang, Y. G., Huber, M. and Lunt, D. J.: The DeepMIP contribution to PMIP4: methodologies 1565 for selection, compilation and analysis of latest Paleocene and early Eocene climate proxy data, incorporating version 0.1 of the DeepMIP database, Geosci. Model Dev., 12(7), 3149–3206, doi:10.5194/gmd-12-3149-2019, 2019.

Homes, A. M., Cieraad, E., Lee, D. E., Lindqvist, J. K., Raine, J. I., Kennedy, E. M. and Conran, J. G.: A diverse fern flora including macrofossils with in situ spores from the late Eocene of southern New Zealand, Rev. Palaeobot. Palynol., 220, 16–28, doi:10.1016/j.revpalbo.2015.04.007, 2015.

1570 Hooker, J. J., Collinson, M. E. and Sille, N. P.: Eocene–Oligocene mammalian faunal turnover in the Hampshire Basin, UK: calibration to the global time scale and the major cooling event, J. Geol. Soc. London., 161(2), 161–172, doi:10.1144/0016-764903-091, 2004.

Houben, A. J. P., van Mourik, C. A., Montanari, A., Coccioni, R. and Brinkhuis, H.: The Eocene–Oligocene transition: Changes in sea level, temperature or both?, Palaeogeogr. Palaeoclimatol. Palaeoecol., 335–336, 75–83, 1575 doi:10.1016/j.palaeo.2011.04.008, 2012.

Hren, M. T., Sheldon, N. D., Grimes, S. T., Collinson, M. E., Hooker, J. J., Bugler, M. and Lohmann, K. C.: Terrestrial cooling in Northern Europe during the Eocene–Oligocene transition, Proc. Natl. Acad. Sci., 110(19), 7562 LP – 7567, doi:10.1073/pnas.1210930110, 2013.

Huang, X., Gohl, K. and Jokat, W.: Variability in Cenozoic sedimentation and paleo-water depths of the Weddell Sea basin 1580 related to pre-glacial and glacial conditions of Antarctica, Glob. Planet. Change, 118, 25–41, doi:10.1016/j.gloplacha.2014.03.010, 2014.

Huber, M.: A Hotter Greenhouse?, Science, 321(5887), 353–354, doi:10.1126/science.1161170, 2008.

Huber, M. and Caballero, R.: The early Eocene equable climate problem revisited, Clim. Past, 7(2), 603–633, doi:10.5194/cp-7-603-2011, 2011.

1585   Huber, M. and Nof, D.: The ocean circulation in the southern hemisphere and its climatic impacts in the Eocene, Palaeogeogr. Palaeoclimatol. Palaeoecol., 231(1–2), 9–28, doi:10.1016/j.palaeo.2005.07.037, 2006.

Huber, M. and Sloan, L. C.: Climatic responses to tropical sea surface temperature changes on a "greenhouse" Earth, Paleoceanography, 15(4), 443–450, doi:10.1029/1999PA000455, 2000.

Huber, M. and Sloan, L. C.: Heat transport, deep waters, and thermal gradients: Coupled simulation of an Eocene greenhouse
1590   climate, Geophys. Res. Lett., 28(18), 3481–3484, doi:10.1029/2001GL012943, 2001.

Huber, M., Sloan, L. and Shellito, C.: Early Paleogene oceans and climate: A fully coupled modeling approach using the NCAR CCSM, in: Causes and consequences of globally warm climates in the Early Paleogene, Geol. Soc. Am. Spec. Pap., 369, 25–47, 2003.

Huber, M., Brinkhuis, H., Stickley, C. E., Döös, K., Sluijs, A., Warnaar, J., Schellenberg, S. A. and Williams, G. L.: Eocene
1595   circulation of the Southern Ocean: Was Antarctica kept warm by subtropical waters?, Paleoceanography, 19(4), PA4026, doi:10.1029/2004PA001014, 2004.

Hurley, S. J., Elling, F. J., Könneke, M., Buchwald, C., Wankel, S. D., Santoro, A. E., Lipp, J. S., Hinrichs, K.-U. and Pearson, A.: Influence of ammonia oxidation rate on thaumarchaeal lipid composition and the TEX$_{86}$ temperature proxy, Proc. Natl. Acad. Sci., 113(28), 7762 LP – 7767, doi:10.1073/pnas.1518534113, 2016.

1600   Hutchinson, D. K., de Boer, A. M., Coxall, H. K., Caballero, R., Nilsson, J. and Baatsen, M.: Climate sensitivity and meridional overturning circulation in the late Eocene using GFDL CM2.1, Clim. Past, 14, 789–810, doi:10.5194/cp-14-789-2018, 2018.

Hutchinson, D. K., Coxall, H. K., O'Regan, M., Nilsson, J., Caballero, R. and de Boer, A. M.: Arctic closure as a trigger for Atlantic overturning at the Eocene-Oligocene Transition, Nat. Commun., 10, 3797, doi:10.1038/s41467-019-11828-z, 2019.

Hyeong, K., Kuroda, J., Seo, I. and Wilson, P. A.: Response of the Pacific inter-tropical convergence zone to global cooling
1605   and initiation of Antarctic glaciation across the Eocene Oligocene Transition, Sci. Rep., 6, 30647, doi:10.1038/srep30647, 2016.

Inglis, G. N., Farnsworth, A., Lunt, D., Foster, G. L., Hollis, C. J., Pagani, M., Jardine, P. E., Pearson, P. N., Markwick, P., Galsworthy, A. M. J., Raynham, L., Taylor, K. W. R. and Pancost, R. D.: Descent toward the Icehouse: Eocene sea surface cooling inferred from GDGT distributions, Paleoceanography, 30(7), 1000–1020, doi:10.1002/2014PA002723, 2015.

1610   Jacobs, B. F., Pan, A. D. and Scotese, C. R.: A review of the Cenozoic vegetation history of Africa, in Cenozoic mammals of Africa, edited by W. J. Werdelin, L., Sanders, pp. 57–72, University of California Press Berkeley., 2010.

Japsen, P., Bonow, J. M., Green, P. F., Chalmers, J. A. and Lidmar-Bergström, K.: Elevated, passive continental margins: Long-term highs or Neogene uplifts? New evidence from West Greenland, Earth Planet. Sci. Lett., 248(1), 330–339, doi:10.1016/j.epsl.2006.05.036, 2006.

1615   Japsen, P., Green, P. F. and Bonow, J. M.: Investigation of the Burial and Exhumation History of East Greenland Based On Apatite-fission Track Analysis, Stratigraphic Landform Analysis and the Geological Record, OTC Arct. Technol. Conf., 8, doi:10.4043/25562-MS, 2015.

Jin, J.-H., Herman, A. B., Spicer, R. A. and Kodrul, T. M.: Palaeoclimate background of the diverse Eocene floras of South

China, Sci. Bull., 62(22), 1501–1503, doi:10.1016/j.scib.2017.11.002, 2017.

1620 John, E. H., Pearson, P. N., Coxall, H. K., Birch, H., Wade, B. S. and Foster, G. L.: Warm ocean processes and carbon cycling in the Eocene, Philos. Trans. R. Soc. A Math. Phys. Eng. Sci., 371(2001), doi:10.1098/rsta.2013.0099, 2013.

John, E. H., Wilson, J. D., Pearson, P. N. and Ridgwell, A.: Temperature-dependent remineralization and carbon cycling in the warm Eocene oceans, Palaeogeogr. Palaeoclimatol. Palaeoecol., 413, 158–166, doi:10.1016/j.palaeo.2014.05.019, 2014.

St. John, K.: Cenozoic ice-rafting history of the central Arctic Ocean: Terrigenous sands on the Lomonosov Ridge, 1625 Paleoceanography, 23(1), doi:10.1029/2007PA001483, 2008.

Katz, M. E., Miller, K. G., Wright, J. D., Wade, B. S., Browning, J. V, Cramer, B. S. and Rosenthal, Y.: Stepwise transition from the Eocene greenhouse to the Oligocene icehouse, Nat. Geosci., 1, 329 [online] Available from: http://dx.doi.org/10.1038/ngeo179, 2008.

Katz, M. E., Cramer, B. S., Toggweiler, J. R., Esmay, G., Liu, C., Miller, K. G., Rosenthal, Y., Wade, B. S. and Wright, J. D.: 1630 Impact of Antarctic Circumpolar Current development on late Paleogene ocean structure., Science, 332(6033), 1076–1079, doi:10.1126/science.1202122, 2011.

Kennedy-Asser, A. T., Lunt, D. J., Farnsworth, A. and Valdes, P. J.: Assessing Mechanisms and Uncertainty in Modeled Climatic Change at the Eocene-Oligocene Transition, Paleoceanogr. Paleoclimatology, 34(1), 16–34, doi:10.1029/2018PA003380, 2019.

1635 Kennedy-Asser, A. T., Lunt, D. J., Valdes, P. J., Ladant, J.-B., Frieling, J. and Lauretano, V.: Changes in the high-latitude Southern Hemisphere through the Eocene--Oligocene transition: a model--data comparison, Clim. Past, 16(2), 555–573, doi:10.5194/cp-16-555-2020, 2020.

Kennedy, A. T., Farnsworth, A., Lunt, D. J., Lear, C. H. and Markwick, P. J.: Atmospheric and oceanic impacts of Antarctic glaciation across the Eocene–Oligocene transition, Phil. Trans. R. Soc. A, 373(2054), 20140419, doi:10.1098/rsta.2014.0419, 1640 2015.

Kennett, J. P.: Cenozoic Evolution of Antarctic Glaciation, the Circum-Antarctic Ocean, and Their Impact on Global Paleoceanography, J. Geophys. Res., 82(27), 3843–3860, doi:10.1029/JC082i027p03843, 1977.

Kennett, J. P. and Shackleton, N. J.: Oxygen isotopic evidence for the development of the psychrosphere 38 Myr ago, Nature, 260, 513, doi:10.1038/260513a0, 1976.

1645 Kennett, J. P., Houtz, R. E., Andrews, P. B., Edwards, A. R., Gostin, V. A., Hajos, M., Hampton, M., Jenkins, D. G., Margolis, S. V, Ovenshine, A. T. and Perch-Nielsen, K.: Cenozoic paleoceanography in the Southwest Pacific Ocean, Antarctic glaciation, and the development of the Circum-Antarctic Current, Initial Rep. Deep Sea Drill. Proj., 29, 1155, 1975.

Kiehl, J. T. and Shields, C. A.: Sensitivity of the Palaeocene–Eocene Thermal Maximum climate to cloud properties, Philos. Trans. R. Soc. A Math. Phys. Eng. Sci., 371(2001), 20130093, doi:10.1098/rsta.2013.0093, 2013.

1650 Kim, J.-H., van der Meer, J., Schouten, S., Helmke, P., Willmott, V., Sangiorgi, F., Koç, N., Hopmans, E. C. and Damsté, J. S. S.: New indices and calibrations derived from the distribution of crenarchaeal isoprenoid tetraether lipids: Implications for past sea surface temperature reconstructions, Geochim. Cosmochim. Acta, 74(16), 4639–4654, doi:10.1016/j.gca.2010.05.027, 2010.

Kim, S. L., Eberle, J. J., Bell, D. M., Fox, D. A. and Padilla, A.: Evidence from shark teeth for a brackish Arctic Ocean in the 1655 Eocene greenhouse, Geology, 42(8), 695–698, doi:10.1130/G35675.1, 2014.

Kobashi, T., Grossman, E. L., Dockery, D. T. and Ivany, L. C.: Water mass stability reconstructions from greenhouse (Eocene) to icehouse (Oligocene) for the northern Gulf Coast continental shelf (USA), Paleoceanography, 19(1), PA1022, doi:10.1029/2003PA000934, 2004.

1660 Kocsis, L., Ozsvárt, P., Becker, D., Ziegler, R., Scherler, L. and Codrea, V.: Orogeny forced terrestrial climate variation during the late Eocene–early Oligocene in Europe, Geology, 42(8), 727–730, doi:10.1130/G35673.1, 2014.

Kohn, M. J., Josef, J. A., Madden, R., Kay, R., Vucetich, G. and Carlini, A. A.: Climate stability across the Eocene-Oligocene transition, southern Argentina, Geology, 32(7), 621–624, doi:10.1130/G20442.1, 2004.

Kohn, M. J., Strömberg, C. A. E., Madden, R. H., Dunn, R. E., Evans, S., Palacios, A. and Carlini, A. A.: Quasi-static Eocene– Oligocene climate in Patagonia promotes slow faunal evolution and mid-Cenozoic global cooling, Palaeogeogr. 1665 Palaeoclimatol. Palaeoecol., 435, 24–37, doi:https://doi.org/10.1016/j.palaeo.2015.05.028, 2015.

Konrad, W., Roth-Nebelsick, A. and Grein, M.: Modelling of stomatal density response to atmospheric CO_2, J. Theor. Biol., 253(4), 638–658, doi:10.1016/j.jtbi.2008.03.032, 2008.

Kovar-Eder, J.: Early Oligocene plant diversity along the Upper Rhine Graben: The fossil flora of Rauenberg, Germany, Acta Palaeobot., 56, 329, doi:10.1515/acpa-2016-0011, 2016.

1670 Krylov, A. A., Andreeva, I. A., Vogt, C., Backman, J., Krupskaya, V. V, Grikurov, G. E., Moran, K. and Shoji, H.: A shift in heavy and clay mineral provenance indicates a middle Miocene onset of a perennial sea ice cover in the Arctic Ocean, Paleoceanography, 23(1), doi:10.1029/2007PA001497, 2008.

Kunzmann, L., Kvaček, Z., Teodoridis, V., Müller, C. and Moraweck, K.: Vegetation dynamics of riparian forest in central Europe during the late Eocene, Palaeontogr. Abteilung B, 295(1–3), 69–89, doi:10.1127/palb/295/2016/69, 2016.

1675 Kürschner, W. M., Kvaček, Z. and Dilcher, D. L.: The impact of Miocene atmospheric carbon dioxide fluctuations on climate and the evolution of terrestrial ecosystems, Proc. Natl. Acad. Sci., 105(2), 449 LP – 453, doi:10.1073/pnas.0708588105, 2008.

Kvaček, Z., Teodoridis, V., Mach, K., Přikryl, T. and Dvořák, Z.: Tracing the Eocene-Oligocene transition: a case study from North Bohemia., Bull. Geosci., 89(1), 21–66, doi:10.3140/bull.geosci.1411, 2014.

Ladant, J.-B., Donnadieu, Y. and Dumas, C.: Links between CO_2, glaciation and water flow: reconciling the Cenozoic history 1680 of the Antarctic Circumpolar Current, Clim. Past, 10(6), 1957–1966, doi:10.5194/cp-10-1957-2014, 2014a.

Ladant, J.-B., Donnadieu, Y., Lefebvre, V. and Dumas, C.: The respective role of atmospheric carbon dioxide and orbital parameters on ice sheet evolution at the Eocene-Oligocene transition, Paleoceanography, 29(8), 810–823, doi:10.1002/2013PA002593, 2014b.

Langton, S. J., Rabideaux, N. M., Borrelli, C. and Katz, M. E.: Southeastern Atlantic deep-water evolution during the late- 1685 middle Eocene to earliest Oligocene (Ocean Drilling Program Site 1263 and Deep Sea Drilling Project Site 366), Geosphere, 12(3), 1032–1047, doi:10.1130/GES01268.1, 2016.

Larsen, H. C., Saunders, A. D., Clift, P. D., Beget, J., Wei, W. and Spezzaferri, S.: Seven Million Years of Glaciation in Greenland, Science, 264(5161), 952 LP – 955, doi:10.1126/science.264.5161.952, 1994.

Lear, C. H., Elderfield, H. and Wilson, P. A.: Cenozoic Deep-Sea Temperatures and Global Ice Volumes from Mg/Ca in 1690 Benthic Foraminiferal Calcite, Science, 287(5451), 269 LP – 272, doi:10.1126/science.287.5451.269, 2000.

Lear, C. H., Rosenthal, Y., Coxall, H. K. and Wilson, P. A.: Late Eocene to early Miocene ice sheet dynamics and the global carbon cycle, Paleoceanography, 19(4), doi:10.1029/2004PA001039, 2004.

Lear, C. H., Bailey, T. R., Pearson, P. N., Coxall, H. K. and Rosenthal, Y.: Cooling and ice growth across the Eocene-Oligocene transition, Geology, 36(3), 251, doi:10.1130/G24584A.1, 2008.

1695 Lear, C. H., Mawbey, E. M. and Rosenthal, Y.: Cenozoic benthic foraminiferal Mg/Ca and Li/Ca records: Toward unlocking temperatures and saturation states, Paleoceanography, 25(4), doi:10.1029/2009PA001880, 2010.

Lear, C. H., Coxall, H. K., Foster, G. L., Lunt, D. J., Mawbey, E. M., Rosenthal, Y., Sosdian, S. M., Thomas, E. and Wilson, P. A.: Neogene ice volume and ocean temperatures: Insights from infaunal foraminiferal Mg/Ca paleothermometry, Paleoceanography, 30(11), 1437–1454, doi:10.1002/2015PA002833, 2015.

1700 Lefebvre, V., Donnadieu, Y., Sepulchre, P., Swingedouw, D. and Zhang, Z.-S.: Deciphering the role of southern gateways and carbon dioxide on the onset of the Antarctic Circumpolar Current, Paleoceanography, 27(4), PA4201, doi:10.1029/2012PA002345, 2012.

Lielke, K., Manchester, S. and Meyer, H.: Reconstructing the environment of the northern Rocky Mountains during the Eocene/Oligocene transition: constraints from the palaeobotany and geology of south-western Montana, USA, Acta Palaeobot., 1705 52(2), 317–358 [online] Available from: http://bomax.botany.pl/pubs-new/#article-3604, 2012.

Linnemann, U., Su, T., Kunzmann, L., Spicer, R. A., Ding, W.-N., Spicer, T. E. V, Zieger, J., Hofmann, M., Moraweck, K., Gärtner, A., Gerdes, A., Marko, L., Zhang, S.-T., Li, S.-F., Tang, H., Huang, J., Mulch, A., Mosbrugger, V. and Zhou, Z.-K.: New U-Pb dates show a Paleogene origin for the modern Asian biodiversity hot spots, Geology, 46(1), 3–6, doi:10.1130/G39693.1, 2017.

1710 Liu, W., Xie, S.-P., Liu, Z. and Zhu, J.: Overlooked possibility of a collapsed Atlantic Meridional Overturning Circulation in warming climate, Sci. Adv., 3(1), doi:10.1126/sciadv.1601666, 2017.

Liu, X. Y., Gao, Q., Han, M. and Jin, J. H.: Estimates of late middle Eocene CO2 based on stomatal density of modern and fossil Nageia leaves, Clim. Past, 12(2), 241–253, doi:10.5194/cp-12-241-2016, 2016.

Liu, Z., Tuo, S., Zhao, Q., Cheng, X. and Huang, W.: Deep-water Earliest Oligocene Glacial Maximum (EOGM) in South 1715 Atlantic, Chinese Sci. Bull., 49(20), 2190–2197, doi:10.1007/BF03185787, 2004.

Liu, Z., Pagani, M., Zinniker, D., DeConto, R., Huber, M., Brinkhuis, H., Shah, S. R., Leckie, R. M. and Pearson, A.: Global Cooling During the Eocene-Oligocene Climate Transition, Science, 323(5918), 1187–1190, doi:10.1126/science.1166368, 2009.

Liu, Z., He, Y., Jiang, Y., Wang, H., Liu, W., Bohaty, S. M. and Wilson, P. A.: Transient temperature asymmetry between 1720 hemispheres in the Palaeogene Atlantic Ocean, Nat. Geosci., 11, 656–660, doi:10.1038/s41561-018-0182-9, 2018.

Livermore, R., Hillenbrand, C.-D., Meredith, M. and Eagles, G.: Drake Passage and Cenozoic climate: An open and shut case?, Geochemistry, Geophys. Geosystems, 8(1), Q01005, doi:10.1029/2005GC001224, 2007.

Lunt, D. J., Foster, G. L., Haywood, A. M. and Stone, E. J.: Late Pliocene Greenland glaciation controlled by a decline in atmospheric CO2 levels, Nature, 454(7208), 1102–5, doi:10.1038/nature07223, 2008.

1725 Lunt, D. J., Dunkley Jones, T., Heinemann, M., Huber, M., LeGrande, A., Winguth, A., Loptson, C., Marotzke, J., Roberts, C. D., Tindall, J., Valdes, P. and Winguth, C.: A model–data comparison for a multi-model ensemble of early Eocene atmosphere–ocean simulations: EoMIP, Clim. Past, 8(5), 1717–1736, doi:10.5194/cp-8-1717-2012, 2012.

Lunt, D. J., Farnsworth, A., Loptson, C., Foster, G. L., Markwick, P., O'Brien, C. L., Pancost, R. D., Robinson, S. A. and Wrobel, N.: Palaeogeographic controls on climate and proxy interpretation, Clim. Past, 12(5), 1181–1198, doi:10.5194/cp-12-1730 1181-2016, 2016.

Lyell, C. and Deshayes, G. P.: Principles of Geology: being an attempt to explain the former changes of the Earth's surface, by reference to causes now in operation, John Murray., 1830.

Macphail, M.: Australian palaeoclimates: Cretaceous to Tertiary a review of palaeobotanical and related evidence to the year 2000, CRC LEME Open File Report 151,., 2007.

1735   Maher, K. and Chamberlain, C. P.: Hydrologic Regulation of Chemical Weathering and the Geologic Carbon Cycle, Science, 343(6178), 1502 LP – 1504, doi:10.1126/science.1250770, 2014.

Mai, D. H.: Tertiäre Vegetationsgeschichte Europas, Feddes Repert., 106(3–4), 331, doi:10.1002/fedr.19951060333, 1995.

Markwick, P. J.: The palaeogeographic and palaeoclimatic significance of climate proxies for data-model comparisons, in Deep-time perspectives on climate change: marrying the signal from computer models and biological proxies, pp. 251–312,
1740   Micropalaeontol. Soc. Spec. Publ. London., 2007.

Markwick, P. J.: Palaeogeography in exploration, Geol. Mag., 156(2), 366–407, doi:10.1017/S0016756818000468, 2019.

Markwick, P. J. and Valdes, P. J.: Palaeo-digital elevation models for use as boundary conditions in coupled ocean–atmosphere GCM experiments: a Maastrichtian (late Cretaceous) example, Palaeogeogr. Palaeoclimatol. Palaeoecol., 213(1), 37–63, doi:10.1016/j.palaeo.2004.06.015, 2004.

1745   Martin, H. A.: Cenozoic climatic change and the development of the arid vegetation in Australia, J. Arid Environ., 66(3), 533–563, doi:10.1016/j.jaridenv.2006.01.009, 2006.

Martini, E.: Standard Tertiary and Quaternary calcareous nannoplankton zonation, in Proc. II Planktonic Conference, Roma 1970, Roma, Tecnoscienza, edited by A. Farinacci, pp. 739–785., 1971.

Maslin, M. A., Li, X. S., Loutre, M.-F. and Berger, A.: The contribution of orbital forcing to the progressive intensification of
1750   Northern Hemisphere glaciation, Quat. Sci. Rev., 17(4), 411–426, doi:10.1016/S0277-3791(97)00047-4, 1998.

Maxbauer, D. P., Royer, D. L. and LePage, B. A.: High Arctic forests during the middle Eocene supported by moderate levels of atmospheric CO2, Geology, 42(12), 1027–1030, doi:10.1130/G36014.1, 2014.

McElwain, J. C. and Chaloner, W. G.: Stomatal Density and Index of Fossil Plants Track Atmospheric Carbon Dioxide in the Palaeozoic, Ann. Bot., 76(4), 389–395, doi:10.1006/anbo.1995.1112, 1995.

1755   McKay, R. M., Barrett, P. J., Levy, R. S., Naish, T. R., Golledge, N. R. and Pyne, A.: Antarctic Cenozoic climate history from sedimentary records: ANDRILL and beyond, Philos. Trans. R. Soc. A Math. Phys. Eng. Sci., 374(2059), doi:10.1098/rsta.2014.0301, 2016.

McKinley, C. C., Thomas, D. J., LeVay, L. J. and Rolewicz, Z.: Nd isotopic structure of the Pacific Ocean 40–10 Ma, and evidence for the reorganization of deep North Pacific Ocean circulation between 36 and 25 Ma, Earth Planet. Sci. Lett., 521,
1760   139–149, doi:10.1016/j.epsl.2019.06.009, 2019.

Merico, A., Tyrrell, T. and Wilson, P. A.: Eocene/Oligocene ocean de-acidification linked to Antarctic glaciation by sea-level fall, Nature, 452(7190), 979–982, doi:10.1038/nature06853, 2008.

Meyers, J. A.: Terrestrial Eocene-Oligocene vegetation and climate in the Pacific Northwest, in From Greenhouse to Icehouse: The Marine Eocene-Oligocene Transition, edited by D. R. Prothero, L. C. Ivany, and E. A. Nesbitt, pp. 171–185, Columbia
1765   University Press, New York., 2003.

Mihlbachler, M. C., Rivals, F., Solounias, N. and Semprebon, G. M.: Dietary Change and Evolution of Horses in North

America, Science, 331(6021), 1178 LP – 1181, doi:10.1126/science.1196166, 2011.

Mikolajewicz, U., Maier-Reimer, E., Crowley, T. J. and Kim, K.-Y.: Effect of Drake and Panamanian Gateways on the circulation of an ocean model, Paleoceanography, 8(4), 409–426, doi:10.1029/93PA00893, 1993.

1770 Miller, K. G., Janecek, T. R., Katz, M. E. and Keil, D. J.: Abyssal circulation and benthic foraminiferal changes near the Paleocene/Eocene boundary, Paleoceanography, 2(6), 741–761, doi:10.1029/PA002i006p00741, 1987.

Miller, K. G., Wright, J. D. and Fairbanks, R. G.: Unlocking the Ice House: Oligocene-Miocene oxygen isotopes, eustasy, and margin erosion, J. Geophys. Res. Solid Earth, 96(B4), 6829–6848, doi:10.1029/90JB02015, 1991.

Miller, K. G., Browning, J. V, Aubry, M.-P., Wade, B. S., Katz, M. E., Kulpecz, A. A. and Wright, J. D.: Eocene–Oligocene 1775 global climate and sea-level changes: St. Stephens Quarry, Alabama, GSA Bull., 120(1–2), 34–53, doi:10.1130/B26105.1, 2008.

Moraweck, K., Grein, M., Konrad, W., Kva\vcek, J., Kova-Eder, J., Neinhuis, C., Traiser, C. and Kunzmann, L.: Leaf traits of long-ranging Paleogene species and their relationship with depositional facies, climate and atmospheric CO2 level, Palaeontogr. Abteilung B, 298(4–6), 93–172, doi:10.1127/palb/2019/0062, 2019.

1780 Mudelsee, M., Bickert, T., Lear, C. H. and Lohmann, G.: Cenozoic climate changes: A review based on time series analysis of marine benthic δ 18 O records, Rev. Geophys., 52(3), 333–374, doi:10.1002/2013RG000440, 2014.

Müller, P. J., Kirst, G., Ruhland, G., von Storch, I. and Rosell-Melé, A.: Calibration of the alkenone paleotemperature index U37K′ based on core-tops from the eastern South Atlantic and the global ocean (60°N-60°S), Geochim. Cosmochim. Acta, 62(10), 1757–1772, doi:10.1016/S0016-7037(98)00097-0, 1998.

1785 Müller, R. D., Sdrolias, M., Gaina, C. and Roest, W. R.: Age, spreading rates, and spreading asymmetry of the world's ocean crust, Geochemistry, Geophys. Geosystems, 9(4), Q04006, doi:10.1029/2007GC001743, 2008.

Negri, F. R., Bocquentin-Villanueva, J., Ferigolo, J. and Antoine, P.-O.: A Review of Tertiary Mammal Faunas and Birds from Western Amazonia, in Amazonia: Landscape and Species Evolution, pp. 243–258, Wiley-Blackwell Publishing Ltd., 2009.

Nocchi, M., Parisi, G., Monaco, P., Monechi, S., Madile, M., Napoleone, G., Ripepe, M., Orlando, M., Premoli Silva, I. and 1790 Bice, D. M.: The Eocene-Oligocene Boundary in the Umbrian Pelagic Sequences, Italy, in termbal eocene events, vol. 9, edited by C. Pomerol and I. B. T.-D. in P. and S. Premoli-Silva, pp. 25–40, Elsevier., 1986.

Nof, D., Van Gorder, S. and de Boer, A.: Does the Atlantic meridional overturning cell really have more than one stable steady state?, Deep Sea Res. Part I Oceanogr. Res. Pap., 54(11), 2005–2021, doi:10.1016/j.dsr.2007.08.006, 2007.

O'Regan, M., Williams, C. J., Frey, K. E. and Jakobsson, M.: A Synthesis of the Long-Term Paleoclimatic Evolution of the 1795 Arctic, Oceanography, 24, doi:10.5670/oceanog.2011.57, 2011.

Oboh-Ikuenobe, F. E. and Jaramillo, C. A.: Palynological patterns in the uppermost Eocene to lower Oligocene sedimentary, in From Greenhouse to Icehouse: The Marine Eocene-Oligocene Transition, p. 269, Columbia University Press., 2003.

Olivarez Lyle, A. and Lyle, M. W.: Missing organic carbon in Eocene marine sediments: Is metabolism the biological feedback that maintains end-member climates?, Paleoceanography, 21(2), PA2007, doi:10.1029/2005PA001230, 2006.

1800 Olivetti, V., Balestrieri, M. L., Rossetti, F. and Talarico, F. M.: Tectonic and climatic signals from apatite detrital fission track analysis of the Cape Roberts Project core records, South Victoria Land, Antarctica, Tectonophysics, 594, 80–90, doi:10.1016/j.tecto.2013.03.017, 2013.

Olivetti, V., Balestrieri, M. L., Rossetti, F., Thomson, S. N., Talarico, F. M. and Zattin, M.: Evidence of a full West Antarctic Ice Sheet back to the early Oligocene: insight from double dating of detrital apatites in Ross Sea sediments., Terra Nov., 27(3), 1805 238–246, doi:10.1111/ter.12153, 2015.

Opdyke, B. N. and Wilkinson, B. H.: Surface area control of shallow cratonic to deep marine carbonate accumulation, Paleoceanography, 3(6), 685–703, doi:10.1029/PA003i006p00685, 1988.

Pagani, M., Zachos, J. C., Freeman, K. H., Tipple, B. and Bohaty, S.: Marked Decline in Atmospheric Carbon Dioxide Concentrations During the Paleogene, Science, 309(5734), 600 LP – 603, doi:10.1126/science.1110063, 2005.

1810 Pagani, M., Huber, M., Liu, Z., Bohaty, S. M., Henderiks, J., Sijp, W., Krishnan, S. and DeConto, R. M.: The Role of Carbon Dioxide During the Onset of Antarctic Glaciation, Science, 334(6060), 1261–1264, doi:10.1126/science.1203909, 2011.

Page, M., Licht, A., Dupont-Nivet, G., Meijer, N., Barbolini, N., Hoorn, C., Schauer, A., Huntington, K., Bajnai, D., Fiebig, J., Mulch, A. and Guo, Z.: Synchronous cooling and decline in monsoonal rainfall in northeastern Tibet during the fall into the Oligocene icehouse, , doi:10.1130/G45480.1, 2019.

1815 Palike, H., Lyle, M. W., Nishi, H., Raffi, I., Ridgwell, A., Gamage, K., Klaus, A., Acton, G., Anderson, L., Backman, J., Baldauf, J., Beltran, C., Bohaty, S. M., BownPaul, Busch, W., Channell, J. E. T., Chun, C. O. J., Delaney, M., Dewangan, P., Dunkley Jones, T., Edgar, K. M., Evans, H., Fitch, P., Foster, G. L., Gussone, N., Hasegawa, H., Hathorne, E. C., Hayashi, H., Herrle, J. O., Holbourn, A., Hovan, S., Hyeong, K., Iijima, K., Ito, T., Kamikuri, S., Kimoto, K., Kuroda, J., Leon-Rodriguez, L., Malinverno, A., Moore Jr, T. C., Murphy, B. H., Murphy, D. P., Nakamura, H., Ogane, K., Ohneiser, C., Richter, C., 1820 Robinson, R., Rohling, E. J., Romero, O., Sawada, K., Scher, H., Schneider, L., Sluijs, A., Takata, H., Tian, J., Tsujimoto, A., Wade, B. S., Westerhold, T., Wilkens, R., Williams, T., Wilson, P. A., Yamamoto, Y., Yamamoto, S., Yamazaki, T. and Zeebe, R. E.: A Cenozoic record of the equatorial Pacific carbonate compensation depth, Nature, 488(7413), 609–614, doi:10.1038/nature11360, 2012.

Pan, A. D., Jacobs, B. F., Dransfield, J. and Baker, W. J.: The fossil history of palms (Arecaceae) in Africa and new records 1825 from the Late Oligocene (28–27 Mya) of north-western Ethiopia, Bot. J. Linn. Soc., 151(1), 69–81, doi:10.1111/j.1095-8339.2006.00523.x, 2006.

Passchier, S., Bohaty, S. M., Jiménez-Espejo, F., Pross, J., Röhl, U., van de Flierdt, T., Escutia, C. and Brinkhuis, H.: Early Eocene to middle Miocene cooling and aridification of East Antarctica, Geochemistry, Geophys. Geosystems, 14(5), 1399–1410, doi:10.1002/ggge.20106, 2013.

1830 Passchier, S., Ciarletta, D. J., Miriagos, T. E., Bijl, P. K. and Bohaty, S. M.: An Antarctic stratigraphic record of stepwise ice growth through the Eocene-Oligocene transition, GSA Bull., 129(3–4), 318–330, doi:10.1130/B31482.1, 2017.

Pearson, A. and Ingalls, A. E.: Assessing the Use of Archaeal Lipids as Marine Environmental Proxies, Annu. Rev. Earth Planet. Sci., 41(1), 359–384, doi:10.1146/annurev-earth-050212-123947, 2013.

Pearson, P. N. and Palmer, M. R.: Middle Eocene Seawater pH and Atmospheric Carbon Dioxide Concentrations, Science, 1835 284(5421), 1824 LP – 1826, doi:10.1126/science.284.5421.1824, 1999.

Pearson, P. N. and Palmer, M. R.: Atmospheric carbon dioxide concentrations over the past 60 million years, Nature, 406, 695, doi:10.1038/35021000, 2000.

Pearson, P. N., Ditchfield, P. W., Singano, J., Harcourt-Brown, K. G., Nicholas, C. J., Olsson, R. K., Shackleton, N. J. and Hall, M. A.: Warm tropical sea surface temperatures in the Late Cretaceous and Eocene epochs, Nature, 413(6855), 481–487, 1840 doi:10.1038/35097000, 2001.

Pearson, P. N., van Dongen, B. E., Nicholas, C. J., Pancost, R. D., Schouten, S., Singano, J. M. and Wade, B. S.: Stable warm

tropical climate through the Eocene Epoch, Geology, 35(3), 211–214, doi:10.1130/G23175A.1, 2007.

Pearson, P. N., McMillan, I. K., Wade, B. S., Jones, T. D., Coxall, H. K., Bown, P. R. and Lear, C. H.: Extinction and environmental change across the Eocene-Oligocene boundary in Tanzania, Geology, 36(2), 179–182, doi:10.1130/G24308A.1, 2008.

Pearson, P. N., Foster, G. L. and Wade, B. S.: Atmospheric carbon dioxide through the Eocene–Oligocene climate transition, Nature, 461(7267), 1110–1113, doi:10.1038/nature08447, 2009.

Peck, V. L., Yu, J., Kender, S. and Riesselman, C. R.: Shifting ocean carbonate chemistry during the Eocene-Oligocene climate transition: Implications for deep-ocean Mg/Ca paleothermometry, Paleoceanography, 25(4), doi:10.1029/2009PA001906, 2010.

Pérez, L. F., Nielsen, T., Knutz, P. C., Kuijpers, A. and Damm, V.: Large-scale evolution of the central-east Greenland margin: New insights to the North Atlantic glaciation history, Glob. Planet. Change, 163, 141–157, doi:10.1016/j.gloplacha.2017.12.010, 2018.

Petersen, S. V and Schrag, D. P.: Antarctic ice growth before and after the Eocene-Oligocene transition: New estimates from clumped isotope paleothermometry, Paleoceanography, 30(10), 1305–1317, doi:10.1002/2014PA002769, 2015.

Piepjohn, K., von Gosen, W. and Tessensohn, F.: The Eurekan deformation in the Arctic: an outline, J. Geol. Soc. London., 173(6), 1007–1024, doi:10.1144/jgs2016-081, 2016.

Piga, E.: How Hot is Hot? Tropical Ocean Temperatures and Plankton Communities in the Eocene Epoch, PhD Thesis, Cardiff University, submitted., 2020.

Pocknall, D. T.: Palynostratigraphy of the Te Kuiti Group (late Eocene-Oligocene), Waikato Basin, New Zealand, New Zeal. J. Geol. Geophys., 34(4), 407–417, doi:10.1080/00288306.1991.9514479, 1991.

Pollard, D.: A retrospective look at coupled ice sheet–climate modeling, Clim. Change, 100(1), 173–194, doi:10.1007/s10584-010-9830-9, 2010.

Pollard, D. and DeConto, R. M.: Hysteresis in Cenozoic Antarctic ice-sheet variations, Glob. Planet. Change, 45(1–3), 9–21, doi:10.1016/j.gloplacha.2004.09.011, 2005.

Pomerol, C. and Premoli Silva, I.: The Eocene-Oligocene Transition: Events and Boundary, in Terminal Eocene Events, vol. 9, edited by C. Pomerol and I. B. T.-D. in P. and S. Premoli-Silva, pp. 1–24, Elsevier., 1986.

Postigo Mijarra, J. M., Barrón, E., Gómez Manzaneque, F. and Morla, C.: Floristic changes in the Iberian Peninsula and Balearic Islands (south-west Europe) during the Cenozoic, J. Biogeogr., 36(11), 2025–2043, doi:10.1111/j.1365-2699.2009.02142.x, 2009.

Pound, M. J. and Salzmann, U.: Heterogeneity in global vegetation and terrestrial climate change during the late Eocene to early Oligocene transition, Sci. Rep., 7, 43386, doi:10.1038/srep43386, 2017.

Premoli Silva, I. and Jenkins, D. G.: Decision on the Eocene-Oligocene boundary stratotype, Episodes, 16(3), 379–382, 1993.

Pross, J., Contreras, L., Bijl, P. K., Greenwood, D. R., Bohaty, S. M., Schouten, S., Bendle, J. A., Röhl, U., Tauxe, L., Raine, J. I., Huck, C. E., van de Flierdt, T., Jamieson, S. S. R., Stickley, C. E., van de Schootbrugge, B., Escutia, C. and Brinkhuis, H.: Persistent near-tropical warmth on the Antarctic continent during the early Eocene epoch, Nature, 488, 73, doi:10.1038/nature11300, 2012.

Prothero, D.: Cenozoic Mammals and Climate Change: The Contrast between Coarse-Scale versus High-Resolution Studies Explained by Species Sorting, Geosci. , 2(2), doi:10.3390/geosciences2020025, 2012.

1880 Prothero, D. R.: Did impacts, volcanic eruptions, or climate change affect mammalian evolution?, Palaeogeogr. Palaeoclimatol. Palaeoecol., 214(3), 283–294, doi:10.1016/j.palaeo.2004.04.010, 2004.

Pusz, A. E., Thunell, R. C. and Miller, K. G.: Deep water temperature, carbonate ion, and ice volume changes across the Eocene-Oligocene climate transition, Paleoceanography, 26(2), PA2205, doi:10.1029/2010PA001950, 2011.

Qin, W., Carlson, L. T., Armbrust, E. V., Devol, A. H., Moffett, J. W., Stahl, D. A. and Ingalls, A. E.: Confounding effects of 1885 oxygen and temperature on the TEX86 signature of marine Thaumarchaeota, Proc. Natl. Acad. Sci., 112(35), 10979 LP – 10984, doi:10.1073/pnas.1501568112, 2015.

Quattrocchio, M. E., Martínez, M. A., Hinojosa, L. F. and Jaramillo, C.: Quantitative analysis of Cenozoic palynofloras from Patagonia, southern South America, Palynology, 37(2), 246–258, doi:10.1080/01916122.2013.787126, 2013.

Raymo, M. E.: The Initiation of Northern Hemisphere Glaciation, Annu. Rev. Earth Planet. Sci., 22(1), 353–383, 1890 doi:10.1146/annurev.ea.22.050194.002033, 1994.

Raymo, M. E. and Ruddiman, W. F.: Tectonic forcing of late Cenozoic climate, Nature, 359(6391), 117–122, doi:10.1038/359117a0, 1992.

Retallack, G. J.: Late Eocene and Oligocene paleosols from Badlands National Park, South Dakota, Geological Society of America., 1983.

1895 Retallack, G. J.: A 300-million-year record of atmospheric carbon dioxide from fossil plant cuticles, Nature, 411, 287, doi:10.1038/35077041, 2001.

Retallack, G. J., Wynn, J. G. and Fremd, T. J.: Glacial-interglacial–scale paleoclimatic change without large ice sheets in the Oligocene of central Oregon, Geology, 32(4), 297–300, doi:10.1130/G20247.1, 2004.

Ridgway, K. D. and Sweet, A. R.: Climatically induced floristic changes across the Eocene–Oligocene transition in the northern 1900 high latitudes, Yukon Territory, Canada, GSA Bull., 107(6), 676–696, doi:10.1130/0016-7606(1995)107<0676:CIFCAT>2.3.CO;2, 1995.

Robert, C. and Kennett, J. P.: Antarctic continental weathering changes during Eocene-Oligocene cryosphere expansion: Clay mineral and oxygen isotope evidence, Geology, 25(7), 587–590, doi:10.1130/0091-7613(1997)025%3C0587:ACWCDE%3E2.3.CO;2, 1997.

1905 Roberts, C. D., LeGrande, A. N. and Tripati, A. K.: Climate sensitivity to Arctic seaway restriction during the early Paleogene, Earth Planet. Sci. Lett., 286(3–4), 576–585, doi:10.1016/j.epsl.2009.07.026, 2009.

Roth-Nebelsick, A., Utescher, T., Mosbrugger, V., Diester-Haass, L. and Walther, H.: Changes in atmospheric CO2 concentrations and climate from the Late Eocene to Early Miocene: palaeobotanical reconstruction based on fossil floras from Saxony, Germany, Palaeogeogr. Palaeoclimatol. Palaeoecol., 205(1), 43–67, doi:https://doi.org/10.1016/j.palaeo.2003.11.014, 1910 2004.

Roth-Nebelsick, A., Grein, M., Utescher, T. and Konrad, W.: Stomatal pore length change in leaves of Eotrigonobalanus furcinervis (Fagaceae) from the Late Eocene to the Latest Oligocene and its impact on gas exchange and CO2 reconstruction, Rev. Palaeobot. Palynol., 174, 106–112, doi:10.1016/j.revpalbo.2012.01.001, 2012.

Roth-Nebelsick, A., Oehm, C., Grein, M., Utescher, T., Kunzmann, L., Friedrich, J.-P. and Konrad, W.: Stomatal density and

1915   index data of Platanus neptuni leaf fossils and their evaluation as a CO_2 proxy for the Oligocene, Rev. Palaeobot. Palynol., 206, 1–9, doi:10.1016/j.revpalbo.2014.03.001, 2014.

Roth-Nebelsick, A., Grein, M., Traiser, C., Moraweck, K., Kunzmann, L., Kovar-Eder, J., Kvaček, J., Stiller, S. and Neinhuis, C.: Functional leaf traits and leaf economics in the Paleogene — A case study for Central Europe, Palaeogeogr. Palaeoclimatol. Palaeoecol., 472, 1–14, doi:10.1016/j.palaeo.2017.02.008, 2017.

1920   Royer, D. L., Wing, S. L., Beerling, D. J., Jolley, D. W., Koch, P. L., Hickey, L. J. and Berner, R. A.: Paleobotanical Evidence for Near Present-Day Levels of Atmospheric CO_2 During Part of the Tertiary, Science, 292(5525), 2310–2313, doi:10.1126/science.292.5525.2310, 2001.

Royer, D. L., Berner, R. A., Montañez, I. P., Tabor, N. J. and Beerling, D. J.: CO_2 as a primary driver of phanerozoic climate, GSA today, 14(3), 4–10, doi:10.1130/1052-5173(2004)014<4:CAAPDO>2.0.CO;2, 2004.

1925   Sagoo, N., Valdes, P., Flecker, R. and Gregoire, L. J.: The Early Eocene equable climate problem: can perturbations of climate model parameters identify possible solutions?, Philos. Trans. R. Soc. A Math. Phys. Eng. Sci., 371(2001), 20130123, doi:10.1098/rsta.2013.0123, 2013.

Schaefer, J. M., Finkel, R. C., Balco, G., Alley, R. B., Caffee, M. W., Briner, J. P., Young, N. E., Gow, A. J. and Schwartz, R.: Greenland was nearly ice-free for extended periods during the Pleistocene, Nature, 540, 252, doi:10.1038/nature20146, 1930   2016.

De Schepper, S., Gibbard, P. L., Salzmann, U. and Ehlers, J.: A global synthesis of the marine and terrestrial evidence for glaciation during the Pliocene Epoch, Earth-Science Rev., 135, 83–102, doi:10.1016/j.earscirev.2014.04.003, 2014.

Scher, H. D., Bohaty, S. M., Zachos, J. C. and Delaney, M. L.: Two-stepping into the icehouse: East Antarctic weathering during progressive ice-sheet expansion at the Eocene–Oligocene transition, Geology, 39(4), 383–386, doi:10.1130/G31726.1, 1935   2011.

Scher, H. D., Bohaty, S. M., Smith, B. W. and Munn, G. H.: Isotopic interrogation of a suspected late Eocene glaciation, Paleoceanography, 29(6), 628–644, doi:10.1002/2014PA002648, 2014.

Scher, H. D., Whittaker, J. M., Williams, S. E., Latimer, J. C., Kordesch, W. E. C. and Delaney, M. L.: Onset of Antarctic Circumpolar Current 30 million years ago as Tasmanian Gateway aligned with westerlies, Nature, 523(7562), 580–583, 1940   doi:10.1038/nature14598, 2015.

Schouten, S., Hopmans, E. C., Schefuß, E. and Sinninghe Damsté, J. S.: Distributional variations in marine crenarchaeotal membrane lipids: a new tool for reconstructing ancient sea water temperatures?, Earth Planet. Sci. Lett., 204(1), 265–274, doi:10.1016/S0012-821X(02)00979-2, 2002.

Scotese, C. R. and Wright, N. M.: PALEOMAP Paleodigital Elevation Models (PaleoDEMS) for the Phanerozoic 1945   PALEOMAP Project. [online] Available from: https://www.earthbyte.org/paleodem-resource-scotese-and-wright-2018, 2018.

Scotese, C. R., Gahagan, L. M. and Larson, R. L.: Plate tectonic reconstructions of the Cretaceous and Cenozoic ocean basins, Tectonophysics, 155(1), 27–48, doi:10.1016/0040-1951(88)90259-4, 1988.

Seton, M., Müller, R. D., Zahirovic, S., Gaina, C., Torsvik, T., Shephard, G., Talsma, A., Gurnis, M., Turner, M., Maus, S. and Chandler, M.: Global continental and ocean basin reconstructions since 200Ma, Earth-Science Rev., 113(3), 212–270, 1950   doi:10.1016/j.earscirev.2012.03.002, 2012.

Sewall, J. O., Sloan, L. C., Huber, M. and Wing, S.: Climate sensitivity to changes in land surface characteristics, Glob. Planet. Change, 26(4), 445–465, doi:10.1016/S0921-8181(00)00056-4, 2000.

Sexton, P. F., Wilson, P. A. and Pearson, P. N.: Microstructural and geochemical perspectives on planktic foraminiferal preservation: "Glassy" versus "Frosty," Geochemistry, Geophys. Geosystems, 7(12), doi:10.1029/2006GC001291, 2006.

1955   Shackleton, N. J. and Kennett, J. P.: Paleotemperature History of the Cenozoic and the Initiation of Antarctic Glaciation: Oxygen and Carbon Isotope Analyses in DSDP Sites 277, 279 and 281, Initial Rep. Deep Sea Drill. Proj., 29, 743, 1975.

Shackleton, N. J., Backman, J., Zimmerman, H., Kent, D. V, Hall, M. A., Roberts, D. G., Schnitker, D., Baldauf, J. G., Desprairies, A., Homrighausen, R., Huddlestun, P., Keene, J. B., Kaltenback, A. J., Krumsiek, K. A. O., Morton, A. C., Murray, J. W. and Westberg-Smith, J.: Oxygen isotope calibration of the onset of ice-rafting and history of glaciation in the North
1960   Atlantic region, Nature, 307(5952), 620–623, doi:10.1038/307620a0, 1984.

Sheldon, N. D. and Tabor, N. J.: Quantitative paleoenvironmental and paleoclimatic reconstruction using paleosols, Earth-Science Rev., 95(1), 1–52, doi:10.1016/j.earscirev.2009.03.004, 2009.

Sheldon, N. D., Costa, E., Cabrera, L. and Garcés, M.: Continental Climatic and Weathering Response to the Eocene-Oligocene Transition, J. Geol., 120(2), 227–236, doi:10.1086/663984, 2012.

1965   Sheldon, N. D., Grimes, S. T., Hooker, J. J., Collinson, M. E., Bugler, M. J., Hren, M. T., Price, G. D. and Sutton, P. A.: Coupling of marine and continental oxygen isotope records during the Eocene-Oligocene transition, GSA Bull., 128(3–4), 502–510, doi:10.1130/B31315.1, 2016.

Shellito, C. J., Sloan, L. C. and Huber, M.: Climate model sensitivity to atmospheric CO2 levels in the Early–Middle Paleogene, Palaeogeogr. Palaeoclimatol. Palaeoecol., 193(1), 113–123, doi:10.1016/S0031-0182(02)00718-6, 2003.

1970   Sijp, W. P. and England, M. H.: Effect of the Drake Passage Throughflow on Global Climate, J. Phys. Oceanogr., 34(5), 1254–1266, doi:10.1175/1520-0485(2004)034<1254:EOTDPT>2.0.CO;2, 2004.

Sijp, W. P., England, M. H. and Toggweiler, J. R.: Effect of Ocean Gateway Changes under Greenhouse Warmth, J. Clim., 22(24), 6639–6652, doi:10.1175/2009JCLI3003.1, 2009.

Sijp, W. P., England, M. H. and Huber, M.: Effect of the deepening of the Tasman Gateway on the global ocean,
1975   Paleoceanography, 26(4), PA4207, doi:10.1029/2011PA002143, 2011.

Sijp, W. P., von der Heydt, A. S., Dijkstra, H. A., Flögel, S., Douglas, P. M. J. and Bijl, P. K.: The role of ocean gateways on cooling climate on long time scales, Glob. Planet. Change, 119(0), 1–22, doi:10.1016/j.gloplacha.2014.04.004, 2014.

Sijp, W. P., von der Heydt, A. S. and Bijl, P. K.: Model simulations of early westward flow across the Tasman Gateway during the early Eocene, Clim. Past, 12(4), 807–817, doi:10.5194/cp-12-807-2016, 2016.

1980   Śliwińska, K. K., Thomsen, E., Schouten, S., Schoon, P. L. and Heilmann-Clausen, C.: Climate- and gateway-driven cooling of Late Eocene to earliest Oligocene sea surface temperatures in the North Sea Basin, Sci. Rep., 9(1), 4458, doi:10.1038/s41598-019-41013-7, 2019.

Sluijs, A., Schouten, S., Donders, T. H., Schoon, P. L., Röhl, U., Reichart, G.-J., Sangiorgi, F., Kim, J.-H., Sinninghe Damsté, J. S. and Brinkhuis, H.: Warm and wet conditions in the Arctic region during Eocene Thermal Maximum 2, Nat. Geosci., 2,
1985   777, doi:10.1038/ngeo668, 2009.

Solgaard, A. M., Bonow, J. M., Langen, P. L., Japsen, P. and Hvidberg, C. S.: Mountain building and the initiation of the Greenland Ice Sheet, Palaeogeogr. Palaeoclimatol. Palaeoecol., 392, 161–176, doi:10.1016/j.palaeo.2013.09.019, 2013.

Sorlien, C. C., Luyendyk, B. P., Wilson, D. S., Decesari, R. C., Bartek, L. R. and Diebold, J. B.: Oligocene development of the West Antarctic Ice Sheet recorded in eastern Ross Sea strata, Geology, 35(5), 467–470, doi:10.1130/G23387A.1, 2007.

1990   Sosdian, S. M., Greenop, R., Hain, M. P., Foster, G. L., Pearson, P. N. and Lear, C. H.: Constraining the evolution of Neogene ocean carbonate chemistry using the boron isotope pH proxy, Earth Planet. Sci. Lett., 498, 362–376, doi:10.1016/j.epsl.2018.06.017, 2018.

Spicer, R. A.: Tibet, the Himalaya, Asian monsoons and biodiversity – In what ways are they related?, Plant Divers., 39(5), 233–244, doi:10.1016/j.pld.2017.09.001, 2017.

1995   Spray, J. F., Bohaty, S. M., Davies, A., Bailey, I., Romans, B. W., Cooper, M. J., Milton, J. A. and Wilson, P. A.: North Atlantic Evidence for a Unipolar Icehouse Climate State at the Eocene-Oligocene Transition, Paleoceanogr. Paleoclimatology, 34(7), 1124–1138, doi:10.1029/2019PA003563, 2019.

Srokosz, M. A. and Bryden, H. L.: Observing the Atlantic Meridional Overturning Circulation yields a decade of inevitable surprises, Science, 348(6241), doi:10.1126/science.1255575, 2015.

2000   Stärz, M., Jokat, W., Knorr, G. and Lohmann, G.: Threshold in North Atlantic-Arctic Ocean circulation controlled by the subsidence of the Greenland-Scotland Ridge, Nat. Commun., 8, 15681, doi:10.1038/ncomms15681, 2017.

Steinthorsdottir, M. and Vajda, V.: Early Jurassic (late Pliensbachian) CO_2 concentrations based on stomatal analysis of fossil conifer leaves from eastern Australia, Gondwana Res., 27(3), 932–939, doi:10.1016/j.gr.2013.08.021, 2015.

Steinthorsdottir, M., Jeram, A. J. and McElwain, J. C.: Extremely elevated CO_2 concentrations at the Triassic/Jurassic
2005   boundary, Palaeogeogr. Palaeoclimatol. Palaeoecol., 308(3), 418–432, doi:10.1016/j.palaeo.2011.05.050, 2011.

Steinthorsdottir, M., Wohlfarth, B., Kylander, M. E., Blaauw, M. and Reimer, P. J.: Stomatal proxy record of CO_2 concentrations from the last termination suggests an important role for CO_2 at climate change transitions, Quat. Sci. Rev., 68, 43–58, doi:10.1016/j.quascirev.2013.02.003, 2013.

Steinthorsdottir, M., Porter, A. S., Holohan, A., Kunzmann, L., Collinson, M. and McElwain, J. C.: Fossil plant stomata
2010   indicate decreasing atmospheric CO_2 prior to the Eocene-Oligocene boundary, Clim. Past, 12(2), 439–454, doi:10.5194/cp-12-439-2016, 2016.

Steinthorsdottir, M., Vajda, V., Pole, M. and Holdgate, G.: Moderate levels of Eocene pCO_2 indicated by Southern Hemisphere fossil plant stomata, Geology, doi:10.1130/G46274.1, 2019.

Stickley, C. E., Brinkhuis, H., Schellenberg, S. A., Sluijs, A., Röhl, U., Fuller, M., Grauert, M., Huber, M., Warnaar, J. and
2015   Williams, G. L.: Timing and nature of the deepening of the Tasmanian Gateway, Paleoceanography, 19(4), PA4027, doi:10.1029/2004PA001022, 2004.

Stickley, C. E., St John, K., Koç, N., Jordan, R. W., Passchier, S., Pearce, R. B. and Kearns, L. E.: Evidence for middle Eocene Arctic sea ice from diatoms and ice-rafted debris, Nature, 460, 376–379, doi:10.1038/nature08163, 2009.

Stocchi, P., Escutia, C., Houben, A. J. P., Vermeersen, B. L. A., Bijl, P. K., Brinkhuis, H., DeConto, R. M., Galeotti, S.,
2020   Passchier, S., Pollard, D., Brinkhuis, H., Escutia, C., Klaus, A., Fehr, A., Williams, T., Bendle, J. A. P., Bijl, P. K., Bohaty, S. M., Carr, S. A., Dunbar, R. B., Flores, J. A., Gonzàlez, J. J., Hayden, T. G., Iwai, M., Jimenez-Espejo, F. J., Katsuki, K., Kong, G. S., McKay, R. M., Nakai, M., Olney, M. P., Passchier, S., Pekar, S. F., Pross, J., Riesselman, C., Röhl, U., Sakai, T., Shrivastava, P. K., Stickley, C. E., Sugisaki, S., Tauxe, L., Tuo, S., van de Flierdt, T., Welsh, K. and Yamane, M.: Relative sea-level rise around East Antarctica during Oligocene glaciation, Nat. Geosci., 6, 380, doi:10.1038/ngeo1783, 2013.

2025   Strömberg, C. A. E., Dunn, R. E., Madden, R. H., Kohn, M. J. and Carlini, A. A.: Decoupling the spread of grasslands from the evolution of grazer-type herbivores in South America, Nat. Commun., 4, 1478, doi:10.1038/ncomms2508, 2013.

Strother, S. L., Salzmann, U., Sangiorgi, F., Bijl, P. K., Pross, J., Escutia, C., Salabarnada, A., Pound, M. J., Voss, J. and

Woodward, J.: A new quantitative approach to identify reworking in Eocene to Miocene pollen records from offshore Antarctica using red fluorescence and digital imaging, Biogeosciences, 14(8), 2089–2100, doi:10.5194/bg-14-2089-2017, 2017.

Su, T., Li, S.-F., Tang, H., Huang, Y.-J., Li, S.-H., Deng, C.-L. and Zhou, Z.-K.: Hemitrapa Miki (Lythraceae) from the earliest Oligocene of southeastern Qinghai-Tibetan Plateau and its phytogeographic implications, Rev. Palaeobot. Palynol., 257, 57–63, doi:10.1016/j.revpalbo.2018.06.001, 2018.

Teodoridis, V. and Kvaček, Z.: Palaeoenvironmental evaluation of cainozoic plant assemblages from the Bohemian Massif (Czech Republic) and adjacent Germany, Bull. Geosci., 90(3), 695–720, doi:10.3140/bull.geosci.1553, 2015.

Thomas, D. J., Korty, R., Huber, M., Schubert, J. A. and Haines, B.: Nd isotopic structure of the Pacific Ocean 70-30 Ma and numerical evidence for vigorous ocean circulation and ocean heat transport in a greenhouse world, Paleoceanography, 29(5), 454–469, doi:10.1002/2013PA002535, 2014.

Thomson, S. N., Reiners, P. W., Hemming, S. R. and Gehrels, G. E.: The contribution of glacial erosion to shaping the hidden landscape of East Antarctica, Nat. Geosci., 6, 203, doi:10.1038/ngeo1722, 2013.

Tierney, J. E. and Tingley, M. P.: A TEX86 surface sediment database and extended Bayesian calibration, Sci. Data, 2, 150029, doi:10.1038/sdata.2015.29, 2015.

Tiffney, B. H. and Wing, S. L.: Paleoenvironment of the Oligocene Jebel Qatrani Formation, Fayum depression, northern Egypt, based on floral remains, in 23rd meeting of the Geological Society of America, San Diego, CA, October, pp. 21–24., 1991.

Tigchelaar, M., von der Heydt, A. S. and Dijkstra, H. A.: A new mechanism for the two-step delta 18O signal at the Eocene-Oligocene boundary, Clim. Past, 7(1), 235–247, doi:10.5194/cp-7-235-2011, 2011.

Toggweiler, J. R. and Bjornsson, H.: Drake Passage and palaeoclimate, J. Quat. Sci., 15(4), 319–328, doi:10.1002/1099-1417(200005)15:4<319::AID-JQS545>3.0.CO;2-C, 2000.

Torsvik, T. H., Van der Voo, R., Preeden, U., Mac Niocaill, C., Steinberger, B., Doubrovine, P. V, van Hinsbergen, D. J. J., Domeier, M., Gaina, C., Tohver, E., Meert, J. G., McCausland, P. J. A. and Cocks, L. R. M.: Phanerozoic polar wander, palaeogeography and dynamics, Earth-Science Rev., 114(3), 325–368, doi:10.1016/j.earscirev.2012.06.007, 2012.

Tripati, A. and Darby, D.: Evidence for ephemeral middle Eocene to early Oligocene Greenland glacial ice and pan-Arctic sea ice, Nat. Commun., 9(1), 1038, doi:10.1038/s41467-018-03180-5, 2018.

Tripati, A., Backman, J., Elderfield, H. and Ferretti, P.: Eocene bipolar glaciation associated with global carbon cycle changes, Nature, 436, 341, doi:10.1038/nature03874, 2005.

Tripati, A. K., Eagle, R. A., Morton, A., Dowdeswell, J. A., Atkinson, K. L., Bahé, Y., Dawber, C. F., Khadun, E., Shaw, R. M. H., Shorttle, O. and Thanabalasundaram, L.: Evidence for glaciation in the Northern Hemisphere back to 44 Ma from ice-rafted debris in the Greenland Sea, Earth Planet. Sci. Lett., 265(1), 112–122, doi:https://doi.org/10.1016/j.epsl.2007.09.045, 2008.

Vahlenkamp, M., Niezgodzki, I., De Vleeschouwer, D., Bickert, T., Harper, D., Kirtland Turner, S., Lohmann, G., Sexton, P., Zachos, J. and Pälike, H.: Astronomically paced changes in deep-water circulation in the western North Atlantic during the middle Eocene, Earth Planet. Sci. Lett., 484, 329–340, doi:10.1016/j.epsl.2017.12.016, 2018a.

Vahlenkamp, M., Niezgodzki, I., De Vleeschouwer, D., Lohmann, G., Bickert, T. and Pälike, H.: Ocean and climate response to North Atlantic seaway changes at the onset of long-term Eocene cooling, Earth Planet. Sci. Lett., 498, 185–195,

2030

2035

2040

2045

2050

2055

2060

2065

doi:10.1016/j.epsl.2018.06.031, 2018b.

Via, R. K. and Thomas, D. J.: Evolution of Atlantic thermohaline circulation: Early Oligocene onset of deep-water production in the North Atlantic, Geology, 34(6), 441–444, doi:10.1130/G22545.1, 2006.

Viebahn, J. P., von der Heydt, A. S., Le Bars, D. and Dijkstra, H. A.: Effects of Drake Passage on a strongly eddying global
2070 ocean, Paleoceanography, 31(5), 564–581, doi:10.1002/2015PA002888, 2016.

Waddell, L. M. and Moore, T. C.: Salinity of the Eocene Arctic Ocean from oxygen isotope analysis of fish bone carbonate, Paleoceanography, 23(1), PA1S12, doi:10.1029/2007PA001451, 2008.

Wade, B. S. and Pearson, P. N.: Planktonic foraminiferal turnover, diversity fluctuations and geochemical signals across the Eocene/Oligocene boundary in Tanzania, Mar. Micropaleontol., 68(3), 244–255, doi:10.1016/j.marmicro.2008.04.002, 2008.

2075 Wade, B. S., Pearson, P. N., Berggren, W. A. and Pälike, H.: Review and revision of Cenozoic tropical planktonic foraminiferal biostratigraphy and calibration to the geomagnetic polarity and astronomical time scale, Earth-Science Rev., 104(1), 111–142, doi:10.1016/j.earscirev.2010.09.003, 2011.

Wade, B. S., Houben, A. J. P., Quaijtaal, W., Schouten, S., Rosenthal, Y., Miller, K. G., Katz, M. E., Wright, J. D. and Brinkhuis, H.: Multiproxy record of abrupt sea-surface cooling across the Eocene-Oligocene transition in the Gulf of Mexico,
2080 Geology, 40(2), 159–162, doi:10.1130/G32577.1, 2012.

Wagner, F., Below, R., Klerk, P. D., Dilcher, D. L., Joosten, H., Kürschner, W. M. and Visscher, H.: A natural experiment on plant acclimation: lifetime stomatal frequency response of an individual tree to annual atmospheric CO_2 increase, Proc. Natl. Acad. Sci., 93(21), 11705 LP – 11708, doi:10.1073/pnas.93.21.11705, 1996.

Walker, J. C. G., Hays, P. B. and Kasting, J. F.: A negative feedback mechanism for the long-term stabilization of Earth's
2085 surface temperature, J. Geophys. Res. Ocean., 86(C10), 9776–9782, doi:10.1029/JC086iC10p09776, 1981.

Wei, W.: Opening of the Australia–Antarctica Gateway as dated by nannofossils, Mar. Micropaleontol., 52(1), 133–152, doi:10.1016/j.marmicro.2004.04.008, 2004.

Wellner, J. S., Anderson, J. B., Ehrmann, W., Weaver, F. M., Kirshner, A., Livsey, D. and Simms, A. R.: History of an Evolving Ice Sheet as Recorded in SHALDRIL Cores from the Northwestern Weddell Sea, Antarctica, in Tectonic, Climatic, and
2090 Cryospheric Evolution of the Antarctic Peninsula, pp. 131–151, American Geophysical Union., 2011.

Williams, S. E., Whittaker, J. M. and Müller, R. D.: Full-fit, palinspastic reconstruction of the conjugate Australian-Antarctic margins, Tectonics, 30(6), TC6012, doi:10.1029/2011TC002912, 2011.

Wilson, D. S. and Luyendyk, B. P.: West antarctic paleotopography estimated at the eocene-oligocene climate transition, Geophys. Res. Lett., 36(16), 10–13, doi:10.1029/2009GL039297, 2009.

2095 Wilson, D. S., Jamieson, S. S. R., Barrett, P. J., Leitchenkov, G., Gohl, K. and Larter, R. D.: Antarctic topography at the Eocene–Oligocene boundary, Palaeogeogr. Palaeoclimatol. Palaeoecol., 335–336, 24–34, doi:10.1016/j.palaeo.2011.05.028, 2012.

Wilson, D. S., Pollard, D., DeConto, R. M., Jamieson, S. S. R. and Luyendyk, B. P.: Initiation of the West Antarctic Ice Sheet and estimates of total Antarctic ice volume in the earliest Oligocene, Geophys. Res. Lett., 40(16), 4305–4309,
2100 doi:10.1002/grl.50797, 2013.

Wing, S. L.: Eocene and Oligocene Floras and Vegetation of the Rocky Mountains, Ann. Missouri Bot. Gard., 74(4), 748–784, doi:10.2307/2399449, 1987.

Wing, S. L., Hasiotis, S. T. and Bown, T. M.: First ichnofossils of flank-buttressed trees (late Eocene), Fayum Depression, Egypt, Ichnos, 3(4), 281–286, doi:10.1080/10420949509386398, 1995.

2105 Winguth, A., Shellito, C., Shields, C. and Winguth, C.: Climate Response at the Paleocene–Eocene Thermal Maximum to Greenhouse Gas Forcing—A Model Study with CCSM3, J. Clim., 23(10), 2562–2584, doi:10.1175/2009JCLI3113.1, 2010.

Wolfe, J. A.: Distribution of Major Vegetational Types During the Tertiary, in The Carbon Cycle and Atmospheric CO2: Natural Variations Archean to Present, pp. 357–375, American Geophysical Union., 1985.

Wolfe, J. A.: Tertiary climatic changes at middle latitudes of western North America, Palaeogeogr. Palaeoclimatol. 2110 Palaeoecol., 108(3), 195–205, doi:10.1016/0031-0182(94)90233-X, 1994.

Woodburne, M. O., Goin, F. J., Bond, M., Carlini, A. A., Gelfo, J. N., López, G. M., Iglesias, A. and Zimicz, A. N.: Paleogene land mammal faunas of South America; a response to global climatic changes and indigenous floral diversity, J. Mamm. Evol., 21(1), 1–73, doi:10.1007/s10914-012-9222-1, 2014.

Woodward, F. I.: Stomatal numbers are sensitive to increases in CO2 from pre-industrial levels, Nature, 327, 617, 2115 doi:10.1038/327617a0, 1987.

Xiao, G. Q., Abels, H. A., Yao, Z. Q., Dupont-Nivet, G. and Hilgen, F. J.: Asian aridification linked to the first step of the Eocene-Oligocene climate Transition (EOT) in obliquity-dominated terrestrial records (Xining Basin, China), Clim. Past, 6(4), 501–513, doi:10.5194/cp-6-501-2010, 2010.

Yancey, T. E., Elsik, W. C. and Sancay, R. H.: The palynological record of late Eocene climate change, northwest Gulf of 2120 Mexico, in From Greenhouse to Icehouse: The Marine Eocene-Oligocene Transition, pp. 252–268, Columbia University Press, New York., 2003.

Yang, J., Spicer, R. A., Spicer, T. E. V and Li, C.-S.: 'CLAMP Online': a new web-based palaeoclimate tool and its application to the terrestrial Paleogene and Neogene of North America, Palaeobiodiversity and Palaeoenvironments, 91(3), 163, doi:10.1007/s12549-011-0056-2, 2011.

2125 Yang, S., Galbraith, E. and Palter, J.: Coupled climate impacts of the Drake Passage and the Panama Seaway, Clim. Dyn., 43(1–2), 37–52, doi:10.1007/s00382-013-1809-6, 2014.

Young, D. A., Wright, A. P., Roberts, J. L., Warner, R. C., Young, N. W., Greenbaum, J. S., Schroeder, D. M., Holt, J. W., Sugden, D. E., Blankenship, D. D., van Ommen, T. D. and Siegert, M. J.: A dynamic early East Antarctic Ice Sheet suggested by ice-covered fjord landscapes, Nature, 474, 72, doi:10.1038/nature10114, 2011.

2130 Zaarur, S., Affek, H. P. and Brandon, M. T.: A revised calibration of the clumped isotope thermometer, Earth Planet. Sci. Lett., 382, 47–57, doi:10.1016/j.epsl.2013.07.026, 2013.

Zachos, J., Pagani, M., Sloan, L., Thomas, E. and Billups, K.: Trends, Rhythms, and Aberrations in Global Climate 65 Ma to Present, Science, 292(5517), 686–693, doi:10.1126/science.1059412, 2001.

Zachos, J. C. and Kump, L. R.: Carbon cycle feedbacks and the initiation of Antarctic glaciation in the earliest Oligocene, 2135 Glob. Planet. Change, 47(1), 51–66, doi:10.1016/j.gloplacha.2005.01.001, 2005.

Zachos, J. C., Breza, J. R. and Wise, S. W.: Early Oligocene ice-sheet expansion on Antarctica: Stable isotope and sedimentological evidence from Kerguelen Plateau, southern Indian Ocean, Geology, 20(6), 569–573, doi:10.1130/0091-7613(1992)020%3C0569:EOISEO%3E2.3.CO;2, 1992.

Zachos, J. C., Quinn, T. M. and Salamy, K. A.: High-resolution (10^4 years) deep-sea foraminiferal stable isotope records of

2140   the Eocene-Oligocene climate transition, Paleoceanography, 11(3), 251–266, doi:10.1029/96PA00571, 1996.

Zachos, J. C., Dickens, G. R. and Zeebe, R. E.: An early Cenozoic perspective on greenhouse warming and carbon-cycle dynamics., Nature, 451(7176), 279–83, doi:10.1038/nature06588, 2008.

Zanazzi, A., Kohn, M. J., MacFadden, B. J. and Terry, D. O.: Large temperature drop across the Eocene–Oligocene transition in central North America, Nature, 445, 639, doi:10.1038/nature05551, 2007.

2145   Zhang, Y. G., Pagani, M., Liu, Z., Bohaty, S. M. and DeConto, R.: A 40-million-year history of atmospheric CO2, Philos. Trans. R. Soc. London A Math. Phys. Eng. Sci., 371(2001), doi:10.1098/rsta.2013.0096, 2013.

Zhang, Z., Nisancioglu, K. H., Flatøy, F., Bentsen, M., Bethke, I. and Wang, H.: Tropical seaways played a more important role than high latitude seaways in Cenozoic cooling, Clim. Past, 7(3), 801–813, doi:10.5194/cp-7-801-2011, 2011.

Zhang, Z., Ramstein, G., Schuster, M., Li, C., Contoux, C. and Yan, Q.: Aridification of the Sahara desert caused by Tethys
2150   Sea shrinkage during the Late Miocene, Nature, 513, 401, doi:10.1038/nature13705, 2014.

Zhu, J., Poulsen, C. J. and Tierney, J. E.: Simulation of Eocene extreme warmth and high climate sensitivity through cloud feedbacks, Sci. Adv., 5(9), eaax1874, doi:10.1126/sciadv.aax1874, 2019.